

Investigation of protein-metal ion and protein-protein interactions using mass spectrometry and nuclear magnetic spectroscopy

Faqeer A. Hassem



Thesis presented in partial fulfilment of the requirements for the degree
Master of Science in Biotechnology at the University of the Western Cape

Supervisor: David J. R. Pugh (D.Phil *Oxon*)

Faculty of Natural Sciences

Abstract

Protein-protein interaction networks provide a global picture of cellular function and biological processes. Some proteins act as hub proteins, highly connected to others, whereas some others have few interactions. The dysfunction of a single highly connected interactor can cause widespread disruption of cellular processes including diseases and cancer. Therefore, detailed study of the interactions made by cancer-related proteins will help explain their role in the interaction networks.

The investigation of proteins by mass spectrometry (MS) has provided unique opportunities to gain insight into the dynamics of these proteins at the molecular level. MS uses mass analysis for protein characterization, and is currently the most comprehensive and versatile tool in proteomics. MS can provide confirmation of protein samples of interest, accurate molecular mass measurements of proteins, purity of protein samples, detection of post-translational modifications, and more recently, interactions between two or more proteins.

The conventional way of investigating the structure of proteins involves nuclear magnetic resonance (NMR) or X-ray crystallography. Compared to MS these methods are time consuming methods and, furthermore, require a considerable amount of protein. MS has proved to be useful in this regard as it provides insights into the structural arrangement of proteins, and/or their interacting partners, without the need for crystallization or the tedious process of backbone assignment before structural and functional annotations can be attributed to the protein of interest. However, in many cases, conventional methods are used parallel to MS to serve as validation of the MS data.

The broad objective of this MSc study was to provide structural and functional insights into the function of Retinoblastoma Binding Protein-6 (RBBP6), using a MS approach. The aims were twofold: 1) to investigate metal ion binding by RING (Really Interesting New Gene) finger domains from RBBP6, and 2) to investigate the *in vitro* interaction between RBBP6 and Hsp 70(Heat Shock Protein 70), and between RBBP6 and Murine Double Minute-2 (Mdm2).



Declaration

By submitting this thesis, I declare that the entirety of the work contained therein is my own original work, that I am the sole author thereof (save to the extent explicitly otherwise stated), that reproduction and publication thereof by The University of the Western Cape will not infringe any third party rights and that I have not previously in its entirety or in part submitted it for obtaining any qualification.

August 2013



Acknowledgements

Firstly, I would like to thank the Almighty for giving me the health, strength and knowledge for undertaking this project. To my parents, grandparents, family, and especially my wife, Waafeka, thanks for all your motivation, encouragement and support.

I would like to thank Prof. David Pugh for giving me the opportunity to join his research group to undertake this project and for his guidance and mentorship during the course of the project. My sincerest appreciation to Dr. Andrew Faro for his guidance, assistance and scientific inputs throughout the project. To my fellow peers in the biochemistry lab, thank you for all that you have done for me.

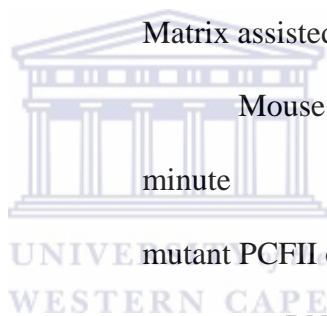
Lastly, I would like to thank the National Research Foundation of South Africa for providing financial support.



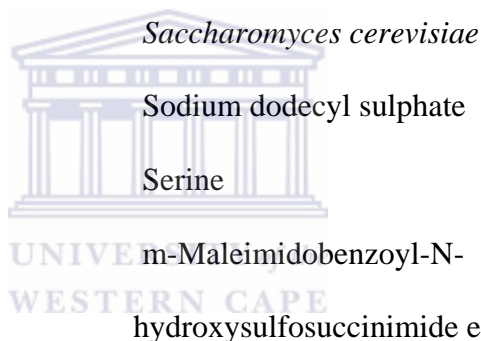
Abbreviations

Å	Angstrom
<i>An</i>	<i>Aspergillus niger</i>
APS	Ammonium persulphate
Asp or D	Aspartic acid
ATP	adenosine tri-phosphate
bp	base pair
BS ³	Bis[sulfosuccinimidyl] suberate
C-terminus	Carboxyl terminus
CV	Column volume
Cys or C	Cysteine
DNA	Deoxyribonucleic acid
dNTP	2'-deoxynucleoside 5'-triphosphate
DTT	1,4-dithio-DL-threitol
E1s	E1 ubiquitin-activating enzyme
E2s	E2 ubiquitin conjugating enzyme/Ubc
E3s	E3 ubiquitin ligase.
EDTA	Ethylenediaminetetra acetic acid
ESI	Electrospray ionization
Fig	Figure
Gln or Q	Glutamine
Glu or E	Glutamic acid
Gly or G	Glycine
GST	Glutathione S-Transferase
HDM2	Human double minute 2

His or H	Histidine
<i>Hs</i>	<i>Homo sapien</i>
Hsp70	Heat shock protein 70
Ile or I	Isoleucine
IPTG	Isopropyl-1-thio -D-galactoside
Kb	kilo base
kDa	kilo Dalton
Leu or L	Leucine
LB	Luria broth
Lys or K	Lysine
MALDI	Matrix assisted laser desorption/ionization
MDM2	Mouse double minute 2
min	minute
Mpe1	mutant PCFII extrogenic suppressor 1
mRNA	messenger RNA
MS	Mass spectrometry
m/z	mass to charge
N-terminus	Amino terminal
p53	protein 53
P2P-R	proliferation potential protein-related
PACT	p53-Associated Cellular protein-Testes derived
PAGE	Polyacrylamide gel electrophoresis
PBS	Phosphate buffer saline
PCR	Polymerase chain reaction



PDB	Protein Data Bank
PHD	Plant homeodomain
Phe or F	Phenylalanine
ppm	parts per million
Rb	Retinoblastoma
RBBP6	Retinoblastoma binding protein 6
RBQ-1	RB-binding Q-protein
RING	Really interesting new gene
RNA	Ribonucleic acid
s	seconds
Sc	<i>Saccharomyces cerevisiae</i>
SDS	Sodium dodecyl sulphate
Ser or S	Serine
Sulfo-MBS	m-Maleimidobenzoyl-N-hydroxysulfosuccinimide ester
TBE	Tris Borate EDTA
TE	Tris EDTA
TFIIH	Transcription factor IIIH
Thr or T	Threonine
Trp or W	Tryptophan
Ubc	Ubiquitin conjugating enzymes
UV	Ultra Violet
Y2H	Yeast-2-Hybrid
Zn ²⁺ /Zn	Zinc



List of figures

Figure 1.1. During electrospray ionization the sample is dissolved in a polar, volatile solvent and pumped through a narrow, stainless steel capillary. The charged droplets diminish in size by solvent evaporation, assisted by a warm flow of nitrogen known as the drying gas, which passes across the front of the ionization source. Charged sample ions, free from solvent, are then released from the droplets into the analyzer of the mass spectrometer. (Figure taken from Steen and Mann 2004).

Figure 1.2. In MALDI the sample to be analyzed is spotted onto an ultraviolet- absorbing matrix, which is normally a low-molecular-weight aromatic acid. On irradiation with a focused laser beam of the appropriate wavelength, the matrix molecules sublime and transfer the embedded non-volatile analyte molecules into the gas phase. After numerous ion-molecule collisions in the plume of ions and molecules, singly protonated analyte ions are formed, which are accelerated by electric potentials into the mass analyzer of choice. Figure taken from Steen and Mann (2004).

Figure 1.3. Products generated from a cross-linking reaction followed by proteolytic digestion. Type 2 cross-links (inter cross-links) are the cross-links most desired during protein-protein interaction experiments. (Figure taken from Leitner *et al.* 2010).

Figure 1.4. Most common ion fragments seen under low-energy conditions. CID, a low-energy fragmentation method gives rise to N-terminal ‘b-ions’ or C-terminal ‘y-ions.’ Figure taken from Schilling *et al.* (2003).

Figure 1.5. Fragmentation spectrum of a cross-linked peptide. The fragment peaks are annotated depending on the peptide that fragmented and the naming convention for peptides. The spectrum features fragments of both cross-linked peptides, thereby leading to confident and unambiguous identification of both peptides. Figure taken from Rappsilber (2011).

Figure 1.6. Domain organization of the RBBP6 protein family. All homologues contain a DWNN domain, a zinc knuckle and a RING finger and are found in all complete eukaryotic genomes analyzed to date. (Taken from Pugh *et al.* 2006).

Figure 1.7. Schematic representation of a RING finger domain indicating the ‘cross-brace’ topology for zinc ion coordination (Figure taken from Chasapis *et al.* 2009).

Figure 1.8. The ubiquitin pathway. A hierarchical set of three types of enzyme is required for substrate ubiquitination: ubiquitin-activating (E1), ubiquitin-conjugating (E2) and ubiquitin-protein ligase (E3) enzymes.

Figure 1.9. Alignment of RING finger domains from RBBP6 orthologues suggests that the *Hs*RING finger binds 2 Zn²⁺ ions, in which 1st and 3rd pair of cysteine residues (red arrows) bind one Zn²⁺ and the 2nd and 4th pairs (blue arrows) the other. The alignment reveals a disruption in the 1st pair of coordinating cysteines in the *An*RING and *Sc*RING homologs. The alignment reveals that some of the residues coordinating the first Zn²⁺ ion (red arrows) are missing from *A. niger* and *S. cerevisiae*, raising the possibility that both of these orthologues may bind only one Zn²⁺ ion.

Figure 3.1. (a) Primers designed for the amplification of *S. cerevisiae* included BamHI and XhoI restriction sites (bold) in the forward and reverse primers respectively, as well as two stop codons (underlined) immediately upstream of the XhoI site. (b) The *A. niger* sequence synthesized by Genscript Inc. was flanked by BamHI and XhoI sites. A

single stop codon was added immediately upstream of the XhoI site. (c) The *A. niger* sequence was optimized by Genscript Inc. to increase the efficiency of expression in *E. coli*. Primers were synthesized by the DNA synthesis facility at the University of Cape Town.

Figure 3.2. Amplification and cloning of the RING finger domain from *S. cerevisiae*. a) *ScRING* amplified directly from genomic DNA yielded the expected product of 267 bp (lanes 2 and 4). Lanes 1 and 3 contained no template DNA. b) Following colony PCR the 267bp fragment corresponding to the *ScRING* validated the successful cloning of the gene into the pGEX-6P-2 expression vector. Lanes 2, 3, 4, 7, 9, 10 correspond to positive clones. Lane 1 is the negative control for the PCR reaction as it contains no template DNA.

Figure 3.3. Sub-cloning of the RING finger domain from *A. niger* into pGEX-6P-2. a) A 252 bp fragment corresponding to the gene of interest was released when the pUC57-*AnRING* was digested with BamHI and XhoI. (b) The *A. niger* RING was successfully sub-cloned into pGEX-6P-2, as confirmed by the presence of a 252 bp fragment, following digestion of plasmid DNA extracted from positive clones. Lanes 1, 3 and 5 represent positive clones.

Figure 3.4. Experimentally determined sequences (Sbjct) for *ScRING* (a) and *AnRING* (b) were in 100 % agreement with expected sequences (Query). Flanking restriction sequences GGATCC (BamHI) and CTCGAG (XhoI) are indicated in yellow.

Figure 3.5. Pure samples of GST-RING finger proteins from *S. cerevisiae* (a), *A. niger* (b) and *H. sapiens* (c) were eluted from the glutathione matrix following addition of 20 mM free glutathione. All three domains exhibit an apparent molecular weight of approximately 35 kDa, as expected, corresponding to 26 kDa (GST) plus 9 kDa (RING).

Figure 3.6. Successful cleavage with 3C protease and separation using glutathione affinity of GST-RING proteins from *S. cerevisiae* (a), *A. niger* (b) and *H. sapiens* (c). In each case the uncleaved fusion can be seen in lane 1 and the cleaved sample in lane 2. Lane 3 and upward show varying degrees of successful separation of GST from the RING finger using a second round of glutathione affinity chromatography.

Figure 3.7. Chromatogram and SDS-PAGE showing the successful purification of the *HsRING* finger domain. Subjecting the sample to size exclusion chromatography separates most of the GST from the RING, to an extent that minimal GST remains in the sample.

Figure 3.8. 1D ^1H spectrum of *S. cerevisiae* RING finger domain at pH 6.0, 25 °C recorded at 600 MHz. The large chemical shift dispersion of resonances and sharp peaks exhibited by the protein is indicative of its foldedness. This is confirmed by the appearance of resonances corresponding to amide protons (H^{N}) in the region 9-11 ppm, α -protons (H^{α}) in the region 5-6 ppm, and methyl groups in the region 0-0.5 ppm. The sharpness of the peaks also indicate that the protein is monomeric.

Figure 3.9 ^{15}N -HSQC spectrum of a 10x diluted *ScRING* (red) superimposed over the concentrated sample (black). Spectra were recorded at pH 6.0, 25°C at 600MHz. The absence of concentration-dependent chemical shift perturbations suggests that the domain is monomeric in solution.

Figure 3.10 1D ^1H spectrum of the *A. niger* RING finger domain at pH 6.0, 25 °C, recorded at 600 MHz. The high level of dispersion (some H^{N} resonances in the region 9-10 ppm, some H^{α} in the region 5-6 ppm and methyl protons in the region 0-0.5 ppm) is an indication that the protein is folded.

Figure 3.11. Deconvoluted ESI MS of *Homo sapiens* RING finger. a) The denaturing ESI spectrum reveals the protein to be 10230 Da when the protein is sprayed into the

mass spectrometer using formic acid. b) The non-denaturing spectrum reveals the most abundant species to be the *HsRING* with 2 Zn^{2+} bound. c) The dimer with no Zn^{2+} bound, the dimer with 2 Zn^{2+} and the dimer binding 4 Zn^{2+} . The other peaks are separated by approximately 22 Da and are likely to correspond to sodium adducts, which is a result of the protein being insufficiently desalted prior to MS

Figure 3.12. Deconvoluted ESI MS of *Saccharomyces cerevisiae* RING finger. a.)The denaturing spectrum indicates the protein with no Zn^{2+} ions bound at 9610 Da. b) The non-denaturing spectrum reveals the most abundant species at the peak of 9673 Da, indicative of the one Zn^{2+} ion bound to the protein. Traces of the protein with no Zn^{2+} bound were also present.

Figure 3.13. Deconvoluted ESI MS of *Aspergillus niger* RING finger. a.)The denaturing ESI spectrum indicates the protein with no Zn^{2+} ions bound at 9200 Da. b.) The non-denaturing spectrum reveals majority of the species binding 2 Zn^{2+} . A peak corresponding to the protein binding 1 Zn^{2+} could not be detected.

Figure 4.1. The N-terminal of RBBP6 interacts with Hsp 70. (A) In a 6-His affinity pull-down assay, 6His-tagged Hsp70 was able to precipitate a GST-DWNN fusion protein (lane 3), but two unrelated His- tagged proteins were not (lanes 1-2). The same amount of DWNN fusion protein was present in each lane. (B) In the reciprocal GST-affinity pull-down assay, GST-DWNN and a larger fragment of RBBP6 (including DWNN), were able to precipitate 6His-tagged Hsp70 (lanes 2-3), but an unrelated GST-fusion protein was not (lane 1) (Kappo *et al.* 2012).

Figure 4.2. Analysis of cross-linked species. a) SDS-PAGE following cross-linking of DWNN and Hsp 70. b) Western blot of cross-linking assay using monoclonal anti-DWNN antibody. The addition of the hetero-bifunctional cross-linker sulfo-MBS creates high molecular weight bands that exceed the molecular weight of Hsp70 (70

kDa). These do not correspond to Hsp70-Hsp70 complexes because the antibody does not recognize Hsp70 at all (lane 2) nor to DWNN-DWNN complexes as they do not appear to any significant content in lane 4, where DWNN alone is cross-linked.

Figure 4.3. Intra-cross-links identified by Mass Matrix. Data generated from the Mass matrix server using the cross-linking application identified Hsp70 whilst no evidence of DWNN was observed, thus revealing intra-cross-links between the Hsp70 protein rather than inter-cross-links with DWNN.

Figure 4.4. Isolation of an interacting complex between the DWNN domain and Hsp70. (a) Size exclusion chromatogram of Hsp70 alone. (b) Size exclusion chromatogram of DWNN and Hsp70. The labels refer to the lanes in (c). (c) SDS-PAGE of fractions corresponding to the fractions indicated in (b). The small peak eluting prior to Hsp70 contains a band consistent with the DWNN domain (lanes 3 and 4), which is seen on its own in lane 1. The bulk of the DWNN domain elutes much later, consistent with its molecular weight of only 9 kDa.

Figure 4.5. Identification of DWNN from excised band. Using the database as the input the MASCOT server identified mainly keratin and trypsin (a), which are a result of sample preparation prior to MS. However, peptides identified match that of the RBBP6 gene. When subjecting the server to the DWNN domain sequence as input (b) the server identified peptides covering 68 % of the DWNN domain sequence (highlighted in green).

Figure 4.6. Primer design for GST-MDM2-RING incorporating BamHI and XhoI restriction sites (red rectangles). Stop codon sites are indicated by the green rectangle.

Figure 4.7. (a) Primers for amplification of MDM2-RING, incorporating an N-terminal NdeI and a C-terminal XhoI site (red boxes) as well as two stop codons immediately following the end of the gene. (b) Cloning into the NdeI and XhoI sites was chosen so

as to incorporate an N-terminal 6His tag. Incorporation of a C-terminal 6His tag was obviated by the stop codons incorporated into the reverse primer. Figure adapted from <http://www.staff.ncl.ac.uk/p.dean/pET.pdf>, accessed 04/07/2013.

Figure 4.8. a) Colony PCR screen of putative clones identified one positive colony (lane 2), which was subjected to sequencing. b) Comparison of the experimental sequence (Query) showed that the construct contained a mismatch (indicated in green). Inspection of the sequencing trace (c) confirmed that the mismatch was indeed present and was not due an error in base calling. Fortunately the mismatch was found to have no effect on the amino acid sequence.

Figure 4.9. GST-affinity pulldown assay using GST-RBBP6-RING as bait and MDM2-RING-6His as prey. MDM2 RING finger was probed for using a monoclonal antibody against the full length MDM2 protein. GST-RBBP6-RING is able to precipitate 6His-MDM2-RING, but a dummy GST-fusion was not.

Figure 4.10. Immunoprecipitation of MDM2-RING-6His and RBBP6-RING. Using an affinity matrix to couple antibodies to a matrix RBBP6-RING finger was used as bait to pull down MDM2-RING-6His finger. MDM2 RING was probed for using a monoclonal antibody against the full length MDM2 protein. b) Using MDM2-RING-6His as bait the RBBP6-RING was precipitated, as detected using a polyclonal antibody against the RBBP6-RING finger.

List of tables

Table 2.1. Restriction digestion of the RING PCR product and pGEX-6P-2 vector.

Table 2.2. Ligation reactions for cloning DNA fragments into pGEX-6P-2 expression vector



Table of Contents

Abstract	ii
Declaration	iv
Acknowledgements	v
Abbreviations	vi
List of figures	ix
List of Tables	xv

Chapter 1: Literature review

1.1 Introduction	1
1.2 Mass Spectrometry	3
1.2.1 Sample preparation	5
1.2.2 Ionization	5
a) Electrospray Ionization (ESI)	6
b) Matrix-Assisted Laser Desorption/Ionization (MALDI)	8
1.2.3 Mass Analyzers	10
a) Ion trap	10
b) Time-of-flight (TOF)	11
c) Quadrupole	11
1.3 Analysis of protein-metal ion binding using mass spectrometry	12
1.4 Analysis of protein-protein interactions using mass spectrometry	12
1.5 The RBBP6 protein family	17
1.6 RING finger domains	21
1.6.1 Classification of RING finger domains	23
1.6.2 RING fingers and ubiquitination	25



1.6.3 Zinc ion coordination in RING fingers	27
1.6.4 The RBBP6 RING finger domain	28
1.7 Objectives of this MSc	31

Chapter 2: Materials and methods

General stock solutions and buffer preparation	32
2.1 Generation of the pGEX-6P-2-RING expression constructs	32
2.2 Bacteria and yeast strains	34
2.3 Antibodies used	35
2.4 Preparation of yeast genomic DNA	35
2.5 PCR amplification of DNA	35
2.6 Double restriction digestion of genomic DNA and PGEX-6P-2vector	36
2.7 Agarose gel electrophoresis of DNA	36
2.8 Cohesive end ligation	37
2.9 Colony PCR assay	38
2.10 Transformation of plasmid DNA into competent cells	38
2.11 Large scale expression of recombinant protein	39
2.12 Glutathione affinity purification of GST-fusion proteins	39
2.13 Cleavage of the GST-fusion proteins using 3C protease	40
2.14 Size exclusion chromatography	40
2.15. SDS-PAGE gel electrophoresis	41
2.16 ESI-MS of RING finger domain protein	42
2.17 Affinity pull-down assays	42
2.18 Chemical cross-linking	43

2.19 Immuno-detection of Proteins	43
2.20 Mass Spectrometry	43

Chapter 3: Results – Protein-metal ion interaction

3.1. Introduction	46
3.2. Generation of GST-RING finger domain expression constructs	46
3.3. Expression and purification of RING finger proteins	52
3.4. ESI-MS of RING finger proteins	60
3.4.1. <i>Homo sapiens</i> RING finger	60
3.4.2. <i>Saccharomyces cerevisiae</i> RING finger	62
3.4.3. <i>Aspergillus niger</i> RING finger	65



Chapter 4: Results – Protein-protein interactions

4.1 Introduction	67
4.2 RBBP6 interacts with Hsp70 through its N-terminal DWNN domain	68
4.3 Cross-linking of DWNN and Hsp70	68
4.4 MS analysis of cross-linked proteins	70
4.5 Size exclusion chromatography of DWNN and Hsp70	73
4.6 Interaction between RBBP6 and Murine-double minute 2 (MDM2)	76
4.6.1 Affinity pull-down assay	76

Chapter 5: Discussion and Conclusion

References	89
------------	----

Chapter 1: Literature review

1.1 Introduction

Really Interesting New Gene proteins, more commonly known as RING finger domains, are small motifs of 70 amino acids in length that stabilize themselves by binding two zinc ions (Dominguez *et al.* 2004). The zinc ions are coordinated by eight cysteine or histidine residues in a so-called cross-brace fashion, in which the first and third pair of coordinating residues in the sequence coordinate one zinc ion, while the second and fourth pair coordinate the second zinc ion. RING finger domains are hallmarks of E3 ubiquitin ligase enzymes, which catalyze the attachment of ubiquitin moieties to substrate proteins. U-box domains adopt a similar structure to that of RING finger domains, although they do not bind any zinc ions, with the stability deficit being made up by increased numbers of hydrogen bonds and salt bridges. Retinoblastoma binding protein 6 (RBBP6) is a 250 kDa human RING finger-containing protein that has been shown to be involved in the regulation of mRNA processing and apoptosis, among other functions (Li *et al.* 2007). It has also been shown to function as an E3 ubiquitin ligase, ubiquitinating both p53 and Y-Box Binding Protein 1 (YB-1) through its RING finger domain (Li *et al.*, 2007, Chibi *et al.*, 2008). NMR studies of the RING finger domain of human RBBP6 has confirmed that it binds two zinc ions (Kappo *et al.*, 2012). However, analysis of the sequences of orthologues from other organisms reveals that in some of them, including the yeast *Saccharomyces cerevisiae*, some of the zinc coordinating residues have been replaced by residues that are unable to coordinate zinc. The conclusion to be drawn is that the RING finger in *S. cerevisiae* RBBP6 (ScRBBP6) binds only one zinc ion. If so, this may be the first report of a single-zinc RING finger domain.

If the resulting protein were folded, it would suggest that the requirement for binding one of the zinc ions has been replaced by the same mechanisms that stabilize U-boxes. The domain may therefore represent an intermediate between RING fingers and U-boxes. This is interesting in view of the fact that, based on their amino acid sequences, the RING fingers from the RBBP6 family bear strong similarities to U-boxes (Aravind and Koonin, 2000), an observation which is supported by the 3-dimensional structure of the human RING finger (Kappo *et al.* 2012). In RING fingers from other members of the RBBP6 family, such as that from the fungus *Aspergillus niger*, one of the zinc coordinating residues has been replaced by an aspartic acid (Kappo *et al.*, 2012).

Non-denaturing mass spectrometry represents another technique for studying the zinc binding of proteins that is potentially much more convenient, rapid, as well as requiring much less sample. However protein mass spectrometry is conventionally performed under denaturing conditions, resulting in unfolding of the protein and loss of any bound zinc. Analysis of zinc binding cannot be performed under denaturing conditions. Even in native conditions there is a high probability of bound zinc being lost during ionization, unless very soft ionisation conditions are used. In recent years mass spectrometry using soft electro-spray ionisation and volatile solvents such as ammonium acetate has been shown to be suitable for studying the folded native state of a number of proteins, including zinc binding and protein-protein interactions (Benesch and Robinson, 2006). One of the aims of this project was therefore to use non-denaturing mass spectrometry to investigate the number of zinc ions bound by RING finger domains from the RBBP6 protein family.

Although possible, investigation of protein-protein interactions using non-denaturing mass spectrometry has proved to be highly demanding from a technical point of view. An alternative method involves stabilization of non-covalent complexes using covalent cross-

linking reagents. The attachment points of these cross-links can then be determined using conventional mass spectrometry, by trypsinizing the complex and using tandem mass spectrometry under denaturing conditions to identify cross-linked fragment from both proteins. A second aim of the project was to test this method using previously identified interactions involving human RBBP6. These included the interaction between the N-terminal DWNN domain of RBBP6 and the Heat shock protein 70 (Hsp70), and between the RING finger domain of RBBP6 and Murine Double Minute 2 (MDM2), better known for its ubiquitination and suppression of the major tumour suppressor protein p53. In order to do that, suitable interacting fragments first had to be expressed in bacteria and shown to interact *in vitro* using other methods, principally immunoprecipitation. Hence a third aim was to express the RING and DWNN domains from human RBBP6 and domains from Hsp70 and MDM2 in bacteria, and use immunoprecipitation to confirm the interactions *in vitro*.

The following subsections in this chapter shed some light on the history and advancements made in both non-denaturing, and denaturing mass spectrometry, ionisation techniques, as well as cross-linking MS, to investigate protein-protein interactions. It then focuses on the RBBP6 family of proteins, particularly RING finger domains, that are involved in many processes, including ubiquitination and pre-mRNA processing.

1.2 Mass spectrometry

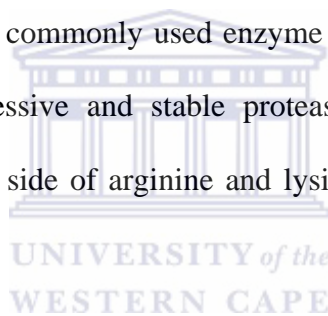
The development of mass spectrometry (MS) has had a profound influence on the study of proteins and protein function (Aebersold and Mann. 2003). The classical proteomic quantification methods using dyes, fluorophores or radioactivity provided very good sensitivity, linearity, and dynamic range, but they suffered from two important shortcomings: i) they required high-resolution protein separation, not typically provided

by 2-dimensional (2-D) gels, which limited their applicability to abundant and soluble proteins, and ii) they could not reveal the identity of any particular protein (Bantscheff *et al.* 2007). Protein sequencing was carried out using Edman degradation, in which polypeptides underwent chemical step-wise degradation from the N-terminus to the C-terminus (Domon and Aebersold. 2006), followed by amino acid identification using ultraviolet (UV) spectroscopy. This required a free amino terminus on the protein of interest, and relied on the fact that degradation cannot be blocked upon the Edman reaction (Steen and Mann. 2004). During the 1990s mass spectrometry, in which biomolecules are ionized and their mass measured by following their specific trajectories in a vacuum system, displaced Edman degradation, because it is much more sensitive and can fragment the peptides in seconds instead of hours or days (Steen and Mann. 2004). Today MS has established itself as the primary method of protein identification from complex mixtures of biological origin (Baldwin. 2004) and has become the powerhouse behind the development of proteomics. It is seen as a powerful analytical tool that elucidates many characteristics of a protein sample, including confirmation of a sample of interest, molecular weight determination of the protein sample, purity of the sample, detection of post-translational modifications (PTMs), disulfide bridge determination and, more recently, protein-protein interactions. The identification of proteins, which are often drug targets and are present at low concentration levels in complicated mixtures, is significantly facilitated by the sensitivity of MS (Glish and Vachet. 2003). In combination with separation techniques such as liquid chromatography, MS can play an important role in identifying and monitoring biomarkers in physiological fluids, which is a useful way of assessing drug efficacy and safety issues (Glish and Vachet. 2003).

1.2.1 Sample preparation

MS is based on producing, differentiating and detecting ions in the gas phase (Siuzdak *et al.* 1994). Mass spectrometry was restricted for a long time to small and thermo-stable compounds because of the lack of effective techniques to softly ionize and transfer the ionized molecules from the condensed phase into the gas phase without excessive fragmentation (Domon and Aebersold. 2006).

Identification of proteins is based on the analysis of peptides generated by proteolytic digestion (Baldwin. 2004). Proteins, being very unpredictable (solubility, oligomerization), first have to be converted to peptides before they can be introduced into the mass spectrometer. The most commonly used enzyme for the conversion of proteins to peptides is trypsin, an aggressive and stable protease which specifically cleaves proteins on the carboxy-terminal side of arginine and lysine residues (Steen and Mann. 2004).



1.2.2 Ionization

The most important reaction to occur in MS is the conversion of the analyte of interest into gas phase ions (Glish and Vachet. 2003). Previous ionization strategies were only suitable for low molecular weight, thermally stable compounds; proteins and peptides, on the other hand, are polar, nonvolatile and thermally unstable species that require an ionization technique that transfers an analyte into the gas phase without extensive degradation (Yates *et al.* 2009).

The emergence of two soft ionization techniques in the 1980s made it possible for proteins and peptides to be analyzed. Electrospray ionization (ESI) and matrix-assisted laser desorption/ionization (MALDI) are the two techniques most commonly used to

volatize and ionize the peptides for mass spectrometric analysis (Aebersold and Mann. 2003). The ionization techniques are described as ‘soft’ because they are able to generate ions from large, nonvolatile analytes such as proteins and peptides without significant analyte fragmentation (Aebersold and Goodlett. 2001). The development of these two techniques has revolutionized the field of biological MS, leading to the award in 2002 of the Nobel Prize in chemistry to John Fenn and Koichi Tanaka.

a) Electrospray Ionization (ESI)

ESI is well suited to the analysis of polar molecules ranging from less than 100 daltons (Da) to more than 1 000 000 Da in molecular mass. Ions are generated at atmospheric pressure by passing a solution-based sample through a small capillary at a potential difference relative to a counter electrode (Glish and Vachet. 2003). This results in the formation of an electrically charged spray, which is followed by formation and desolvation of analyte-solvent droplets (Yates *et al.* 2009). Through the application of a drying gas (usually N₂) or heat, the solvent evaporates and the droplet size decreases, resulting in the formation of desolvated ions (Fig. 1.1). A characteristic of electrospray ionization is the formation of highly charged ions without fragmentation (Yates. 1998). While the ESI process is tolerant to low levels of buffers, salts and detergents, these substances can form adducts with the analyte, causing ambiguous molecular mass determination; they can also suppress the formation of analyte ions (Yates. 1998). Positive attributes of ESI favouring it for biological samples are the lack of a limit to the size of the molecule that can be ionized, as well as the ‘soft’ ionization of the technique that allows for the ionization of intact non-covalent biomacromolecular complexes (Glish and Vachet. 2003), thereby making MS a perfect tool for the elucidation of protein-protein interactions. The downsides to ESI include that sample is constantly being consumed, and its susceptibility to ion suppression effects (Glish and Vachet. 2003).

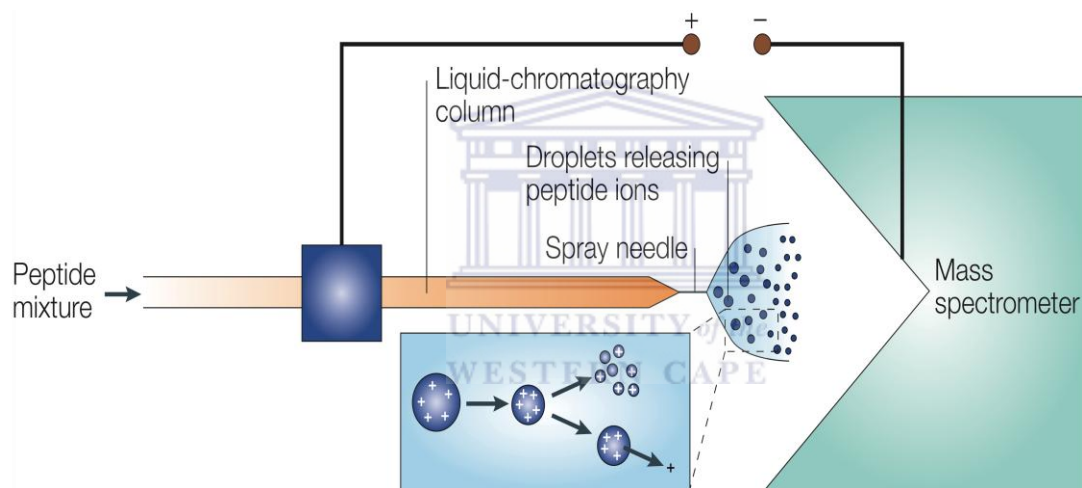


Figure 1.1 During electrospray ionization the sample is dissolved in a polar, volatile solvent and pumped through a narrow, stainless steel capillary. The charged droplets diminish in size by solvent evaporation, assisted by a warm flow of nitrogen known as the drying gas, which passes across the front of the ionization source. Charged sample ions, free from solvent, are then released from the droplets into the analyzer of the mass spectrometer. (Figure taken from Steen and Mann 2004).

Because proteins are identified by the m/z (mass-to-charge) ratios of their peptides and fragments, a high level of separation is required for accurate protein identification (Yates *et al.* 2009). High-pressure liquid chromatography (HPLC) is usually directly coupled to instruments with an ESI source, as the continuous separation via HPLC is compatible with the continuous ionization source provided by ESI (Yates *et al.* 2009). Examples of HPLC chromatographic materials commonly used in MS-based proteomics include ion exchange, reverse phase, affinity, and hybrid material, with high-pressure reverse phase chromatography being the most favoured (Steen and Mann. 2003).

b) Matrix-Assisted Laser Desorption/Ionization (MALDI)

In MALDI ions are produced by pulsed-laser irradiation of the sample of interest (Glish and Vachet. 2003), following adsorption onto a matrix.. The matrix, typically a UV-absorbing weak organic acid, absorbs laser energy and transfers it to the acidified analyte, causing desorption of ions of the analyte into the gas phase (Yates *et al.* 2009). Because the analyte is incorporated into a matrix during crystallization (Fig. 1.2), the process may serve to sequester the analyte from contaminants such as salt and buffers, in addition to direct excitation (Yates. 1998). The ions generated from MALDI are predominantly singly charged (Yates *et al.* 2009), providing a one-to-one correspondence between ions in the mass spectrum and the masses of peptides in the mixture (Yates. 1998). Compared to ESI, very little sample is wasted, thereby achieving very high levels of sensitivity (Glish and Vachet. 2003). However, one of the drawbacks to MALDI is the large degree of chemical noise generated by the matrix, making low molecular weights difficult to analyze.

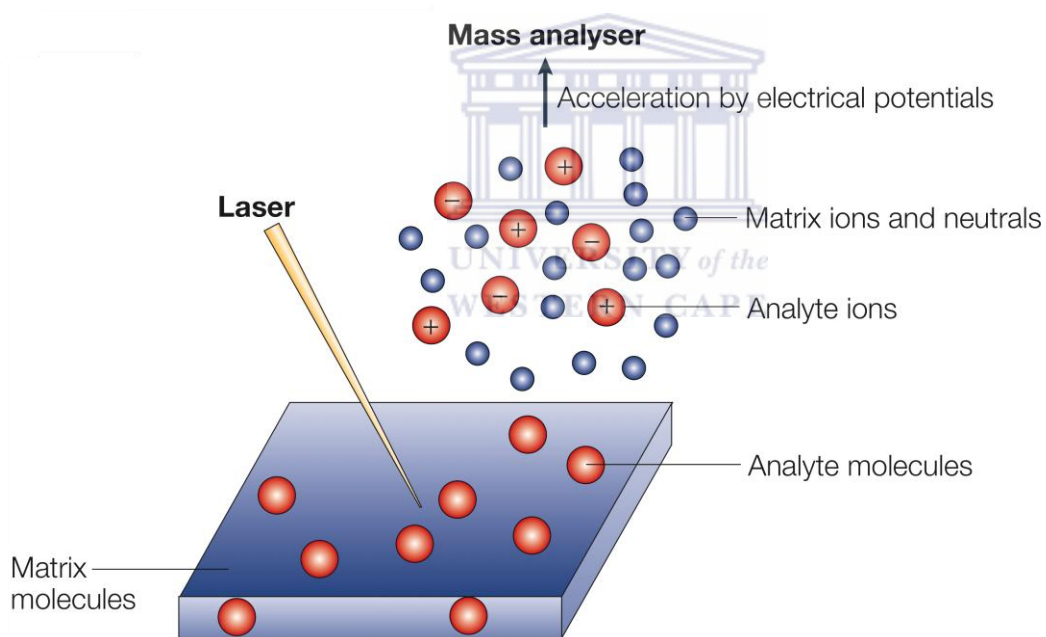


Figure 1.2 In MALDI the sample to be analyzed is spotted onto an ultraviolet- absorbing matrix, which is normally a low-molecular-weight aromatic acid. On irradiation with a focused laser beam of the appropriate wavelength, the matrix molecules sublime and transfer the embedded non-volatile analyte molecules into the gas phase. After numerous ion–molecule collisions in the plume of ions and molecules, singly protonated analyte ions are formed, which are accelerated by electric potentials into the mass analyser of choice. Figure taken from Steen and Mann (2004).

1.2.3 Mass Analyzers

Mass analyzers are differentiated as being either beam analyzers, or trapping analyzers; in the former ions leave the source in a beam and pass through the analyzing field to the detector, whilst the latter traps ions in the analyzing field after being formed in the analyzer itself or being injected from an external source (Glish and Vachet. 2003). Mass analyzers form an integral part of MS instrumentation as they are able to store ions and separate them based on m/z ratios (Yates *et al.* 2009). Each mass analyzer possesses unique qualities, including mass range, analysis speed, resolution, sensitivity, and dynamic range.

a) Ion trap

These are robust, sensitive, inexpensive analyzers, in which ions are captured or ‘trapped’ for a certain period of time, and are then subjected to MS or MS/MS (tandem MS) analyses (Siuzdak *et al.* 1994). MS/MS is the ability to induce fragmentation and perform successive MS experiments on the fragmented ions (Yates *et al.* 2009). Drawbacks of traditional ion-trap analyzers include a relatively low mass accuracy, which has been overcome in recent years by the development of 2D and 3D ion traps. Ion trap analyzers have evolved since their introduction, with the LTQ ion trap being the recent advancement in the field (Schwartz *et al.* 2002). Features of the instrument include a ten-fold higher storage capacity than 3D ion traps, and high resolution at a faster scanning rate (Yates *et al.* 2009). The instrument is ideally suited for bottom-up liquid chromatography LC/MS protein identification from complex mixtures (whole-cell lysates).

The LTQ Orbitrap is a hybrid MS instrument that incorporates recent advances in ion-trap development, where it is used for trapping, ion selection, and ion reactions (Yates et al. 2009). It uses the orbital trapping of ions in its static electrostatic fields in which the ions orbit around a central electrode and oscillate in an axial direction (Yates *et al.* 2009). The orbitrap mass analyzer features high resolution, high mass accuracy, and great dynamic range. When coupled to an LTQ ion trap, the instrument offers the high resolution and mass accuracy of the orbitrap, combined with the speed and sensitivity of the LTQ ion trap (Yates *et al.* 2009).

b) Time-of-flight (TOF)

TOF analyzers are the simplest of mass analyzers. Ions exiting the ion source are accelerated through a fixed potential before travelling a fixed distance and striking the detector (Glish and Vachet. 2003). The time it takes for an ion to reach the detector is related to its mass-to-charge (m/z) ratio (Yates. 1998). The addition of an electrostatic mirror (reflectron) at the end of the flight tube increases the resolution of TOF spectrometry by compensating for small differences in the velocities of ions with the same m/z . The mass range of TOF instruments is therefore vast (Glish and Vachet. 2003).

c) Quadrupole

Quadrupole mass separation is a result of ion motion in a dynamic electric field and is directly dependent on the m/z of the ion (Glish and Vachet. 2003). The electric fields are created by simultaneously applying a direct current voltage and an oscillating voltage on four parallel metal rods, known as quadrupoles (Yates. 1998). Quadrupole mass filters are usually coupled together, thereby allowing for detailed structural information to be inferred (Steen and Mann. 2004). This is achieved by creating a reaction region between two quadrupoles, known as a gas-phase collision cell (Yates. 1998). The benefit of this

collision cell is the ability to re-focus ions scattered from collisions with neutral gases, thereby allowing for efficient fragmentation (Yates *et al.* 2009).

1.3 Analysis of protein-metal ion binding using mass spectrometry

Advances in mass spectrometry have opened up new opportunities for the study of proteins. The development of non-denaturing MS methods has allowed for proteins to be studied in their folded state, opening up the fields of protein-metal ion and protein-protein interactions to MS. Non-denaturing (native) MS provides a direct and accurate measurement of the metal-binding stoichiometry of a protein, based on an observed shift in the mass of a protein arising from the non-covalent binding of the metal ion (Veenstra, 1999). Since its introduction, ESI has been successfully employed to investigate various non-covalently bound protein complexes (Gehrig *et al.* 2000). Advancements in ESI have produced narrower mass spectrum peaks and lower charge states, thereby producing more 'native-like' conformations (Benesch & Robinson, 2006). Today, native ESI-MS has become the method of choice for the elucidation of protein assemblies (Zhang *et al.* 2011), which provides a suitable platform for studying protein-metal ion coordination, as the intact protein survives the desolvation and ionization process and is transferred intact into the gas phase (Stengel *et al.* 2012). It is a rapid, sensitive technique that can provide invaluable information on bound small molecules (Laganowsky *et al.* 2013).

1.4 Analysis of protein-protein interactions using mass spectrometry

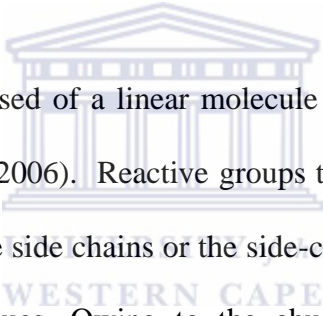
Characterization of non-covalent protein interactions poses an extremely challenging task for the reasons that many protein interactions are not stable, most interactions are transient, and multi-protein complexes possess no common factors or physical properties that can be used as an analytical handle (Tang *et al.* 2005). Protein-protein interactions

constitute the metabolic and signaling pathways that control the growth and development, structure, operation, replication, and selective elimination of cells (Figeys *et al.* 2001). In the past, non-covalent protein-protein interactions were analyzed using fluorescence, circular dichroism (CD) and UV (Veenstra. 1999). These techniques all require meticulous concentration measurements and rely on a change in the signal originating from one of the proteins as it is titrated with the other interacting protein (Veenstra. 1999). The use of MS for interactions provides direct and unambiguous results that are not influenced by concentration measurements (Figeys *et al.* 2001). Although MS, unlike NMR and X-ray crystallography, cannot provide atomic level resolution, it does have advantages when interrogating protein complexes (Zhang *et al.* 2011). MS of intact soluble protein complexes has emerged as a powerful technique to study the stoichiometry, structure-function and dynamics of protein assemblies (Laganowsky *et al.* 2013). A major advantage of studying protein-protein interactions using MS is the facility to detect different species within the same solution, even when their masses are very similar (Benesch & Robinson. 2006). The use of chemical cross-linkers together with MS provides a robust platform for protein-protein interaction analysis, which will be discussed further.

The first step is to generate a complex between the proteins under scrutiny. This can be achieved using Size Exclusion Chromatography (SEC), in which the interacting proteins are incubated together, passed through the SEC column, and eluted as pure complex fractions. Non-covalent interactions are then made covalent through the addition of a cross-linker, followed by SDS-PAGE to isolate the intact complex, Under the denaturing conditions used in SDS-PAGE, cross-linked complexes appear as newly-formed bands of higher molecular mass; bands of interest are excised from the gel and subjected to

digestion in-gel using trypsin. Resulting peptides are submitted for MS analysis, and resulting masses are analyzed using software designed to identify cross-linked products. Subjecting these peptides to peptide mass fingerprinting or other identification methods reveals the identity of the linked polypeptides (Back *et al.* 2003).

Cross-linking MS (CXMS) can also be employed for structural analysis, providing significant advantages over conventional methods even in the more challenging cases (Rappsilber. 2011). It provides data on the tertiary and quaternary structure of proteins in their native state (Rappsilber. 2011), is fast and economical, and supports homology modeling (Chen *et al.* 2011).



A cross-linker is typically composed of a linear molecule with a reactive group at each end, separated by a spacer (Sinz. 2006). Reactive groups target side-chain amino groups of lysines, thiol groups of cysteine side chains or the side-chain carboxylic acid groups of aspartic and glutamic acid residues. Owing to the abundance of lysine residues in proteins, cross-linkers targeting the former increase the chance of achieving successful cross-links (Rappsilber. 2011). The distance created between two interacting residues of the cross-linker is determined by the length of the spacer-arm of the cross-linker. A typical cross-linking reaction results in three different species being created when analyzed by MS: type 0, type 1, and type 2 (Fig. 1.3). Types 0 are peptides linked to cross-linkers with a hydrolyzed, unreactive group at the other end (Schilling *et al.* 2003); in fragmentation spectra, these manifest in the same manner as peptides containing a modified amino acid (Schilling *et al.* 2003). Type 1 relate to peptides containing an internal cross-link on a single peptide chain; like type 0, these carry little information. Type 2, which correspond to cross-linking between two independent peptide chains, are

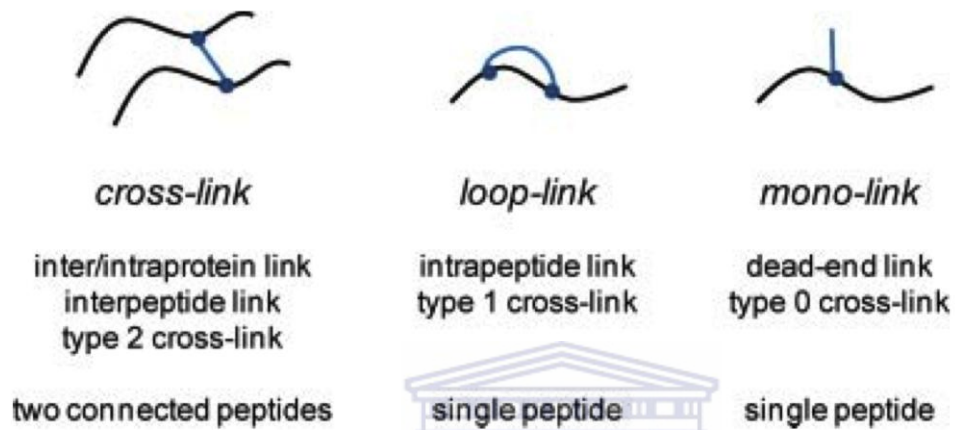
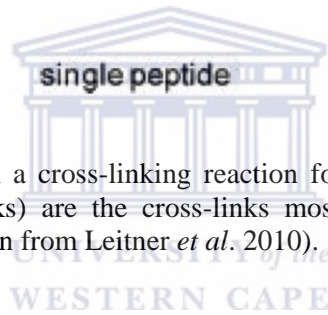


Figure 1.3 Products generated from a cross-linking reaction followed by proteolytic digestion. Type 2 cross-links (inter cross-links) are the cross-links most desired during protein-protein interaction experiments. (Figure taken from Leitner *et al.* 2010).



the most informative; if the peptides belong to different proteins they provide information about protein-protein interactions. If the peptides belong to the same protein, they either provide information about the folded structure of the protein or about the spatial arrangement of the protein in homo-oligomeric complexes.

CXMS has provided a platform for the elucidation of macromolecular interactions, including the spatial rearrangement of protein complexes (Maiolica *et al.* 2007) and protein-protein interactions within larger macromolecular assemblies (Sharon *et al.* 2006). Cross-link analysis can provide positional information on flexible, transient and modular higher-order multi-protein complexes, by mapping regions of partial proximity (Chen *et al.* 2010). It provides precise information concerning the interactions between subunits, thereby enabling improved modeling and docking of subunits (Stengel *et al.* 2012). Advances in cross-linked data analysis and identification has been improved by database searches that identify cross-linked sites in a manner similar to that of protein modification sites (Maiolica *et al.* 2007). Cross-linking data complements X-ray and NMR analysis, as shown by Maiolica *et al.* (2007), in which the spatial organization of a 180 kDa Ndc80 complex was determined. Chen and co-workers (2010) successfully investigated the structure of the RNA polymerase II (Pol II) transcription initiation complex, using cross-linking MS. They were able to extend the Pol II structure to a 15-subunit, 670 kDa complex of Pol II with the initiation factor TFIIF at peptide resolution (Chen *et al.* 2010).

During the MS analysis, the cross-linked peptide first needs to be identified. Mass and fragmentation spectra are first acquired. The fragmentation spectrum reveals the exact or approximate sites of linkage, made possible by the fact that peptides normally follow specific fragmentation rules, breaking predominantly along the backbone at the peptide

bond. Fragment ions for linear peptides are considered to arise from cleavages at three positions of the repeating amide linkages: C α – CO (a, x type) and CO – NH (b, y-type) and NH – C α , with these cleavages being either heterolytic or homolytic, and may also involve the transfer of one or more hydrogens with the charge retention at the N- (a, b, c-type) or C-terminus (x, y, z-type) (Schilling *et al.* 2003). The most common fragmentation method, Collision Induced Dissociation (CID), gives rise to two main fragment types, N-terminal ‘b-ions’ and C-terminal ‘y-ions’ (Fig. 1.4), which are seen under low-energy conditions.

The peaks obtained in fragmentation spectra are labeled using these letters, in conjunction with a subscript for the number of residues contained in the fragment, and a superscript for the number and type (positive or negative) of charges of the ion (Rappasilber. 2011). If a set of fragments is observed that fall upstream and downstream of the cross-linked residues, the exact position of the cross-linking site can be determined (Rappasilber. 2011). A benchmark study for CXMS was established in 2010 by Chen *et al.*, in which the cross-linked complex of PolIII initiation factor TFIIF was investigated. During the analysis of the cross-link and fragmentation data, a spectrum (Fig. 1.5) shows that the fragments determining the linkage sites are red b1 and y13 and green y4/y5 and b4/b5 (Chen *et al.* 2010).

1.5 The RBBP6 protein family

Retinoblastoma Binding Protein-6 (RBBP6), also known as p53-Associated Cellular Protein Testes-derived (PACT) and Proliferation Potential-Related Protein (P2P-R), is a 250 kDa multi-domain nuclear protein, which interacts with the tumor suppressor proteins

pRb and p53 (Sakai *et al.* 1995, Simons *et al.* 1997, Witte and Scott 1997). The protein has been demonstrated

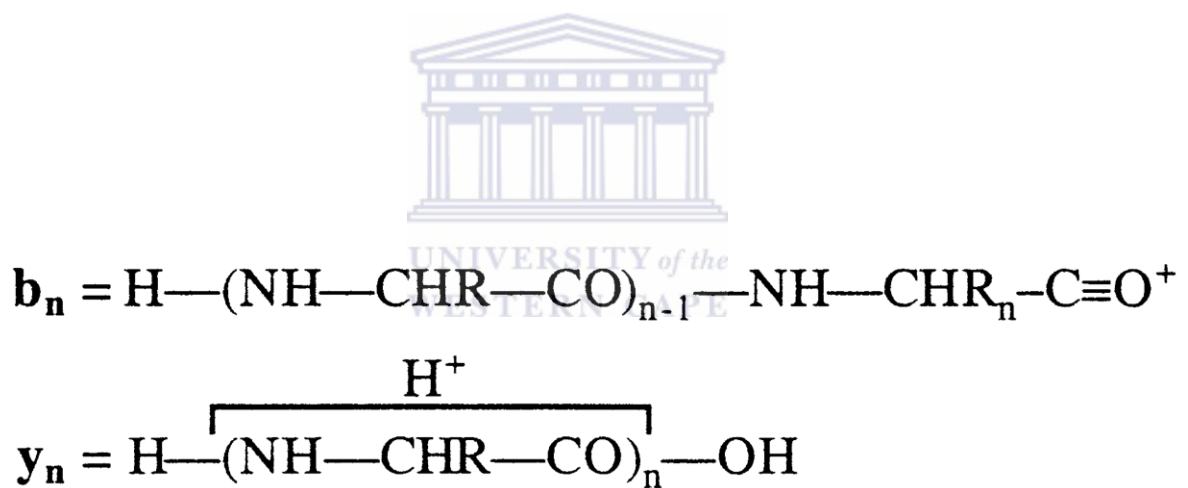


Figure 1.4 Ion fragments most commonly seen under low-energy conditions. CID, a low-energy fragmentation method, gives rise to N-terminal ‘b-ions’ or C-terminal ‘y-ions.’ Figure taken from Schilling *et al.* (2003).

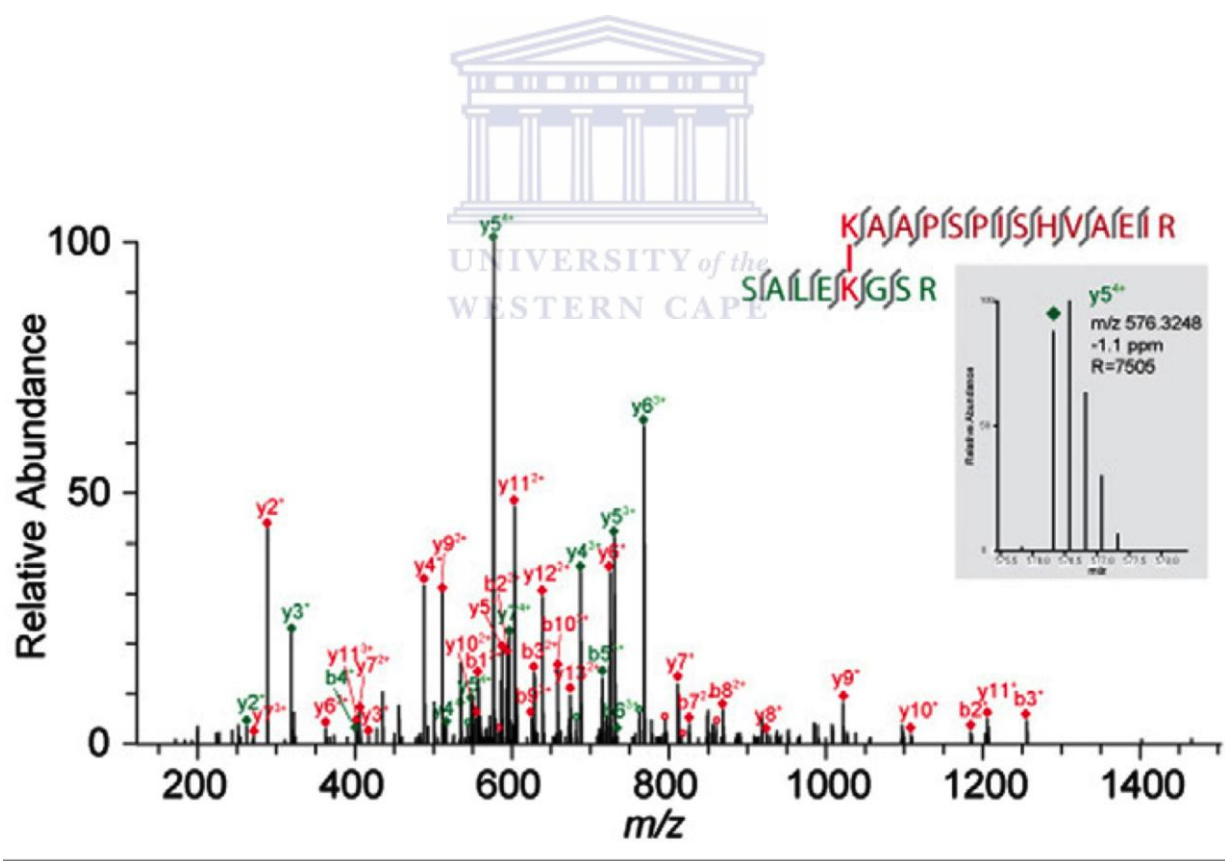


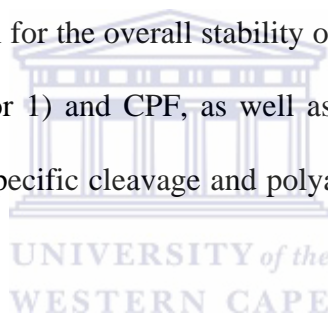
Figure 1.5 Fragmentation spectrum of a cross-linked peptide. The fragment peaks are annotated according to the peptide that fragmented and the naming convention for peptides. The spectrum features fragments of both cross-linked peptides, thereby leading to confident and unambiguous identification of both peptides. Figure taken from Rappsilber (2011).

to be involved in pre-mRNA processing and splicing in yeast (Vo *et al.* 2001), as well as the regulation of apoptosis and cell cycle progression (Li *et al.* 2007). At least three major transcripts are produced from the RBBP6 gene, by a combination of alternative splicing and alternative polyadenylation in humans. These transcripts encode proteins of 1792, 1758 and 118 amino acids respectively, which have been designated isoforms 1, 2 and 3 (Genbank: NP_008841, Genbank: NP_061173, Genbank: NP_116015). The domain organization of RBBP6 proteins from different eukaryotic organisms is shown in Fig. 1.6. The gene is found in all eukaryotic genomes analyzed to date as a single copy.

All RBBP6 homologues have an N-terminal ubiquitin-like domain, called the DWNN domain, followed by a CCHC zinc finger and a RING finger. In humans, the protein contains additional domains, including a proline rich domain (residues 337–349), SR domain (residues 679–773), as well as the pRb (964-1120) and p53 binding domains (residues 1142-1727) (Fig.1.6) (Pugh *et al.* 2006). In humans the DWNN domain is also independently expressed as a single domain protein, consisting of the DWNN domain and a long, unstructured C-terminal tail. In addition to these domains, RBBP6 contains extensive regions that are predicted to be intrinsically disordered.

RBBP6 has been implicated in mRNA processing (Vo *et al.* 2001), cell cycle control and apoptosis (Gao and Scott. 2003). Similarities between the RING-finger-like domain of RBBP6 and members of the U-box family, combined with its association with heat shock proteins, has led to the proposal that RBBP6 plays a role in chaperone-mediated ubiquitination of unfolded protein substrates (Kappo *et al.* 2012). It has been demonstrated in mice that knocking down RBBP6 leads to early embryonic lethality (Li *et al.* 2007). This would suggest that RBBP6 is important for cell growth and embryonic

development (Li *et al.* 2007). The *Saccharomyces cerevisiae* RBBP6 orthologue, Mpe1 (mutant PCFII extrogenic suppressor 1 protein), has 441 amino acids and a molecular weight of 49.5 kDa. Mpe1p is essential for cell viability and has been demonstrated to interact with the PCF11 protein, which encodes a subunit of cleavage factor 1 (CF1) (Vo *et al.* 2001). CF1 is responsible for the specific cleavage and polyadenylation of pre-mRNA. This gene is shorter than its human homologue and only contains the three conserved domains, namely the DWNN, zinc finger and RING domains. Vo *et al.* (2001) demonstrated that neutralization of Mpe1p by anti-Mpe1p antibodies completely inhibits polyadenylation of mRNA transcripts. *In vitro* studies conducted by Vo *et al.* (2001) demonstrated that Mpe1p is an integral subunit of the CPF (Cleavage and Polyadenylation Factor) although it is not essential for the overall stability of the CPF. In *S. cerevisiae* two complexes, CF1 (Cleavage Factor 1) and CPF, as well as the poly (A)-binding protein (Pab1p), are responsible for the specific cleavage and polyadenylation of pre-mRNA (Vo *et al.* 2001).



1.6 RING finger domains

The RING (Really Interesting New Gene) finger domain is one of the most common zinc binding, cysteine-rich motifs and is a hallmark of E3 ubiquitin ligases. The motif consists of the general consensus sequence Cys-X (2)-Cys-X (9-39)-Cys-X (1-3)-His-X (2-3)-Cys-X (2)-Cys-X (4-48)-Cys-X (2)-Cys, where X can be any amino acid. Fig. 1.7 is a diagrammatic representation of the structure of RING finger domains. An analysis of these structures revealed that all RING finger domains adopt a similar fold, but there are still significant differences present (Dominguez. 2004).

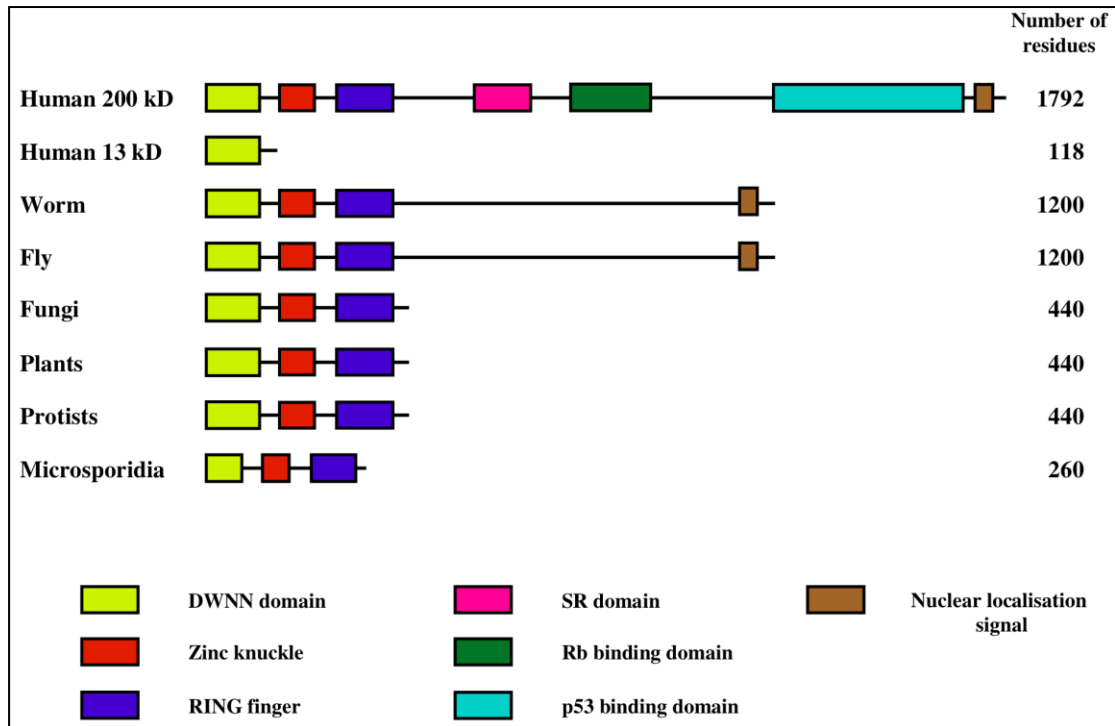


Figure 1.6 Domain organization of the RBBP6 protein family. All eukaryotic genomes contain a single gene containing the DWNN domain, zinc knuckle and RING finger domains, although in higher eukaryotes the gene contains additional C-terminal extensions. A short form containing only the DWNN domain is also found in higher eukaryotes, where it is expressed as an independent protein. (Taken from Pugh *et al.* 2006).

UNIVERSITY of the
WESTERN CAPE

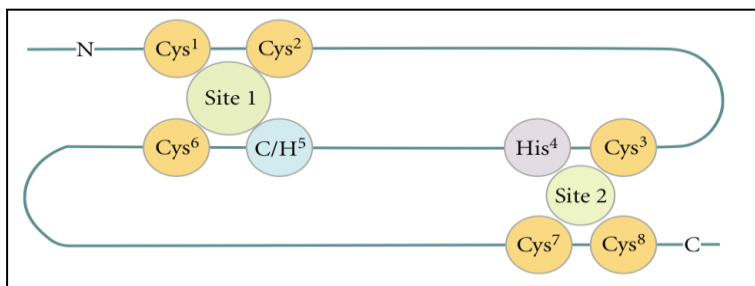


Figure 1.7 Schematic representation of a RING finger domain indicating the 'cross-brace' topology for zinc ion coordination (Figure taken from Chasapis *et al.* 2009).

The overall structure of RING finger domains are characterized by a $\beta\alpha\beta$ fold, but the presence, number, and exact positions of β -strands differ among these domain structures. RING fingers all share the same basic fold consisting of two large loops, each stabilized by a single zinc ion, lying parallel to an α -helix and together packing against a short 3-stranded β -sheet (Kappo *et al.* 2012). A cluster of hydrophobic residues has been shown to be essential in maintaining ternary structures of all RING fingers (Dominguez *et al.* 2004, Hanzawa *et al.* 2001). However, the main differences observed among the nine structures relate to the presence and length of their secondary structural elements. RING domains have been classified into different subclasses based on the variation of these secondary structure elements, as well as Zn^{2+} coordination. These are described in detail in the following section.



1.6.1 Classification of RING finger domains

RING finger domains can be divided into four subclasses: C_3HC_4 , C_3HHC_3 , $\text{C}_2\text{H}_2\text{C}_4$, and C_4C_4 (Dominguez *et al.* 2004). Classification of these domains is based on Zn^{2+} ion coordination, sequence homology, and the presence and length of secondary structural elements. C_3HC_4 , the classical RING domain, is the most common subclass of RING domains. The secondary structure of C_3HC_4 is composed of a three-stranded anti-parallel β -sheet packed against a central α -helix, thus adopting a $\beta\beta\alpha\beta$ global fold (Kellenberger *et al.* 2005). The structure of the C_3HC_4 RING domain was first reported by Barlow and co-workers in which they used 2D proton nuclear magnetic spectroscopy to determine the structure of the RING finger from the immediate-early EHV-1 protein (IEEHV) (Barlow *et al.* 1994). This structure was confirmed by Kellenberger and co-workers in which the structure of the RING finger from MAT1 was determined (Kellenberger *et al.* 2005). The second largest subclass, C_3HHC_3 , is also known as RING-H₂. C_3HHC_3 differs from

C₃HC₄ in that it contains a histidine residue at position 5 instead of a cysteine (as in C₃HC₄) (Katoh *et al.* 2003). Katoh and co-workers illustrated the structure of this subclass using EL5, a protein that is structurally related to the proteins of the *A. thaliana* ATL family (Katoh *et al.* 2003).

Using NMR titration experiments, they showed that amino acids Val136, Cys137, Leu138, Val162, Trp135 and Leu174 form a highly conserved hydrophobic core, which is critical for hydrophobic interaction with an E2 enzyme, thus confirming the role of this domain in ubiquitination (Katoh *et al.* 2003).

The third subclass of the RING domain is that of the C₂H₂C₄ RING motif. This motif is found in the E3 ligase MDM2, which regulates the ubiquitination and degradation relating to the concentration, activity, and stability of p53 (Kostic *et al.* 2006). The first structure of a member of the C₄C₄ subclass was that of the CNOT4 RING domain, which was elucidated using NMR spectroscopy. Hanzawa and co-workers (Hanzawa *et al.* 2001) illustrated that this domain is composed of three loops and an α -helix between loops 2 and 3, with no regular β -sheet. Using NMR Kellenberger and co-authors showed that the RING finger structure of p44 was the same as that of CNOT4, also adopting the C₄C₄ structure (Kellenberger *et al.* 2005). The RING domains of CNOT4 and p44 are involved in transcriptional regulation. The RING finger domain from RBBP6 has also been shown to belong to the C₄C₄ subclass, although the secondary structure bears little resemblance to that of CNOT4 (Kappo *et al.* 2012).

The U-box domain is structurally related to RING fingers but lacks the hallmark metal-coordinating residues of the latter (Aravind and Koonin. 2000). It is a peptide chain of

~70 amino acids that was first identified in the yeast protein UFD2 (ubiquitin fusion degradation protein 2), and subsequently demonstrated by Pringa and co-workers to be present in all eukaryotes (Pringa *et al.* 2000). U-boxes lack zinc-coordinating residues (Houben *et al.* 2005) but instead, hydrophobic residues stabilized by salt bridges and hydrogen bonds replace the zinc coordinating residues, thus stabilizing the U-box (Andersen *et al.* 2004). U-boxes function the same way as RING fingers, by acting as E3 ubiquitin ligases and mediating ubiquitination. U-boxes occur less abundantly than RING fingers, as evident by the fact that only two U-box proteins occur in the *S. cerevisiae* genome (Ohi *et al.* 2003).

1.6.2 RING fingers and ubiquitination

Ubiquitination refers to post-translational modification of proteins by covalent attachment of one or more ubiquitin monomers (Fig. 1.8). Ubiquitin (Ub) is a 76 residue protein that is highly conserved from humans to fungi. Ubiquitination is achieved by the formation of an isopeptide bond between the C-terminal glycine residue of ubiquitin and the ϵ -amino group of a lysine residue from the accepting protein (Deriziotis and Tabrizi. 2008). This process is able to affect the localization, activity, structure and interaction partners of target proteins (Woelk *et al.* 2007). Once cleaved from its precursor polypeptide, Ub is subjected to an enzymatic reaction cascade involving Ub-activating (E1), Ub-conjugating (E2) and Ub-ligating (E3) enzymes (Kirkin. 2007). Ub can be attached as a monomer or as isopeptide-linked polymers (polyubiquitin chains) (Woelk *et al.* 2007). Polyubiquitination is accomplished through seven lysine residues on Ub that can serve as

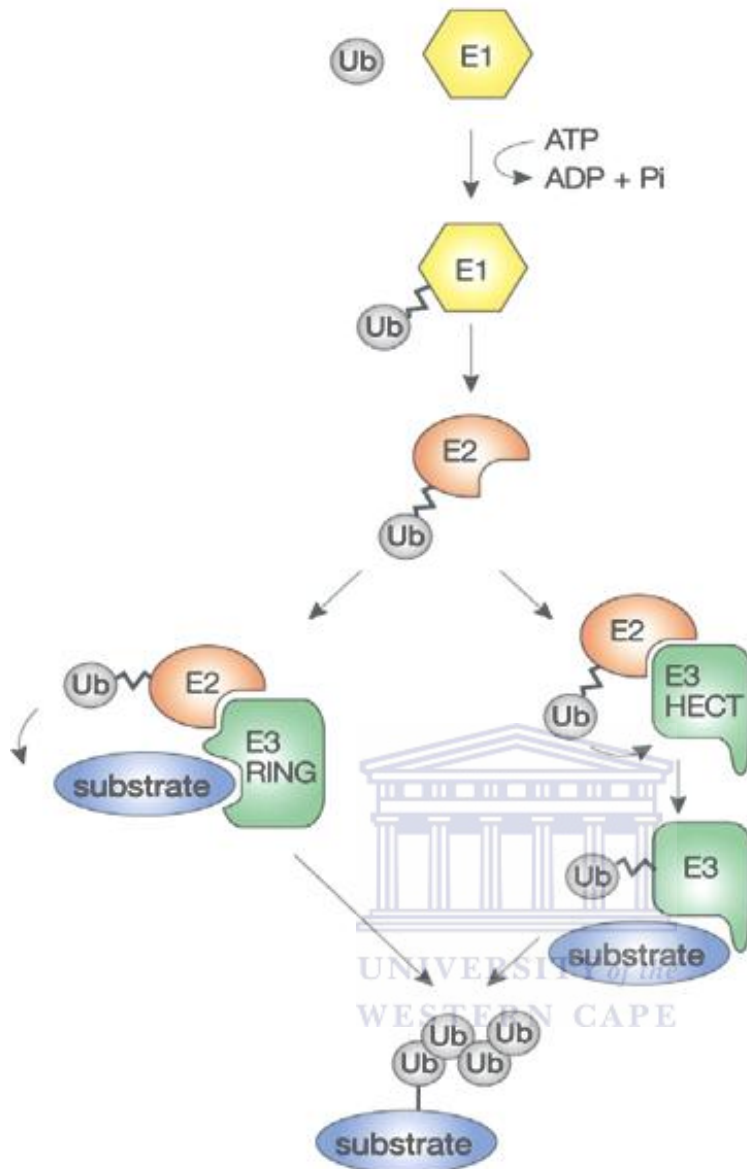


Figure 1.8. The ubiquitination pathway. A hierarchical set of three types of enzyme is required for substrate ubiquitination: ubiquitin-activating (E1), ubiquitin-conjugating (E2) and ubiquitin-protein ligase (E3) enzymes. (Figure taken from Woelk *et al.* 2007).

adaptors for the attachment of other Ub molecules (Woelk *et al.* 2007). An assembly of a chain of at least four ubiquitin molecules linked together via their Lys48 residue marks cellular proteins for degradation by the 26S proteasome, whereas polyubiquitination chains linked together via Lys63 serve as non-proteolytic signals in intracellular trafficking, DNA repair (Hicke *et al.* 2005) and signal transduction (Deshaies and Joazeiro. 2009). According to Kerscher and co-authors, most substrates are modified by multiubiquitin chains in which multiple ubiquitin molecules are linked via isopeptide bonds (Kerscher *et al.* 2006).

Ubiquitination controls a number of fundamental cellular functions. These include apoptosis, antigen processing, DNA repair, intracellular protein trafficking, metabolism, quality control in the endoplasmic reticulum, signal transduction and stress responses (Deriziotis. 2008, Kerscher. 2006). Woelk and co-workers state that the activity of the ubiquitination system needs to be regulated as ubiquitination is often induced by extracellular stimuli and substrates are not constitutively recognized (Woelk *et al.* 2007). Regulation of ubiquitination is often dependent on protein phosphorylation (Gao and Karin. 2005). RING-based E3s are specified by over 600 human genes, and have been linked to the control of many cellular processes and to multiple human diseases (Deshaies and Joazeiro. 2009).

1.6.3 Zinc ion coordination in RING fingers

Zinc (Zn^{2+}), the second most abundant transition metal in the human body, is critical for nucleic acid synthesis and consequently for cell division (Ramalho *et al.* 2009). It plays a central role in regulating cellular metabolism and is an essential cofactor of regulatory proteins, including proteins involved in apoptosis, DNA repair and proteins that control

gene expression (Ramalho *et al.* 2009). Zinc-binding proteins form a large group of metalloproteins in eukaryotic cells with a wide range of functions (Houben *et al.* 2005). The binding of zinc stabilizes the folded conformations of domains so that they may facilitate interactions between the proteins and other macromolecules such as DNA (Berg & Shi. 1996).

Zinc is recognized for its structural role in maintaining the structural configuration of proteins. RING fingers, zinc fingers, and tumor suppressors like p53, are examples of proteins in which zinc plays a structural role. The identification of zinc-binding motifs in DNA-binding proteins has shown that zinc is used more for its structural purposes than for its catalytic roles (Houben *et al.* 2005). Proteins in which zinc plays a structural role may adopt tetrahedral, pentahedral or octahedral zinc coordination schemes (Dudev and Lim. 2003). Tetrahedral coordination is the most stable and seems to be the most favored as zinc is buried away from the solvent thereby neutralizing the positive charges on it. Earlier work by Kamura and co-workers showed that Rbx1 (a subunit of the SCF ubiquitin ligase) requires zinc for proper folding and ligase activity both in vitro and in vivo (Kimura *et al.* 1999). Not all RING domains exhibit intrinsic activity, as seen with BARD1 (Hashizume *et al.* 2001) and MDMX (Linares *et al.* 2003), which require an interaction with another RING domain (BRCA1 and MDM2 respectively), in which the formation of a heterodimer greatly stimulates E3 activity (Deshaies and Jaozeiro. 2009).

1.6.4 The RBBP6 RING finger domain

The RING finger domain of human RBBP6 is able to ubiquitinate YB-1, leading to its degradation in the proteasome (Chibi *et al.* 2008). YB-1 is a member of the cold-shock family of proteins which plays an important role in the maturation of mRNA transcripts.

It also functions as a transcription factor, transducing expression of a range of pro-survival and pro-tumourigenic proteins (Lasham, A., Print, C. G., Woolley, A. G., Dunn, S. E. & Braithwaite, A. W. YB-1: oncoprotein, prognostic marker and therapeutic target? *Biochemical Journal* **449**, 11-23 (2013)). The RING domain of human RBBP6 includes eight cysteine residues that coordinate two Zn^{2+} ions in a 'cross-brace' manner, in which the first and third cysteine pairs (Cys²⁵⁹, Cys²⁶², Cys²⁸¹, Cys²⁸³) coordinate the first Zn^{2+} ion, while the second and fourth pairs (Cys²⁷⁴, Cys²⁷⁵, Cys²⁹⁶, Cys²⁹⁹) coordinate the second Zn^{2+} ion (Kappo *et al.* 2012). It therefore can be classified as a C₄C₄ RING finger (Kappo *et al.* 2012). Kappo and coworkers showed furthermore that the isolated RING homodimerises in solution along the same interface identified in many other RING fingers and U-boxes.



Vo and co-workers identified Mpe1, the *S. cerevisiae* orthologue of human RBBP6, using genetic methods based on its essential role in mRNA processing (Vo *et al.* 2001). They drew attention to the RING domain as a cysteine-rich displaying some of the characteristics of a RING finger (Vo *et al.* 2001). Comparison of the human and yeast RBBP6 protein sequences indicates that the yeast homologue has lost three of the four residues coordinating one of the two zinc ions, suggesting that it may bind only one zinc ion (Fig. 1.9) (Kappo *et al.* 2012).

The *Aspergillus niger* orthologue, when aligned to the *Homo sapiens* RING finger, shows an aspartic acid replacing a cysteine in the 1st zinc ion binding pocket (Fig. 1.9). It may therefore, like its *S. cerevisiae* counterpart, bind one zinc ion or, like its human RING counterpart, bind two.

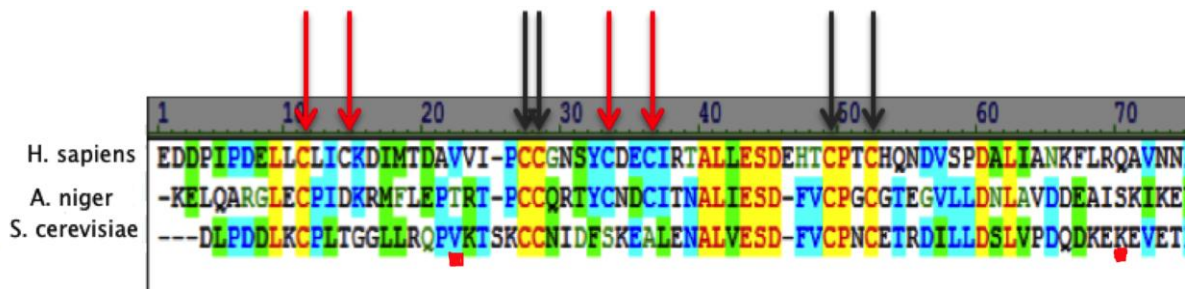


Figure 1.9. Cross-brace configuration for Zn^{2+} binding. Sequence analysis of RING finger domains from RBBP6 homologs reveals that *HsRING* finger binds 2 Zn^{2+} ions, in which the 1st and 3rd pair of cysteine residues (red arrows) bind one Zn^{2+} and the 2nd and 4th pairs (black arrows) the other. The alignment reveals a disruption of the first pair of zinc binding site (red arrows) in the *AnRING* and *ScRING* homologs. The alignment reveals that some of the residues coordinating the first Zn^{2+} ion (red arrows) are missing from *A. niger* and *S. cerevisiae*, raising the possibility that both of these orthologues may bind only one Zn^{2+} .



1.7 Objectives of this MSc project

The aim of this research was to provide structural and functional insights into the function of the RBBP6 protein using mass spectrometry. More specifically, it aims to i) use non-denaturing mass spectrometry to investigate protein-metal ion coordination in RING finger domains from the *S. cerevisiae* and *A. niger* members of the RBBP6 family using non-denaturing ESI-MS and ii) use cross-linking mass spectrometry to investigate previously-reported interactions of RBBP6 with Heat shock protein 70 (Hsp 70) and Mouse Double Minute 2 (MDM2).

To investigate the zinc binding, expression constructs for both proteins first had to be generated, and then the proteins expressed in *E. coli* and purified to homogeneity. Since mass spectrometry under non-denaturing conditions had not previously been carried out successfully in South Africa, the technique first needed to be optimized with the assistance of the operators of instruments at Stellenbosch and Tygerberg.

For the cross-linking analysis, samples of the putative interacting proteins needed to be generated as for aim i). Affinity pull-down and immunoprecipitation assays then needed to be used to confirm the interactions between the domains prior to cross-linking and analysis using tryptic digest-based mass spectrometry.

Chapter 2: Materials and Methods

2.1 General Stock solutions and buffer preparation

Ammonium Persulphate: A 10 % stock solution was prepared in deionised water. The solution was stored at 4 °C.

Ampicillin: A 100 mg/ml stock solution was prepared in deionised water. The solution was filter-sterilized using a 0.22 micron filter and stored at -20 °C.

Chloramphenicol: A 34 mg/ml stock solution was prepared in ethanol. The solution was stored at 4 °C until needed.

Coomassie Staining Solution: 0.25 g Coomassie Blue R-250, 40 % ethanol and 10 % acetic acid in 250 ml deionised water.

Destaining Solution: 15 % (v/v) acetic acid.

Ethidium Bromide: 10 mg/ml stock solution was prepared in water, and stored in the dark at 4 °C.

Protein Extraction Buffer: 50 mM Tris, pH 8, 150 mM NaCl, 100 µg/ml lysozyme, 10 mM β-mercaptoethanol, 0.5% Triton X-100, 20 µg/ml ZnSO₄.

GTE: 50 mM Glucose, 50 mM Tris-HCl and 10 mM EDTA, pH 8.0.

IPTG: A 1 M stock solution was prepared in deionised water. The solution was filter-sterilized, aliquoted and stored at -20 °C.

Luria Agar: 10 g/l Tryptone powder, 5 g/l Yeast extract, 5 g/l NaCl and 14 g/l Bacteriological agar.

Luria Broth: 10 g/l Tryptone powder, 5 g/l Yeast extract, 5 g/l NaCl and 2 g/l Glucose.

Minimal Media: 12.8 g/l $\text{Na}_2\text{HPO}_4 \cdot 7\text{H}_2\text{O}$, 3 g/l KH_2PO_4 , 1 g/l NH_4Cl and 0.5 g/l NaCl .

The pH of this media was adjusted to 7.0 with NaOH and the solution was autoclaved. Immediately prior to use, the solution was supplemented with 2 ml of autoclaved 1 M MgSO_4 , 100 μl of autoclaved 1 M CaCl_2 and 10 ml of filter-sterilized 20 % Glucose. The solution was stored at room temperature. For labeled minimal media 1g/liter ^{15}N - labeled NH_4Cl was added to the media.

NMR Buffer: 100 mM Sodium phosphate buffer pH 6.0, 150 mM NaCl , 5 mM DTT and 0.02 % sodium azide.

Non-denaturing mass spectrometry buffer: 10 mM ammonium acetate, pH 6.0

Phenol/Chloroform: 1 part Tris-saturated phenol and 1 part chloroform. The solutions were mixed together and used fresh.

3C Protease Cleavage Buffer: 50 mM Tris-HCl pH 7.0 containing 150 mM NaCl , 1 mM DTT and 0.01 % Triton X-100. The buffer was prepared fresh immediately prior to use.

Protein Elution Buffer: 20 mM Glutathione and 50 mM Tris-HCl pH 8.0.

Protein Wash Buffer: 50 mM Tris, pH 8.0, 150 mM NaCl and 10 mM β -mercaptoethanol.

2X SDS PAGE Sample Buffer: 4 % SDS, 0.125 M Tris-HCl pH 6.8, 15 % Glycerol and 1 mg/ml Bromophenol Blue. The buffer was stored at room temperature and 100 mM freshly prepared DTT was added immediately prior to use.

10X SDS PAGE Electrophoresis Buffer: 30.2g Tris, 144.1 Glycine and 10 g SDS. The buffer was stored at room temperature and diluted 10-fold when needed.

Separating Buffer: 1.5 M Tris-HCl, adjusted to pH 8.8 with HCl. The buffer was stored at 4 °C.

Stacking Buffer: 0.5 M Tris-HCl, adjusted to pH 6.8 with HCl. The buffer was stored at 4 °C.

5X TBE: 54 g Tris, 27.5 g boric acid, 20 ml 0.5M EDTA, pH 8.0.

Tfb1 Buffer: 30 mM Potassium acetate, 50 mM MnCl₂, 0.1 M KCl, 6.7 mM CaCl₂ and 15 % Glycerol (v/v).

Tbf2 Buffer: 9 mM MOPS, 50 mM CaCl₂, 10 mM KCl and 15 % Glycerol (v/v).

TYM Broth: 20 g/l Tryptone powder, 5 g/l Yeast extract, 3.5 g/l NaCl and 2 g/l MgCl₂.

2.2 Bacteria and yeast strains

Bacteria

1. *E.coli* MC1061 (Casadabhan and Cohen,1980): F-, *araD139*, (*ara leu*) 7697, $\Delta lacx74$, *galU*-, *galK*-, *hs*-, *hsm*+, *strA*
2. *E.coli* BL21 Star™ pLysS (DE3) (Stratagene): F- omp T hsdSB (rB-mB-) gal dcm me131 (DE3)

Yeast:

Matchmaker Y2HGold yeast cells: MATa, *trp1-901*, *leu2-3, 112*, *ura3-52*, *his3-200*, *gal4 Δ* , *gal80 Δ* , LYS2 : : GAL1UAS–Gal1TATA–His3, GAL2UAS–Gal2TATA–Ade2
URA3 : : MEL1UAS–Mel1TATA AUR1-C MEL1 2.1

Yeast cells were a kind gift from Dr. Craig Kinnear, Stellenbosch University, Faculty of Health Sciences, Tygerberg.

2.3 Antibodies used

- Anti-MDM2: mouse monoclonal 4B11, raised against residues 383-491 of human MDM2 (Merck, Darmstadt, Germany)
- Anti-RBBP6-RING: rabbit polyclonal custom raised against residues 249-335 of human RBBP6 (laboratory of Prof Dirk Bellstedt, Department of Biochemistry, University of Stellenbosch).
- Anti-RBBP6-DWNN: mouse monoclonal custom raised against residues 1-81 of human RBBP6, (European Molecular Biology Laboratory, Monterotondo-Scalo, Italy)
- Anti-Hsp70: mouse monoclonal 3A3 (Santa Cruz Biotechnology, Inc., Santa Cruz, CA, USA)

2.4 Preparation of yeast genomic DNA

A single medium-sized *S. cerevisiae* colony was resuspended in 30 µl of 0.2 % SDS in a microfuge tube. The tube was vortexed for 15 seconds and thereafter placed in a 90 °C heating block for 4 minutes. The tube was then centrifuged at 14000 rpm for 1 minute and the supernatant transferred to a new tube. The supernatant, containing the genomic DNA was then used as a template for the subsequent PCR reaction.

2.5 PCR amplification of DNA

PCR amplifications were carried out in reactions containing 1x PCR reaction buffer, 1.5 mM MgCl₂, 10 pmol forward and reverse primers, 0.2 mM dNTPs, and 0.25 U *Taq* polymerase. 1 µl of yeast genomic DNA was used as a template for the PCR reaction. The final volume was made up to 25 µl with sterile autoclaved water. The PCR reaction tubes were briefly centrifuged and the reaction mixture was cycled through the following parameters:

94 °C for 2 minutes (Initial denaturation)

92 °C for 1 min (Denaturation)

60 °C for 1 min (Annealing)

72 °C for 30 seconds (Extension)

72 °C for 5 min (Final extension)

} 30 cycles

The PCR reaction products were then analysed by electrophoresis on 1% agarose gels.

2.6 Double restriction digestion of genomic DNA and pGEX-6P-2vector

Double restriction digests of PCR products and plasmids were carried out as follows:

Table 2.1 Restriction digestion of the RING PCR product and pGEX-6P-2 vector.

Reagent	Species/ vector		
	<i>S. cerevisiae</i>	<i>A. niger</i>	pGEX-6p-2
DNA (1µg)	20µl	15µl	11
10x buffer	10µl	10µl	10µl
BamHI	1µl	1µl	1µl
XhoI	1µl	1µl	1µl
dH2O	68µl	73µl	77µl

The reagents were mixed in a 1.5 ml microfuge tube and incubated at 37 °C for 1.5 hours.

The samples were analyzed by electrophoresis on a 1% agarose gel.

2.7 Agarose gel electrophoresis of DNA

DNA was analyzed by electrophoresis on 1% agarose gels. Gels were prepared by adding the required volume of 1 X TBE to the appropriate mass of electrophoresis grade agarose.

The agarose was boiled and cooled to 55° C followed by the addition of GR Green to a final concentration of 0.5 µg/ml and poured onto a gel-casting tray. 0.5 µl of 6x loading

buffer was mixed with 5-20 μl of the DNA and loaded onto the gel. The marker was loaded in the first lane to show the sizes of the bands. The DNA was visualized by placing the gel under UV light.

2.8 Cohesive end ligation

Ligation reactions were set up as shown in Table 2.2. The ligation reactions were incubated overnight at 4 °C. 10 μl of the ligation was used to transform *E. coli* MC1061 competent cells. Transformed cells were plated on LB agar plates containing 100 $\mu\text{g/ml}$ ampicillin and grown overnight at 37 °C.

Several isolated colonies were picked and screened for inserts by double restriction digests as described in Section 2.6. The remaining cell suspension from positive clones were used to inoculate 10 ml of LB broth containing 100 $\mu\text{g/ml}$ ampicillin and grown overnight at 37 °C. The cells were harvested and plasmid DNA isolated using a Genejet™ plasmid isolation kit (Fermentas). Constructs were then validated using colony PCR, as well as double restriction digest.

Table 2.2 Ligation reactions for cloning DNA fragments into pGEX-6P-2expression vector

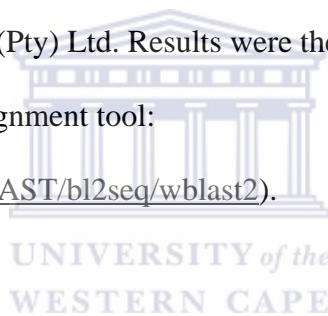
Reagent	Species			
	<i>S. cerevisiae</i>		<i>A. niger</i>	
	Control	Experimental	Control	Experimental
Vector (pGEX-6P-2)	4.5 μl	4.5 μl	5 μl	5 μl
PCR products	0 μl	2 μl	0 μl	2.6 μl
10 X ligation buffer	2 μl	2 μl	2 μl	2 μl
T4 DNA Ligase	1 μl	1 μl	1 μl	1 μl
dH ₂ O	13.5 μl	11.5 μl	12 μl	9.4 μl
Total volume	20 μl	20 μl	20 μl	20 μl

2.9 Colony PCR assay

Colony PCR was used to screen transformed colonies for the presence of the *S. cerevisiae* RING insert. Following transformation, single colonies were picked and resuspended in 20 µl of distilled water. 1 µl of each suspension was added to the PCR reaction and the reaction carried out as described in Section 2.5. Cycling parameters were similar to the PCR reaction carried out earlier with the exception of the denaturation temperature changing to 94 °C, the annealing temperature to 58 °C, and the extension time to 45 seconds.

The sequence identity of positive clones was confirmed by DNA sequencing, carried out at Inqaba Biotechnical Industries (Pty) Ltd. Results were then compared to the expected sequences using the BLAST 2 alignment tool:

(<http://www.ncbi.nlm.nih.gov/BLAST/bl2seq/wblast2>).



2.10 Transformation of plasmid DNA into competent cells

Frozen *E. coli* MC1061 and BL21 (DE3) pLysS competent cells were thawed on ice. 10 µl of the ligation mixture was added to 100 µl of competent cells. The tube was then gently finger-tapped and left on ice for 30 minutes. Cells were heat shocked at 37 °C for 5 minutes and then placed back on ice for 5 minutes. 900 µl of Luria-Bertani broth (no antibiotics) was then added to the tube, which was thereafter incubated for 1 hour at 37 °C. 100 µl of the transformation culture was then spread on a Luria-Bertani agar plate containing 100 µg/ml ampicillin and incubated overnight at 37°C.

2.11 Large-scale expression of recombinant protein

Single colonies of *E. coli* BL21 (DE) pLysS cells transformed with expression plasmids were inoculated into 6 ml LB containing 100 µg/ml ampicillin and 34 µg/ml chloramphenicol and incubated at 37 °C with shaking. After 4 hours, the culture was used to inoculate 200 ml of enriched media (LB) containing 100 µg/ml ampicillin and 34 µg/ml chloramphenicol, and grown overnight at 37 °C. Three hours later the cultures were scaled-up to 2000 ml by addition of media containing the same concentration of ampicillin and incubated at 37 °C with shaking until the OD₅₅₀ reached 0.4 - 0.6.

One hour prior to induction, 100 µM ZnSO₄ was added for proper folding of the protein. Induction was carried out at 25 °C for 16 hours by addition of IPTG to a final concentration of 1 mM for the *S. cerevisiae* RING finger, and 0.5 mM for the *A. niger* and *H. sapiens* RING fingers respectively. Following induction the bacterial cells were harvested by centrifugation at 6000 rpm for 10 minutes at 4 °C. The pellets were resuspended in 25 ml extraction buffer containing protease inhibitor cocktail tablets (Roche Applied Science, Penzberg, Germany) and stored at -20 °C until needed.

Cell lysis was achieved by sonication, which comprised of 5 cycles: 30 seconds pulse, 30 seconds on ice. This was followed by centrifugation at 4 °C at 4300 g, after which the supernatant was held at 4 °C until further purification was performed.

2.12 Glutathione affinity purification of GST-fusion proteins

Glutathione agarose beads (SIGMA, Missouri, USA) were swollen overnight at 4 °C in distilled water according to the manufacturer's instructions.

The beads were thereafter transferred to a 50 ml chromatography column (Bio-rad, Hercules, California) column and washed thoroughly with PBS buffer containing DTT to remove traces of lactose present in the lyophilized beads. For long-term storage the beads were stored in 1 M NaCl at 4 °C. Prior to purification of the GST fusion protein, the column was equilibrated with 2 column volumes of wash buffer (1x PBS with 1 mM DTT). The bacterial lysate was applied to the column and the flow-through collected. The column was washed twice with 10 ml wash buffer and the flow-through collected. The retained fusion protein was eluted with 50 ml elution buffer (20 mM Glutathione in 1x PBS with 1 mM DTT). The beads were thereafter stored in 10 ml 2 M NaCl.

2.13 Cleavage of the GST-fusion proteins using 3C protease

3C protease from human rhinovirus (HRV 3C) was recombinantly expressed as a GST-fusion protein and stored at -20 °C. The purified GST-RING fusion proteins were transferred to a SnakeSkin® Pleated Dialysis Tubing (MWCO 3500Da) (Thermo Scientific, Waltham, Massachusetts, USA) and 100 µl of 3C protease added. The dialysis bag was then placed in 5000 ml cleavage buffer and incubated overnight at 4 °C with stirring.

Following cleavage, the target protein was separated from GST in a second round of glutathione affinity purification, with the target protein remaining in the flow through and GST and 3C protease being retained on the column.

2.14 Size exclusion chromatography

RING finger domains were purified to homogeneity using size exclusion chromatography, achieved using an ÄKTA FPLC chromatography system (GE

Healthcare, Little Chalfont, UK). A 120 ml Superdex 75 16/600 column (Amersham Biosciences, Pittsburgh, USA) was equilibrated with 1 column volume of 1x PBS with 1 mM DTT before concentrated protein samples were loaded onto the column. Eluted proteins were collected in 2 ml fractions.

For cross-linking experiments, interacting proteins were allowed to incubate for at least 2 hours in an equi-molar ratio before being subjected to size exclusion chromatography in order to generate a complex between the two interacting proteins.

2.15 SDS-PAGE gel electrophoresis

Proteins were analyzed by electrophoresis on 16% polyacrylamide gels using Laemmli's method (Laemmli, 1970). The separating gel was prepared from 4 ml 40% acrylamide: bis-acrylamide stock, 2.63 ml separating buffer, 40 μ l 10 % ammonium persulphate, 105 μ l 10% SDS, 7.5 μ l TEMED and the volume was made up to 10 ml using distilled water. The stacking gel was prepared from 0.5 ml 40% 37:5:1 polyacrylamide, 25 μ l 10% APS, 50 μ l 10% SDS, 1.25 ml stacking buffer, 5 μ l TEMED and the volume was made up to 5 ml using distilled water.

Samples were mixed with equal volumes of 2x SDS sample buffer, incubated in a heating block at 95 °C for 10 minutes and centrifuged for 2-3 minutes at 13300 rpm. The samples were then separated by electrophoresis at using a BioRad Mini-Protean system.

Once the dye front had reached the end of the gel, the gel was removed from the caster and incubated in Coomassie staining solution for 15 minutes. Thereafter it was transferred into destaining solution and left to destain until the background was clear.

2.16 ESI-MS of RING finger domain proteins

Pooled fractions of the 3 pure RING finger domain proteins were concentrated and buffer exchanged into 10 mM ammonium acetate using concentrators (Millipore, 3000 MWCO). Protein samples were then subjected to ESI-MS using a Waters API Q-TOF Ultima instrument (Stellenbosch University). Using the column attached to the MS the samples were introduced to the MS using 1% formic acid to obtain a denatured spectrum, after which samples, using 10 mM ammonium acetate were subjected to the MS. MS data were acquired in positive scan mode.

2.17 Affinity pull-down assays

GST and His pull-down assays were performed by expressing the GST/6His -tagged bait proteins in *E. coli*. *E. coli* cell lysates containing GST/His-tagged bait proteins were clarified by centrifugation and the total cellular protein concentration estimated by measuring the absorbance at 280 nm. Untagged purified prey proteins were prepared as described above. Aliquots of tagged bait proteins or GST only were mixed with the prey protein, 20 µl of a 20% glutathione agarose slurry and 500 µl Binding Buffer (50mM Tris, pH 8.0, 5% BSA, 20 µM ZnCl₂, 200 mM NaCl, 20 mM β-mercaptoethanol, 0.5% Triton X-100) and were incubated for 1 hour at room temperature. Additional reactions were included from which the *E. coli* lysate was omitted completely to serve as negative controls. The beads were pelleted by centrifugation and washed 3 times with 500 µl of Binding Buffer, followed by 2 washes with 0.5 M NaCl.

Finally the beads were resuspended in 30 µl of SDS sample buffer, boiled for 5 minutes at 95 °C and loaded onto an SDS-PAGE gel. Prey proteins were immunodetected with the

appropriate antibodies. For immunoprecipitation antibodies were coupled to Affi-gel matrix (Biorad, Hercules, California)

2.18 Chemical cross-linking

Cross-linking involves the conversion of non-covalent interactions between proteins into covalent ones (Rappsilber. 2011). Interacting proteins under scrutiny retain these covalent bonds, even when subjected to denaturing conditions like SDS-PAGE. Purified recombinant proteins were cross-linked using Sulfo-MBS or BS³ (SIGMA, Missouri, USA), after which they were analyzed using SDS-PAGE. Bands of interest were excised, and subjected to MALDI-TOF MS to identify and localize regions of interaction.

2.19 Immuno-detection of Proteins

Protein samples were subjected to SDS-PAGE as described in Section 2.11.5. Thereafter proteins were transferred to nitrocellulose or PVDF membranes using 25 mM Tris, 0.2 M glycine and 20% methanol as transfer buffer. Following the transfer, the membranes were blocked with 5% milk in TBS-T (Tris buffered saline containing 0.1% Tween 20) and then incubated with the appropriate primary and secondary antibodies for 1 hour each. Following three 5-minute washes with TBS-T, the membranes were incubated with SuperSignalR West Pico chemiluminescent substrate solution (Pierce Biotechnology, Rockford, Illinois, USA), exposed to film and developed.

2.20 Mass spectrometry

Gel pieces were cut into smaller cubes and washed twice with water followed by 50% (v/v) acetonitrile for 10 min. The acetonitrile was replaced with 50 mM ammonium bicarbonate and incubated for 10 min, and repeated two more times. All the gel pieces

were then incubated in 100% acetonitrile until they turned white, after which the gel pieces were dried *in vacuo*. Proteins were reduced with 10 mM DTT for 1 h at 57 °C. This was followed by brief washing steps of ammonium bicarbonate followed by 50% acetonitrile before proteins were alkylated with 55 mM iodoacetamide for 1 h in the dark. Following alkylation the gel pieces were washed with ammonium bicarbonate for 10 min followed by 50% acetonitrile for 20 min, before being dried *in vacuo*. The gel pieces were digested with 20 µl of a 10 ng/µl trypsin solution at 37°C overnight. The resulting peptides were extracted twice with 70% acetonitrile in 0.1% formic acid for 30 min, and then dried and stored at -20 °C. Dried peptides were dissolved in 5% acetonitrile in 0.1% formic acid and 10 µl injections were made for nano-LC chromatography.

All experiments were performed on a Thermo Scientific EASY-nLC II connected to a LTQ Orbitrap Velos mass spectrometer (Thermo Scientific, Waltham, Massachusetts, USA) equipped with a nano-electrospray source. For liquid chromatography, separation was performed on a EASY - Column (2 cm, ID 100µm, 5 µm, C18) pre-column followed by a EASY - Column (10 cm, ID 75 µm, 3 µm, C18) column with a flow rate of 300 nl/min.

The gradient used was from 5-40 % B in 20 min, 40-80% B in 5 min and kept at 80% B for 10 min. Solvent A was 100% water in 0.1 % formic acid, and solvent B was 100 % acetonitrile in 0.1% formic acid.

The mass spectrometer was operated in data-dependent mode to automatically switch between Orbitrap-MS and LTQ-MS/MS acquisition. Data were acquired using the Xcaliber software package. The precursor ion scan MS spectra (m/z 400 – 2000) were

acquired in the Orbitrap with resolution $R = 60000$ with the number of accumulated ions being 1×10^6 . The 20 most intense ions were isolated and fragmented in linear ion trap (number of accumulated ions 1.5×10^4) using collision induced dissociation. The lock mass option (polydimethylcyclsiloxane; m/z 445.120025) enabled accurate mass measurement in both the MS and MS/MS modes. In data-dependent LC-MS/MS experiments, dynamic exclusion was used with 60 s exclusion duration. Mass spectrometry conditions were 1.5 kV, capillary temperature of 200 °C, with no sheath and auxiliary gas flow. The ion selection threshold was 500 counts for MS/MS and an activation Q-value of 0.25 and activation time of 10 ms were also applied for MS/MS.

Thermo Proteome Discoverer 1.3 (Thermo Scientific, Waltham, Massachusetts, USA) were used to identify proteins via automated database searching (Mascot, Matrix Science, London, UK) of all tandem mass spectra against the in-house database provided by the host. Carbamidomethyl cysteine was set as fixed modification, and oxidized methionine, N-acetylation and deamidation (NQ) was used as variable modifications. The precursor mass tolerance was set to 10 ppm, and fragment mass tolerance set to 0.8 Da. Two missed tryptic cleavages were allowed.

Proteins were considered positively identified when they were identified with at least 2 tryptic peptides per proteins, a Mascot or Sequest score of more than $p < 0.05$ as determined by Proteome Discoverer 1.3. Percolator was also used for validation of search results. In Percolator a decoy database was searched with a FDR (strict) of 0.02 and FDR (relaxed) of 0.05 with validation based on the q-value.

Chapter 3: Results - Protein-metal ion interactions

3.1 Introduction

The RING finger domain from human Retinoblastoma Binding Protein-6 (RBBP6) binds two Zn^{2+} ions in two zinc binding pockets (Kappo *et al.* 2012). Analysis of the sequences of orthologues from other eukaryotes reveal a number of cases in which zinc coordinating residues were missing, suggesting the possibility that these proteins might only bind one Zn^{2+} . In *Aspergillus niger*, for example, one of the cysteine (C) residues making up zinc binding site 1 has been replaced by aspartic acid (D). In *Saccharomyces cerevisiae* three of the four zinc coordinating residues have been lost. In order to determine how many zinc ions were coordinated by the RING finger domains from *A. niger* and *S. cerevisiae*, these domains were cloned and expressed in *E. coli* and non-denaturing mass spectrometry used to determine the effective molecular weights of the proteins in solution. As a control the human orthologue was subjected to the same analysis, since it had previously been shown, using NMR, to bind two Zn^{2+} ions.

3.2 Generation of GST-RING finger domain expression constructs

Analysis of the genomic sequence of the *S. cerevisiae* orthologue of RBBP6 (NM_001179625) showed that it contained no introns. We therefore decided to amplify it directly out of genomic DNA using a 'colony PCR'-type approach. Yeast cells were a kind from Dr. Craig Kinnear, Stellenbosch University, Health Sciences, Tygerberg. Primers were designed incorporating a BamHI into the forward primer and an XhoI site into the reverse primer (Fig. 3.1), for cloning into the BamHI and XhoI sites of the pGEX-6P-2 expression vector respectively. Two stop codons, TAA and TGA, were included in the reverse primer (Fig 3.1). The ScRING was successfully amplified from yeast

	Primer	Sequence
a.	Forward	5' GAG GCG GGA TCC GAT CTT CCT GAC CAT TTA AAA -3'
	Reverse	5' GAG GCG CTC GAG TCA TTA GCT TCC GTG TAG TTC CTC TTG -3'
b.		<p>GGATCC</p> <p>AAAGAACTGCAGGCGCGTGGCCTGGAATGCCGATTGATAAACGCATGTTTCTGGAACCGACCCGTACGCCGTGC TGTC AACGCACCTATTGCAACGATTGTATTACGAATGCACTGATCGAAAGTGACTTCGTCTGCCCGGGCTGTGGT ACCGAAGGTGTGCTGCTGGATAACCTGGCAGTTGATGACGAAGCTATTAGCAAAATCAAAGAATACGAAGCGGAA AAAGCCGACTCT</p> <p>TAAGTCGAG</p>
c.	Optimized	7 AAAGAACTG CAGGCGCGTGGCCTGGAATGCCGATTGATAAACGCATGTTTCTGGAACCG
	Original	7 AAAGAACTGCAAGCACGTGGTTTAGAGTGTCCGATTGACAAGCGAATGTTTTAGAGCCC
	Optimized	67 ACCCGTACGCCGTGCTGTCAACGCACCTAT TGCAACGATTGTATT ACGAATGCACTGATC
	Original	67 ACGAGAACTCCATGCTGTCAAAGAACATACTGCAATGATTGTATTACCAATGCATTGATC
	Optimized	127 GAAAGTGACTTCGTCTGCCCGGGCTGTGGTACCGAAGGTGTGCTGCTGGATAACCTGGCA
	Original	127 GAGAGCGATTTTGTATGCCCTGGCTGTGGAACGGAGGGAGTGTTACTCGATAACCTTGCC
	Optimized	187 GTTGATGAC GAA GCTATTAGC AAAATCAAAGAATACGAA GCGGAA AAAGCCGACTCT
	Original	187 GTTGATGACGAGGCTATTAGCAAGATTAAGAGTACGAAGCTGAAAAGGCTGATTTCG

Figure 3.1 (a) Primers designed for the amplification of *S. cerevisiae* included BamHI and XhoI restriction sites (bold) in the forward and reverse primers respectively, as well as two stop codons (underlined) immediately upstream of the XhoI site. (b) The *A. niger* sequence synthesized by Genscript Inc. was flanked by BamHI and XhoI sites. A single stop codon was added immediately upstream of the XhoI site. (c) The *A. niger* sequence was optimized by Genscript Inc. to increase the efficiency of expression in *E. coli*. Primers were synthesized by the DNA synthesis facility at the University of Cape Town.

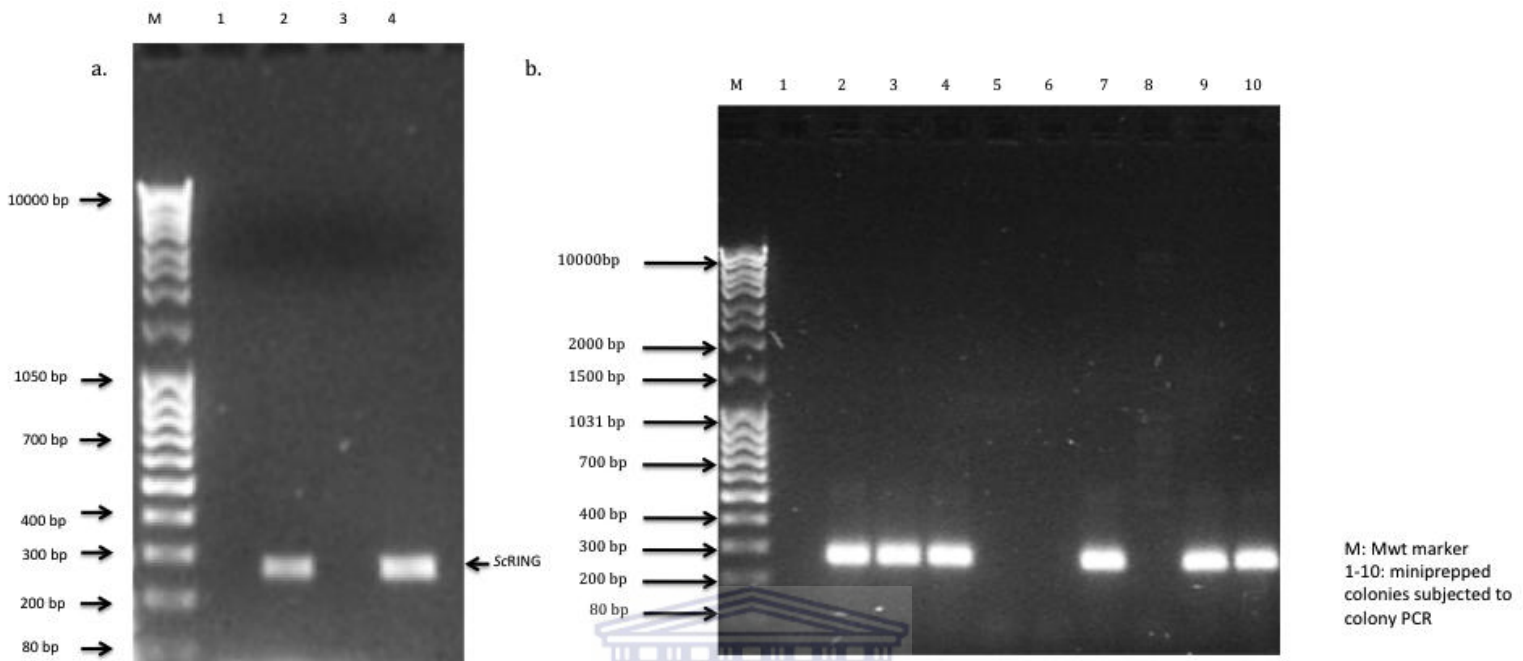
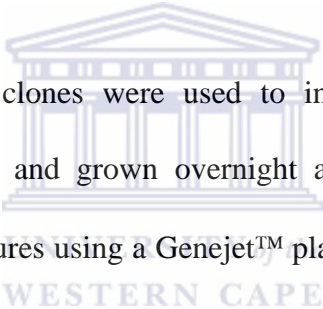


Figure 3.2 Amplification and cloning of the RING finger domain from *S. cerevisiae*. a) ScRING amplified directly from genomic DNA yielded the expected product of 267 bp (lanes 2 and 4). Lanes 1 and 3 contained no template DNA. b) Following colony PCR the 267bp fragment corresponding to the ScRING validated the successful cloning of the gene into the pGEX-6P-2 expression vector. Lanes 2, 3, 4, 7, 9, 10 correspond to positive clones. Lane 1 is the negative control for the PCR reaction as it contains no template DNA.

cells (Fig. 3.2.a) and cloned into the pGEX-6P-2 expression vector (Fig. 3.2.b), as confirmed by the amplified bands in Fig. 3.2 (b) , lanes 2-4, 7, 9 and 10. The AnRING finger (XP_001392158.1) was synthesized by Genscript Inc. (Piscataway, NJ, USA.) and received in a pUC57 vector. The sequence was codon optimized for expression of the protein in *E. coli* and incorporated a BamHI site at the N-terminus and an XhoI site at the C-terminus (Fig. 3.1 (b) and (c)). A single stop codon was incorporated immediately following the end of the gene. The pUC57 vector was digested with restriction enzymes BamHI and XhoI, releasing an insert of 252 bp as expected (Fig.3.3.a). The insert was successfully cloned into *E. coli* MC1061 competent cells, as confirmed by the presence of a fragment of the correct size in lane 5 of Fig. 3.3.b).



Cell suspensions from positive clones were used to inoculate 10 ml of LB broth containing 100 µg/ml ampicillin and grown overnight at 37 °C. Plasmid DNA was isolated from these overnight cultures using a Genejet™ plasmid isolation kit (Fermentas, Vilnius, Lithuania).

Following the isolation of plasmid DNA from positive clones, 10 µl of one of the positive clones were sent for sequencing at Inqaba Biotechnical Industries (Pty) Ltd. Sequences were analyzed as described in Sec. 2.5. Fig. 3.4 shows the sequences of the clones were in 100 % agreement with the expected sequences. Cloned fragments were transformed into the *E. coli* BL21 (DE) pLysS expression strain of competent cells, and single colonies used to grow up proteins.

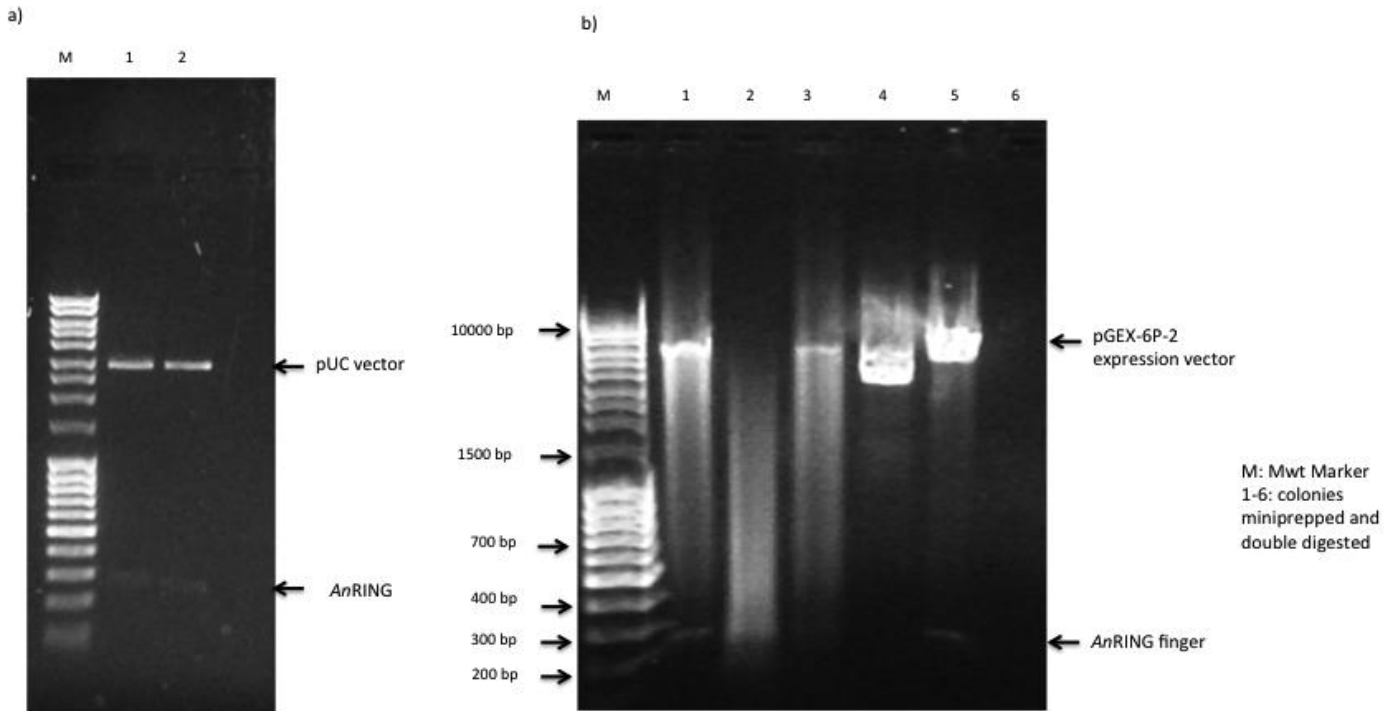


Figure 3.3 Sub-cloning of the RING finger domain from *A. niger* into pGEX-6P-2. a) A 252 bp fragment corresponding to the gene of interest was released when the pUC57-*AnRING* was digested with BamHI and XhoI. (b) The *A. niger* RING was successfully sub-cloned into pGEX-6P-2, as confirmed by the presence of a 252 bp fragment, following digestion of plasmid DNA extracted from positive clones. Lanes 1, 3 and 5 represent positive clones.

a.

Score = 496 bits (268), Expect = 6e-144
 Identities = 268/268 (100%), Gaps = 0/268 (0%)
 Strand=Plus/Plus

Query	1	CCCTGGGATCCGATCTTCCTGACGATTTAAAATGTCCCTTGACAGGTGGTCTTTTGAGGC	60
Sbjct	940	CCCTGGGATCCGATCTTCCTGACGATTTAAAATGTCCCTTGACAGGTGGTCTTTTGAGGC	999
Query	61	AGCCGGTAAAGACAAGCAAGTGCTGTAACATAGATTTCTCAAAGAGGCGCTGGAAAATG	120
Sbjct	1000	AGCCGGTAAAGACAAGCAAGTGCTGTAACATAGATTTCTCAAAGAGGCGCTGGAAAATG	1059
Query	121	CACTGGTAGAGAGCGACTTTGTATGCCCAATTGCGAAACCCGCGATATCCTTCTCGATT	180
Sbjct	1060	CACTGGTAGAGAGCGACTTTGTATGCCCAATTGCGAAACCCGCGATATCCTTCTCGATT	1119
Query	181	CTTTAGTACCCGACCAGGACAAGGAAAAGGAGGTCGAAACGTTTTTGAAGAAACAAGAGG	240
Sbjct	1120	CTTTAGTACCCGACCAGGACAAGGAAAAGGAGGTCGAAACGTTTTTGAAGAAACAAGAGG	1179
Query	241	AACTACACGGAAGCTAATGACTCGAGCG	268
Sbjct	1180	AACTACACGGAAGCTAATGACTCGAGCG	1207

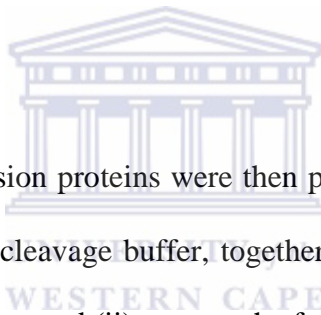
b.

Score	Expect	Identities	Gaps	Strand
484 bits(262)	7e-142	262/262(100%)	0/262(0%)	Plus/Plus
Query	1	CCCTGGGATCCAAAGAAGTGCAGGCGCGTGGCCTGGAATGCCCGATTGATAAACGCATGT	60	
Sbjct	1	CCCTGGGATCCAAAGAAGTGCAGGCGCGTGGCCTGGAATGCCCGATTGATAAACGCATGT	60	
Query	61	TTCTGGAACCGACCCGTACGCCGTGCTGTCAACGCACCTATTGCAACGATTGTATTACGA	120	
Sbjct	61	TTCTGGAACCGACCCGTACGCCGTGCTGTCAACGCACCTATTGCAACGATTGTATTACGA	120	
Query	121	ATGCACTGATCGAAAAGTACTTCGTCCTGCCGGGCTGTGGTACCGAAGGTGTGCTGCTGG	180	
Sbjct	121	ATGCACTGATCGAAAAGTACTTCGTCCTGCCGGGCTGTGGTACCGAAGGTGTGCTGCTGG	180	
Query	181	ATAACCTGGCAGTTGATGACGAAGCTATTAGCAAAATCAAAGAATACGAAGCGGAAAAAG	240	
Sbjct	181	ATAACCTGGCAGTTGATGACGAAGCTATTAGCAAAATCAAAGAATACGAAGCGGAAAAAG	240	
Query	241	CCGACTCTTAACTCGAGCGGCC	262	
Sbjct	241	CCGACTCTTAACTCGAGCGGCC	262	

Figure 3.4 Experimentally determined sequences (Sbjct) were in 100 % agreement with expected sequences (Query) for *Sc*RING (a) and *An*RING (b). Flanking sequences for restriction enzymes BamHI (GGATCC) and XhoI (CTCGAG) are indicated in yellow.

3.3 Expression and purification of RING finger proteins

Expressed, soluble proteins were then separated from insoluble proteins and cell debris by centrifugation at 16000 rpm for one hour. The pGEX-6P-2 expression vector used allowed for the expression of the proteins of interest as fusions with GST, allowing the purification of the proteins on a glutathione agarose column. Cell lysates, containing GST-fusion proteins, were passed through a prepared glutathione agarose column and GST-fusion proteins were retained on the column, and separated from unwanted *E. coli* proteins. Fusion proteins were eluted from the column following the addition of 20 mM reduced glutathione. Fig. 3.5 shows that the RING finger fusion proteins were all expressed at high levels and successfully purified using GST glutathione affinity chromatography.



Fractions corresponding to the fusion proteins were then pooled together and placed in a SnakeSkin dialysis membrane in cleavage buffer, together with human rhinovirus 3C in order to (i) to cleave off the GST tag and (ii) remove the free glutathione from the sample. In a second round of GST affinity chromatography the cleaved sample was then re-loaded onto the glutathione-agarose column and cleaved GST and uncleaved fusion protein were retained on the column while the target protein remained in the flow-through (Fig. 3.6).

Fractions containing RING proteins were loaded onto a size exclusion column to remove remaining GST and 3C protease (Fig.3.7). Finally RING domains were exchanged either into non-denaturing mass spectrometry buffer or NMR buffer.

1D proton NMR spectra were acquired at 600 MHz to assess the state of foldedness of both samples. The high level of chemical shift dispersion of the spectra shown in Figs. 3.8

and 3.10 shows that the RING fingers from *S. cerevisiae* and *A. niger* were folded prior to MS. ^{15}N -enriched samples of the *S. cerevisiae* domain were expressed in minimal media supplemented with ^{15}N -ammonium chloride (Cambridge Isotope Laboratories, Andover MA, USA) and used to record 2D ^{15}N -HSQC spectra. The spectra in Fig 3.9 are very well dispersed in both ^1H and ^{15}N dimensions and there is very little overlap, suggesting that this protein would be suitable for detailed structural analysis using triple-resonance NMR. Fig. 3.9 shows a superposition of spectra corresponding to the protein at 1x (black) and 10x (red) dilution respectively; the lack of significant changes suggests that the protein is likely to be monomeric in solution. This can be contrasted with the human RING finger domain, which showed robust concentration-dependent chemical shift changes consisted with it forming a homodimer in solution.



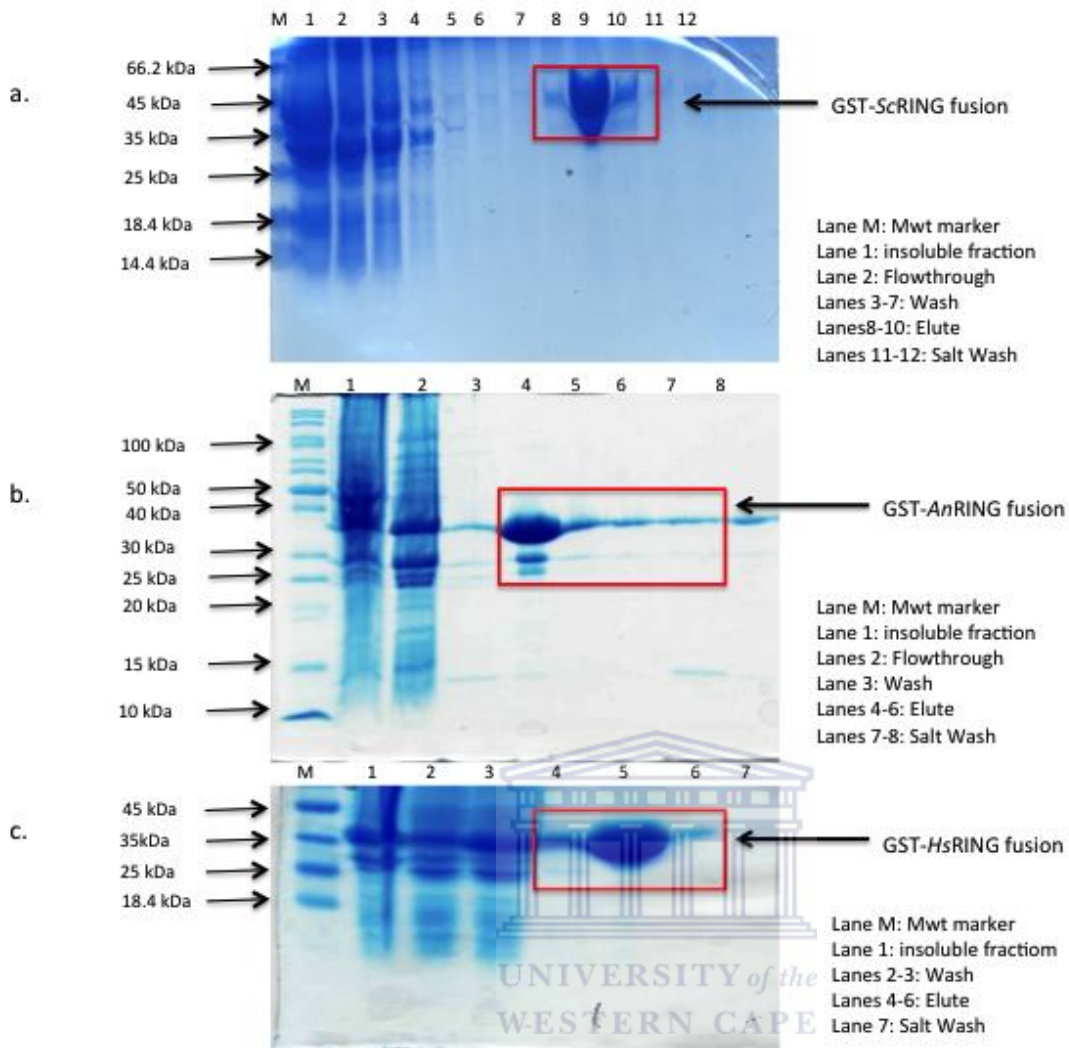


Figure 3.5 Pure samples of GST-RING finger proteins from *S. cerevisiae* (a), *A. niger* (b) and *H. sapiens* (c) were eluted from the glutathione matrix following addition of 20 mM free glutathione. All three domains exhibit an apparent molecular weight of approximately 35 kDa, as expected, corresponding to 26 kDa (GST) plus 9 kDa (RING).

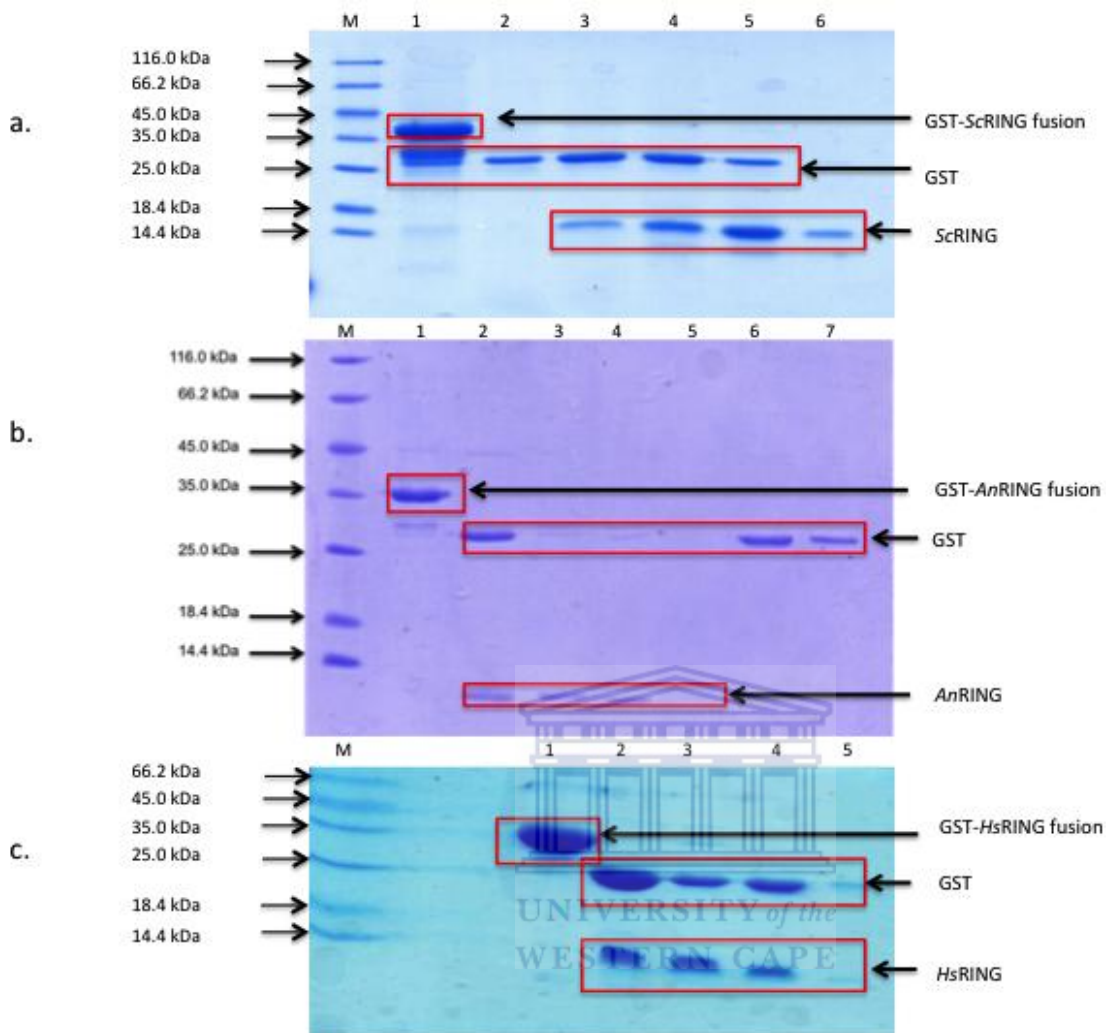


Figure 3.6 Successful cleavage with 3C protease and separation using glutathione affinity chromatography of GST-RING proteins from *S. cerevisiae* (a), *A. niger* (b) and *H. sapiens* (c). In each case the un-cleaved fusion can be seen in lane 1 and the cleaved sample in lane 2. Lane 3 and upward show varying degrees of successful separation of GST from the RING finger using a second round of glutathione affinity chromatography.

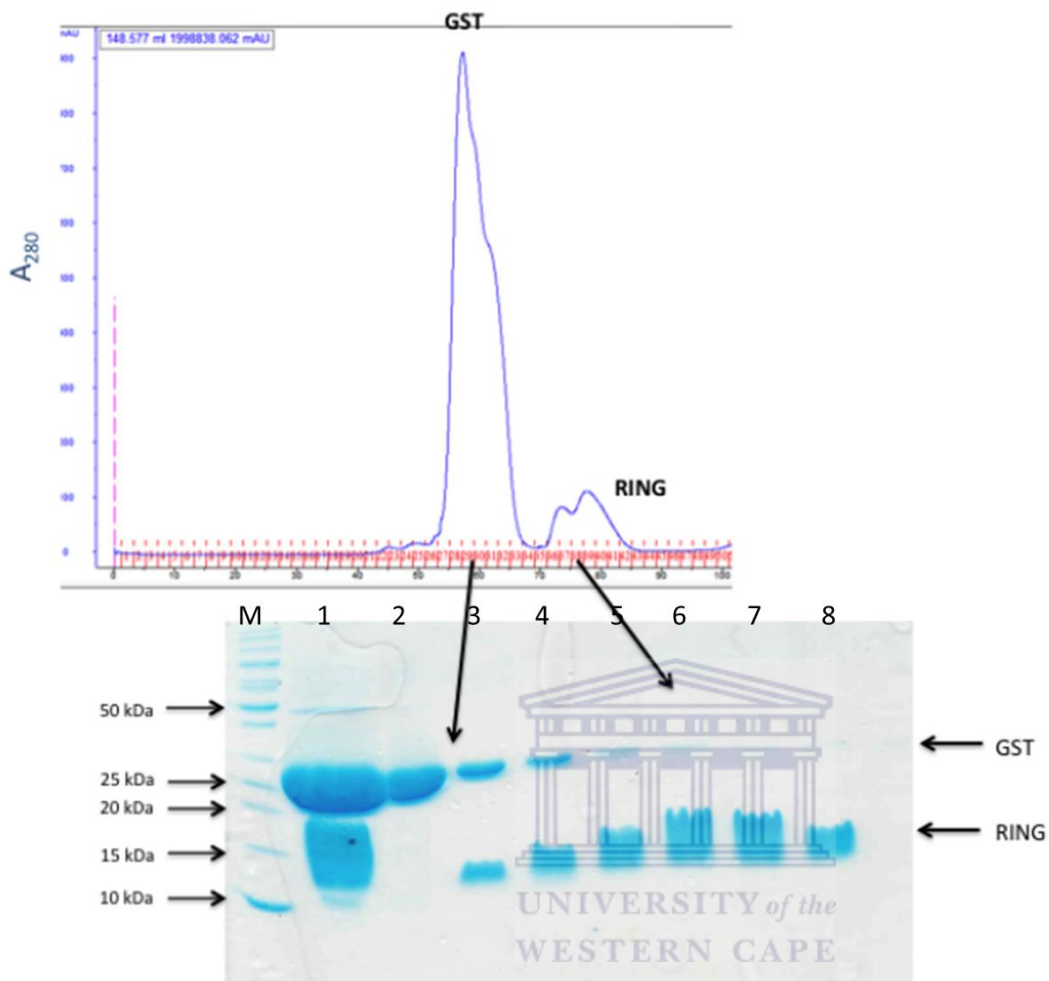


Figure 3.7 Size exclusion chromatogram and associated SDS-PAGE showing successful purification of the *HsRING* finger domain. With the exception of a small amount of overlap in lanes 3 and 4, the procedure successfully separated the cleaved GST from the target protein.

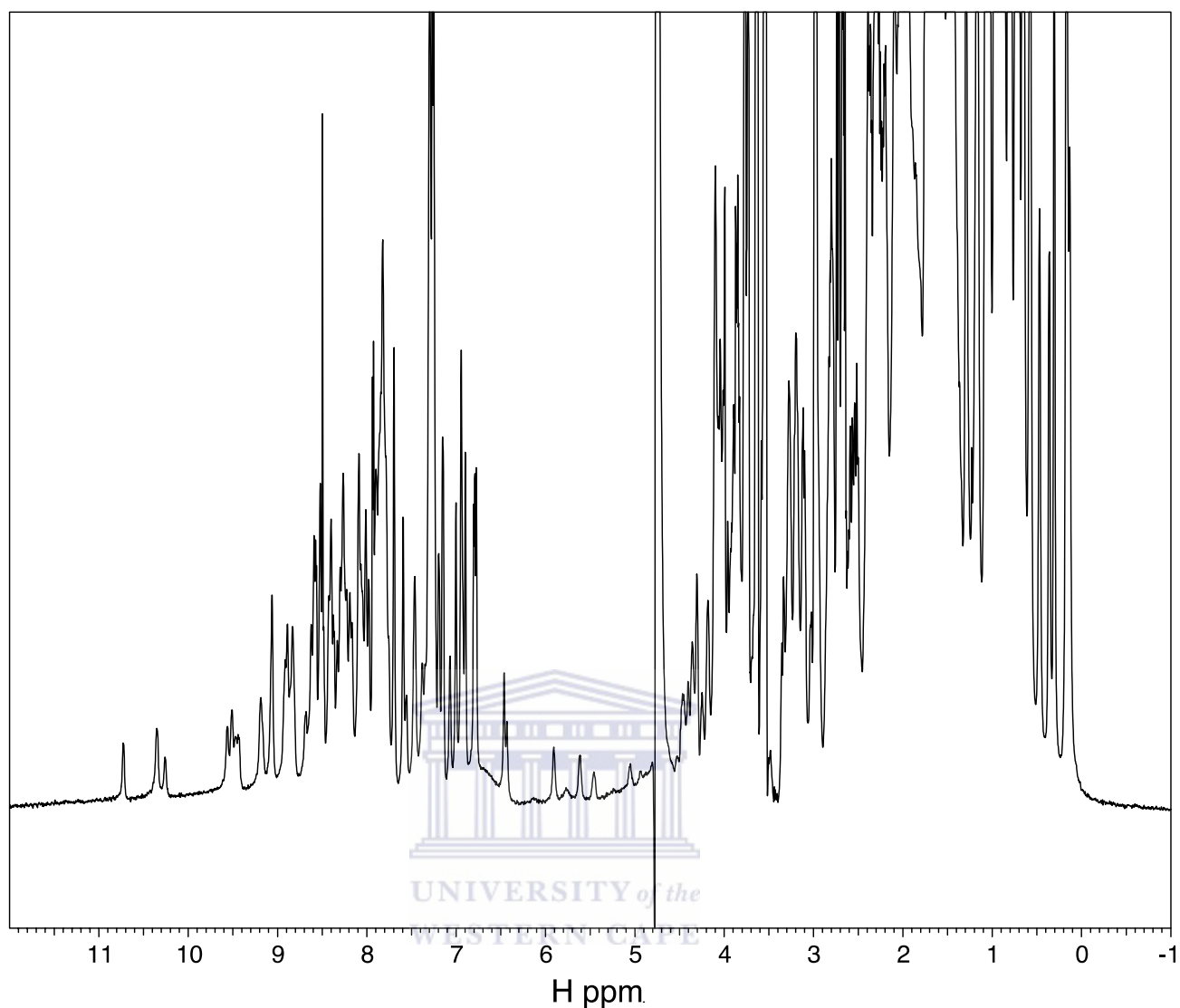


Figure 3.8 1D ^1H spectrum of *S. cerevisiae* RING finger domain at pH 6.0, 25 °C recorded at 600 MHz. The large chemical shift dispersion of resonances and sharp peaks exhibited by the protein is indicative of its foldedness. This is confirmed by the appearance of resonances corresponding to amide protons (H^{N}) in the region 9-11 ppm, α -protons (H^{α}) in the region 5-6 ppm, and methyl groups in the region 0-0.5 ppm. The sharpness of the peaks also indicate that the protein is monomeric.

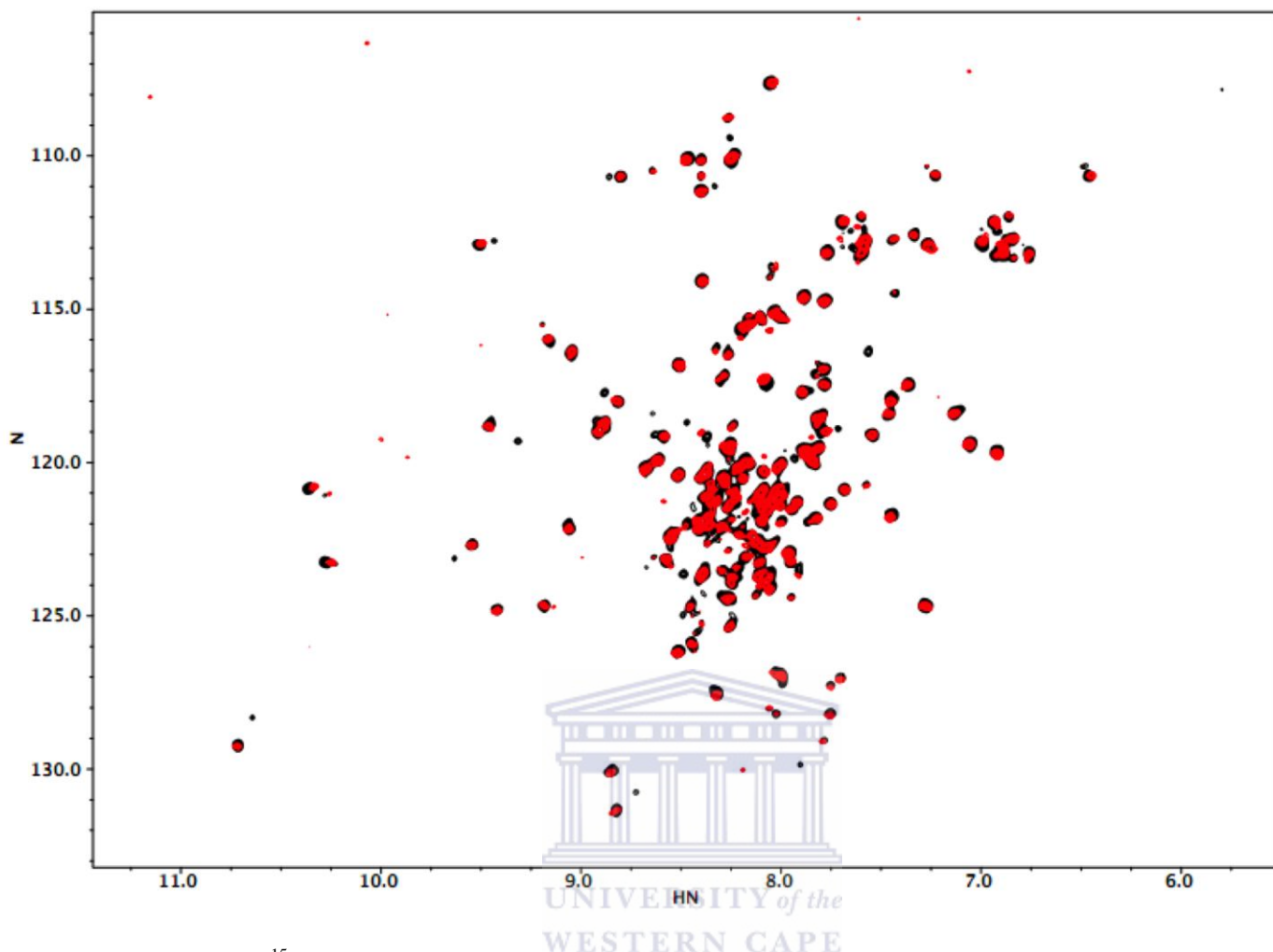


Figure 3.9 ^{15}N -HSQC spectrum of a 10x diluted ScRING (red) superimposed over the concentrated sample (black). Spectra were recorded at pH 6.0, 25°C at 600MHz. The absence of concentration-dependent chemical shift perturbations suggests that the domain is monomeric in solution.

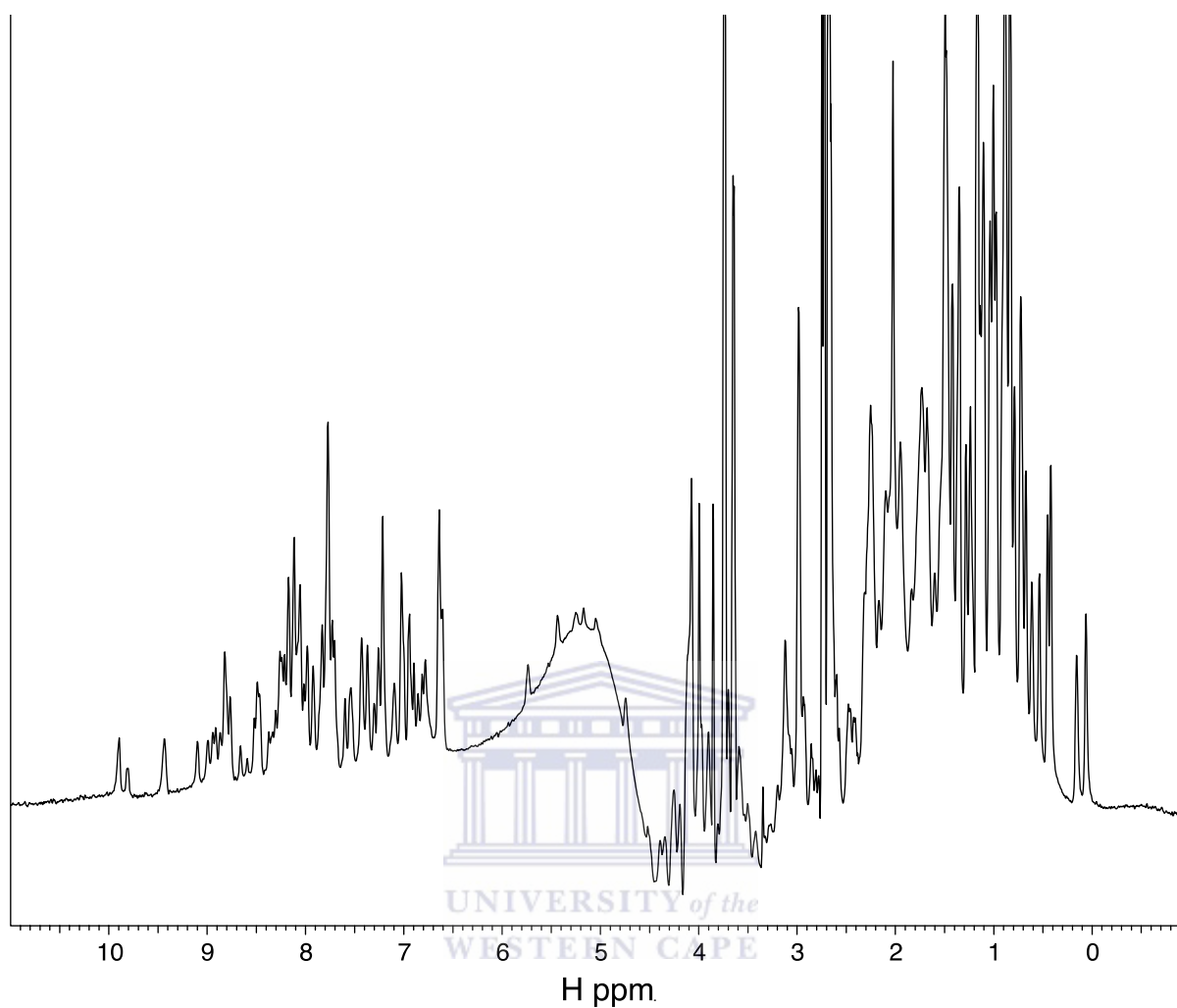


Figure 3.10 1D ^1H spectrum of the *A. niger* RING finger domain at pH 6.0, 25 °C, recorded at 600 MHz. The high level of dispersion (some H^{N} resonances in the region 9-10 ppm, some H^{α} in the region 5-6 ppm and methyl protons in the region 0-0.5 ppm) is an indication that the protein is folded.

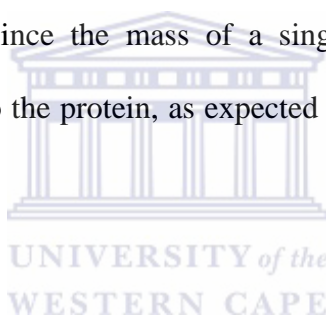
3.4 ESI-MS of RING finger proteins

3.4.1 *Homo sapiens* RING finger

From its amino acid sequence, excluding bound zinc ions, the expected mass of the human RING finger was calculated to be 10 229 Da (<http://web.expasy.org/protparam/>).

Under denaturing conditions (non-denaturing mass spectrometry buffer with the addition of 1 % formic acid) the mass of the protein was found to be 10 230 Da (Fig. 3.11.a). This is expected, since the denatured protein is not expected to be able to bind zinc ions.

Under non-denaturing conditions (no formic acid) the mass of the most abundant species was 10 356 Da (Fig. 3.11.b); since the mass of a single Zn^{2+} ion is 65.4 Da, this corresponds to two Zn^{2+} bound to the protein, as expected on the basis of previous NMR studies (Kappo *et al.* 2012).



Evidence of the *HsRING* finger occurring as a homodimer was also found (Fig. 3.11.c); the predominant species, at 20 711 Da, is consistent with the mass of two monomers, each binding two zinc ions (i.e. twice the mass of the monomer in (b)). Peaks corresponding to the homodimer binding a total of 3 (20 655 Da), 2 (20 588 Da), 1 (20 522 Da) and 0 (20 458 Da) zinc ions can also be seen, none of which are present in denaturing conditions (a). The other peaks corresponding to additions of 22 Da correspond to Na-adducts, which result from incomplete de-salting of samples prior to ESI-MS.

Non-denaturing ESI is therefore consistent with results previously obtained using solution state NMR: that the RING finger from *H. sapiens* RBBP6 binds two zinc ions and has a tendency to form homodimers.

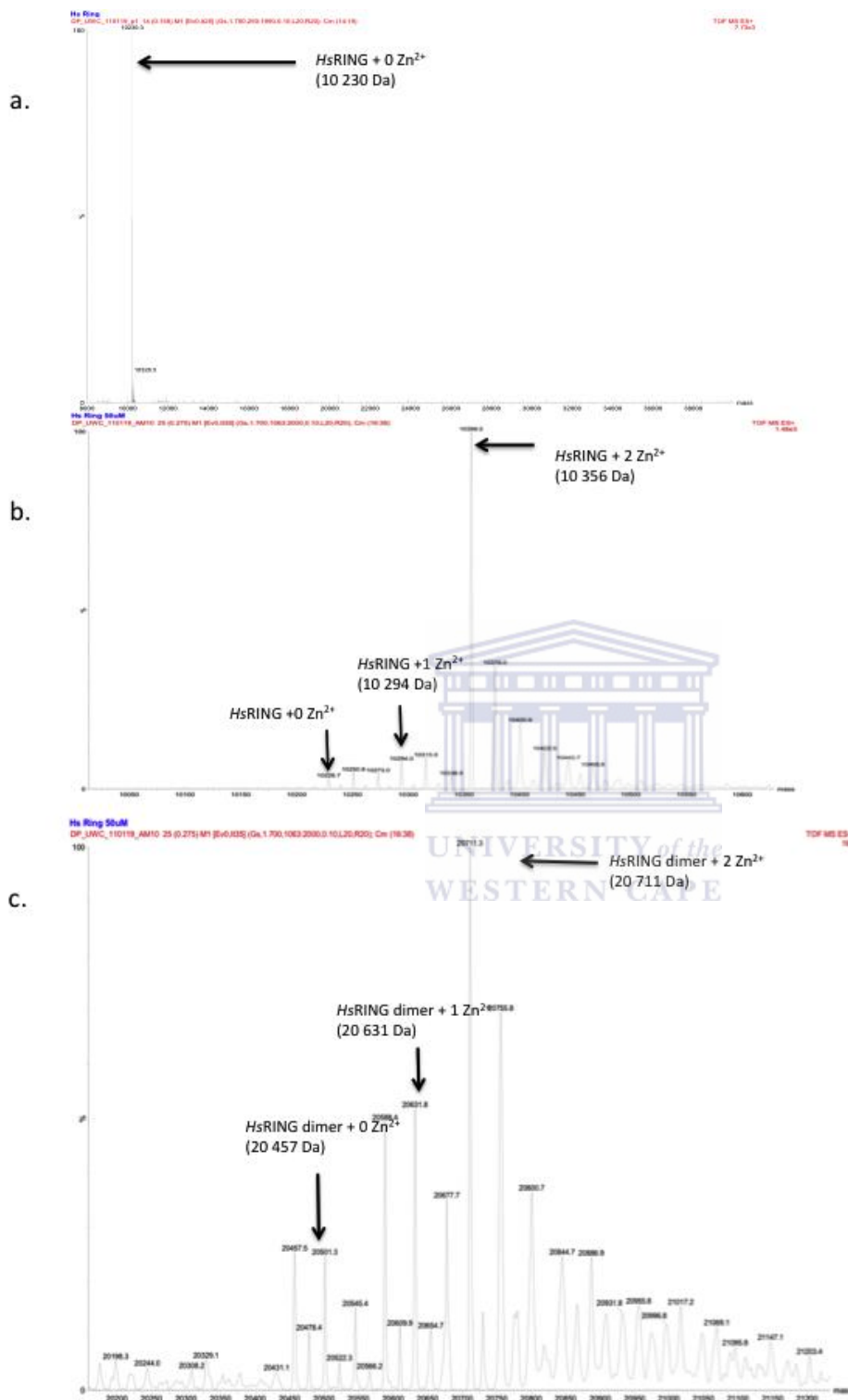
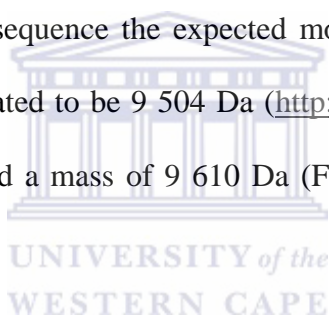


Figure 3.11 Deconvoluted ESI-MS of *Homo sapiens* RING finger. a) The denaturing ESI spectrum reveals the protein to be 10230 Da when the protein is sprayed into the mass spectrometer using formic acid. b) The non-denaturing spectrum reveals the most abundant species to be the *HsRING* with 2 Zn^{2+} bound. c) The dimer with no Zn^{2+} bound, the dimer with 2 Zn^{2+} and the dimer binding 4 Zn^{2+} . The other peaks are separated by approximately 22 Da and are likely to correspond to sodium adducts, which is a result of the protein being insufficiently desalted prior to MS.

3.4.2 *Saccharomyces cerevisiae* RING finger

The amino acid sequence of the *S. cerevisiae* orthologue of RBBP6 showed that the first Zn²⁺ binding pocket had been disrupted (Fig. 1.9), from which we hypothesized that it would bind only one Zn²⁺ ion. The 1D ¹H and 15N-HSQC spectra of the ScRING (Fig. 3.8 and 3.9) revealed that the protein was folded prior to MS. The sharpness and well dispersed peaks of the ¹H spectrum reveals that the ScRING is well folded (Fig 3.8) and the ¹⁵N-HSQC spectrum reveals that the protein remains monomeric in solution in a concentration dependent manner (Fig. 3.9).

On the basis of the amino acid sequence the expected molecular weight of the protein excluding bound zinc was calculated to be 9 504 Da (<http://web.expasy.org/protparam/>). However, denaturing MS returned a mass of 9 610 Da (Fig.3.12.a), 106 Da larger than expected.



Re-sequencing of the construct revealed two mutations, resulting in substitution of amino acid Valine (V) for Arginine (R), and Lysine for Phenylalanine, as is indicated with red dots in Fig. 1.9. Together these substitutions account for the observed mass increase of 105 Da.

Since neither of the mutated residues was expected to disrupt either of the two zinc binding sites, it was considered unlikely that the zinc binding properties would be affected. Hence the non-denaturing MS was carried out using the mutated construct.

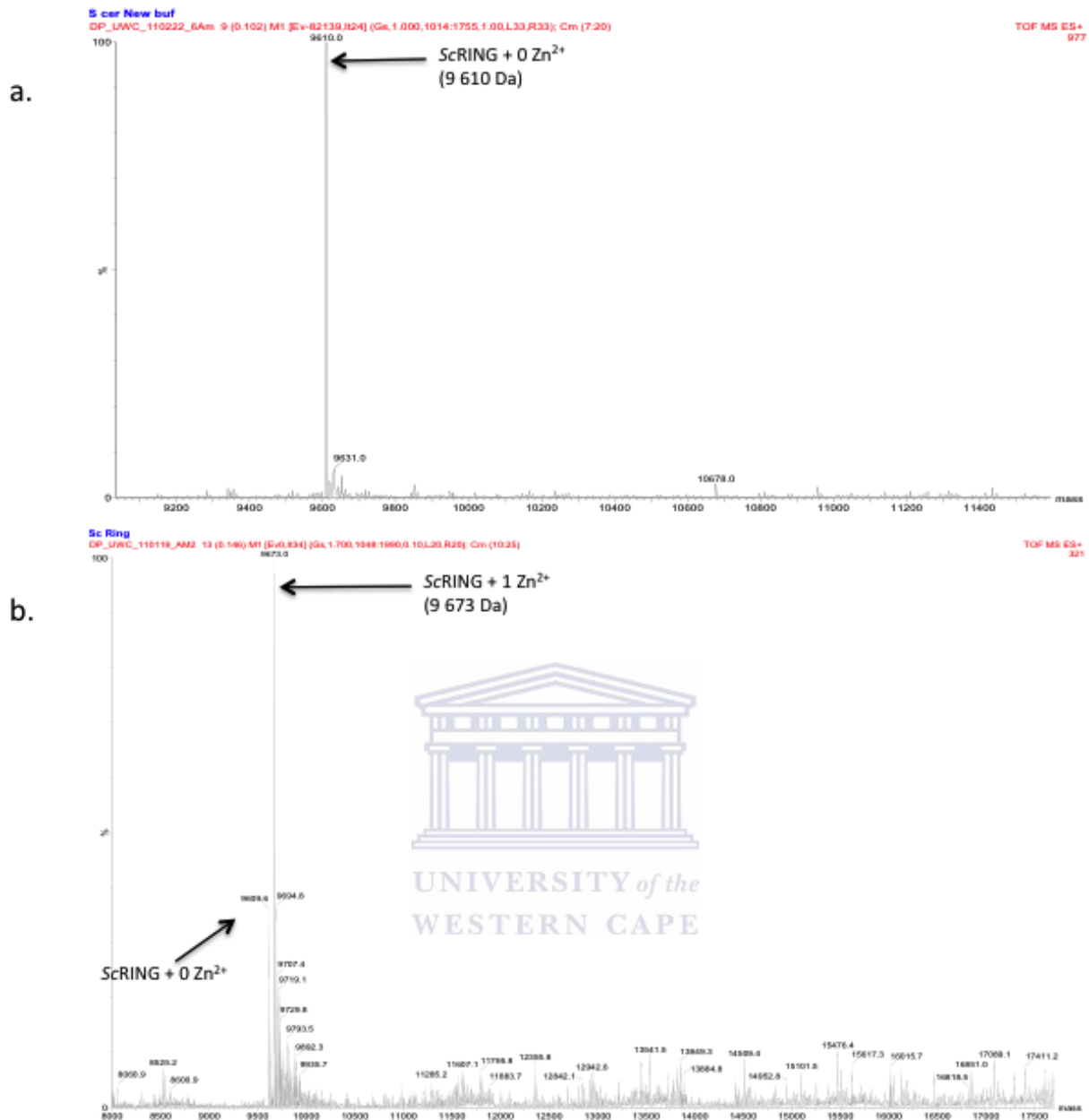


Figure 3.12 Deconvoluted ESI-MS of *Saccharomyces cerevisiae* RING finger. a) The denaturing spectrum indicates the protein with no Zn²⁺ ions bound at 9610 Da. b) The non-denaturing spectrum reveals the most abundant species at 9673 Da, indicative of the one Zn²⁺ ion bound to the protein. Traces of the protein with no Zn²⁺ bound were also present, but there is no evidence of two bound zinc ions.

However, a correct form of the expression construct was subsequently made and the sequence found to be 100 % correct (Fig. 3.4.a). The non-denaturing spectrum of the mutated protein yielded a mass of 9 673 Da indicative of the protein with one Zn²⁺ bound (Fig. 3.12.b). A peak corresponding to no bound zinc ions (9 609 Da) was also observed; however there was no evidence of a peak at 9 738 Da corresponding to two bound zinc ions. Hence our hypothesis that this was a RING finger protein which bound only one zinc ion was confirmed.

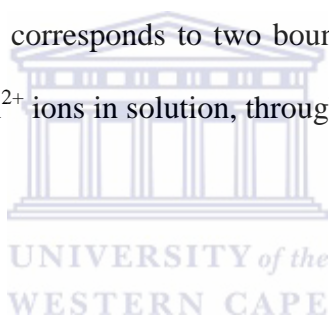
Evidence of +11 adducts at the 1 Zn²⁺ bound state suggests that the protein displays characteristics of a dimer; the reason is that the software used to deconvolute the m/z spectra to produce a spectrum as a function of m. It incorrectly interprets a small fraction of homodimers as monomers. If these homodimers contain an odd number of sodium ions (2n+1, where n=1, 2, 3...), then the peaks appear at $\frac{1}{2} (2n+1) \times 22 \text{ Da} = (2n+1) \times 11 \text{ Da}$. Such peaks can only originate from homodimers. We conclude that despite its unusual zinc binding characteristics, MS suggests that the ScRING still forms homodimers, similar to the human RING domain. However, further elucidation is needed.

The presence of a significant peak corresponding to zero Zn²⁺ ions bound cannot be interpreted as implying that a corresponding fraction of the sample binds no zinc ions in solution. ESI-MS takes place in the gas phase and, although ionization conditions are as gentle as possible, there is still a significant likelihood of zinc ions being lost.

However, the lack of any evidence at all for a second bound zinc, when compared to the human orthologue, can be taken as convincing evidence that only one zinc ion is bound to the *S. cerevisiae* orthologue.

3.4.3 *Aspergillus niger* RING finger

Analysis of the sequence of the *AnRING* shows an aspartic acid replacing one of the zinc coordinating cysteines in the first pocket (Fig. 1.9). Prior to MS the *AnRING* was prepared for NMR to determine the foldedness of the protein. The good dispersion and sharp peaks are indicative of the *AnRING* being folded (Fig 3.10). This suggests that either the protein binds only one zinc ion (in the second pocket), or it binds 2 zinc ions in a CDCCC4 motif. If so, it would be the first report of a CDCCC4 motif for zinc binding. The denaturing mass spectrum of the *AnRING* shows a peak at 9 200 Da (Fig. 3.13.a), corresponding to the unfolded protein with no zinc ions bound. The non-denaturing MS shows a peak at 9 326 Da which corresponds to two bound zinc ions (Fig. 3.13.b). We conclude that *AnRING* binds 2 Zn^{2+} ions in solution, through a novel CDCCC4 motif.



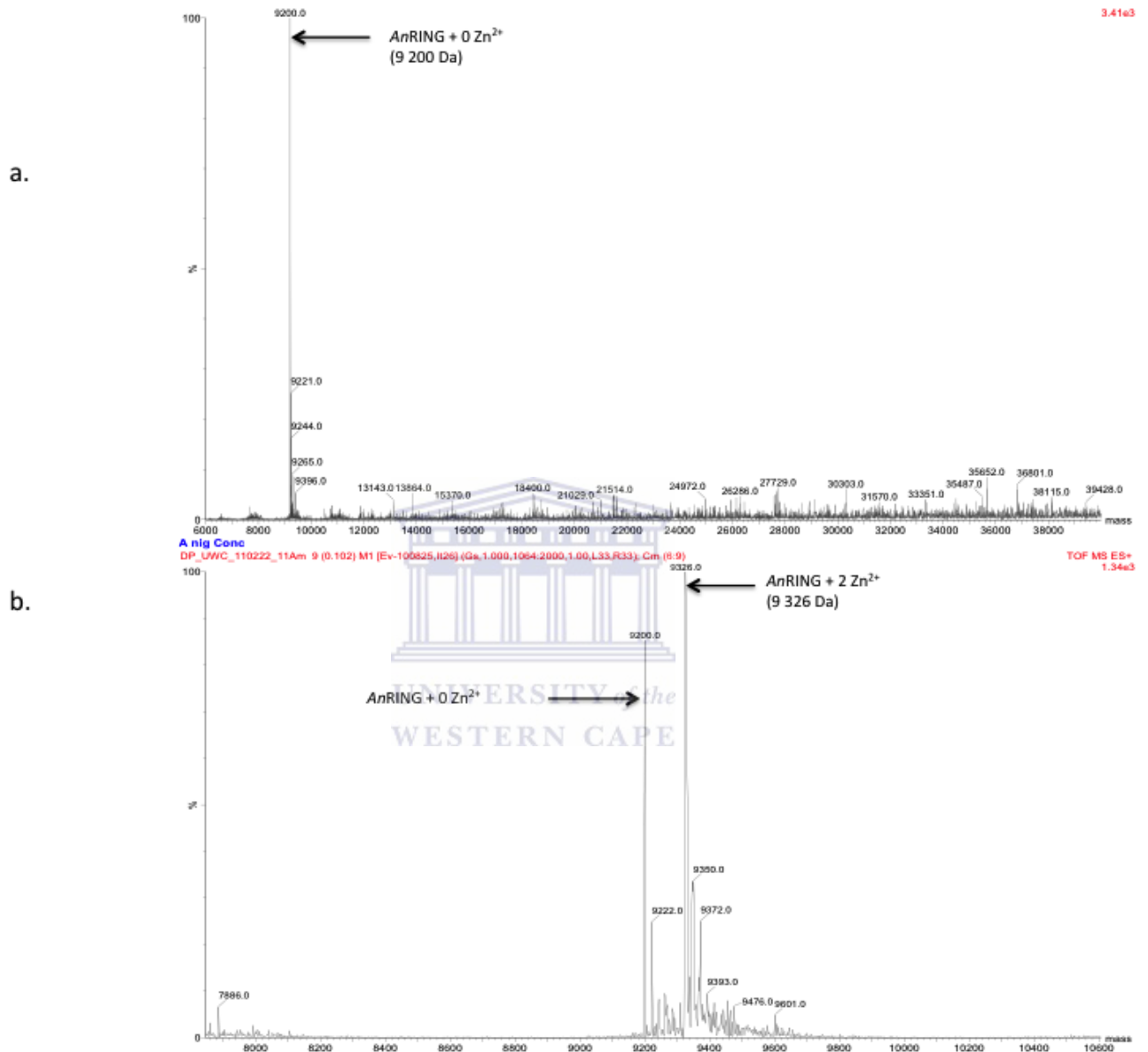
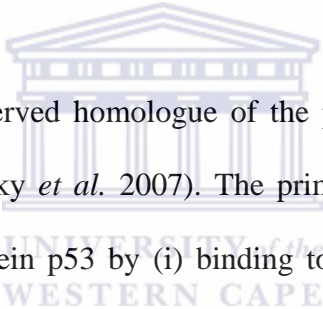


Figure 3.13 Deconvoluted ESI-MS of *Aspergillus niger* RING finger. a) The denaturing ESI spectrum indicates the protein with no Zn²⁺ ions bound at 9200 Da. b) The non-denaturing spectrum reveals the majority of the species binding two Zn²⁺.

Chapter 4: Results - Protein-protein interactions

4.1 Introduction

Previous work conducted by Chibi *et al.* (2008) identified Heat shock protein 70 (Hsp70) as a potential interactor with RBBP6. The similarities between the structures of the RING domain of RBBP6 and that of U-boxes, which are found in E3 ligases associated with chaperone-mediated ubiquitination of unfolded proteins, suggested that the RBBP6/Hsp70 interaction may provide evidence for the involvement of RBBP6 in this process. The aim was therefore to establish an *in vitro* immunoprecipitation procedure with which to narrow down the interaction site on Hsp70, for future NMR-based studies.



Human MDM2 is a highly conserved homologue of the product of the murine double minute (MDM2) gene (Poyurovsky *et al.* 2007). The primary function of MDM2 is to inhibit the tumor suppressor protein p53 by (i) binding to and masking the N-terminal transactivation domain of p53 and ii) by promoting the proteasomal degradation of p53 (Haupt *et al.* 1997, in Poyurovsky *et al.* 2007). MDM2 acts as an E3 ligase through its RING finger domain, which catalyzes the transfer of ubiquitin from the E2 onto substrates such as p53. RBBP6 also contains a RING finger domain and has been shown to catalyze the ubiquitination of the mRNA-associated protein Y-Box Binding Protein (YB-1), a protein that is also strongly linked to tumorigenesis and chemotherapeutic resistance in cancers. RBBP6 has also been shown to play a role in ubiquitination of p53 and to interact directly with MDM2. Li *et al.* (2007) reported that RBBP6 cannot ubiquitinate p53 on its own, but potentially acts as a scaffold, positioning p53 for ubiquitination by MDM2. However the precise details of the interaction between RBBP6 and MDM2 are still unknown.

4.2 RBBP6 interacts with Hsp70 through its N-terminal DWNN domain

Affinity pull-down assays were conducted to localize the interaction between RBBP6 and Hsp70. 6His-tagged Hsp70 and GST-tagged DWNN (RBBP₁₋₈₁) were expressed in *E. coli* and 6His-affinity pull-down assays carried out, detecting with a monoclonal antibody against the DWNN domain as shown in Fig. 4.1.A. Hsp70 was able to precipitate the DWNN domain (lane 3) but two unrelated 6His-tagged proteins were not (lanes 1 and 2).

When the reciprocal assay was carried out, precipitating with glutathione agarose and detecting with an antibody against Hsp70 (Fig. 4.1.B), RBBP6 fragments containing the DWNN domain were able to precipitate Hsp70 (lanes 2 and 3), but an unrelated GST-fusion protein was not (lane 1). Lane 4 contains Hsp70 that had been subjected to immunoprecipitation, in order to show where it appears on an SDS-PAGE gel.

4.3 Cross-linking of DWNN and Hsp70

The next step was to identify the part of Hsp70 directly interacting with the DWNN domain. One method shown to be useful in this regard is cross-linking combined with MS. Non-covalent complexes are cross-linked using a compound such as sulfo-MBS, which generates NHS-ester-amino group linkages on one end and maleimide-sulfhydryl linkages at the other. This should manifest as higher molecular weight species on SDS-PAGE, corresponding to the combined molecular weights of the linked proteins. The cross-linked species are then excised and subjected to MALDI MS in order to identify the identities of the cross-linked residues. This information could be used as a constraint in making a model of the interaction.

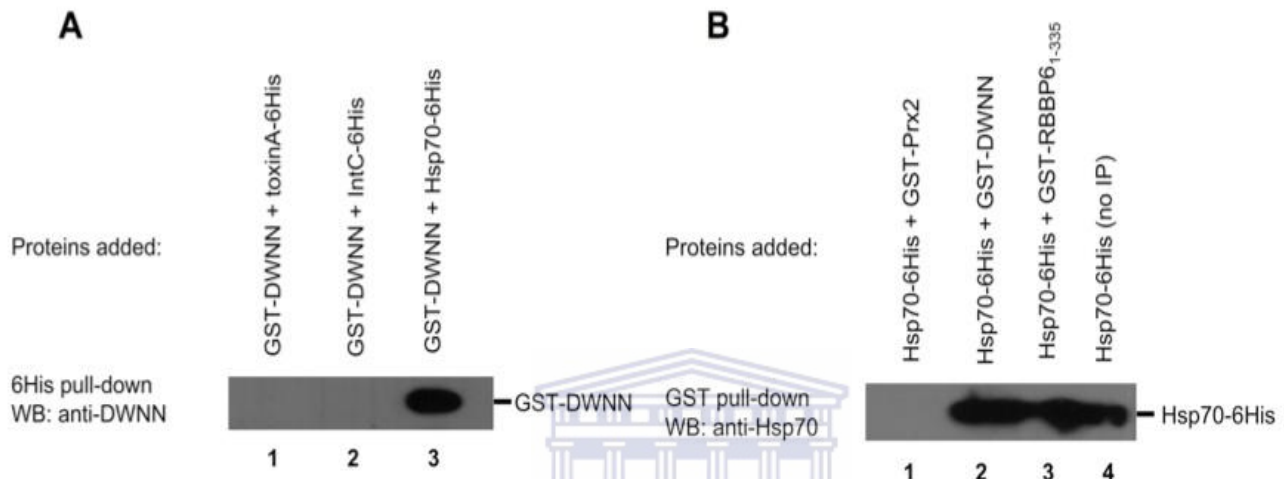


Figure 4.1 The N-terminal DWNN domain of RBBP6 interacts with Hsp70. (A) In a 6His affinity pull-down assay, 6His-tagged Hsp70 was able to precipitate a GST-DWNN fusion protein (lane 3), but two unrelated His-tagged proteins were not (lanes 1-2). The same amount of DWNN fusion protein was present in each lane. (B) In the reciprocal GST-affinity pull-down assay, GST-DWNN and a larger fragment of RBBP6 (including DWNN), were able to precipitate 6His-tagged Hsp70 (lanes 2-3), but an unrelated GST-fusion protein was not (lane 1) (Kappo *et al.* 2012).

The addition of sulfo-MBS cross-linker to a sample containing the DWNN domain and Hsp70 yielded a ladder of bands of molecular weight greater than Hsp70 (lanes 6 and 7) (Fig. 4.2a). To address this deficiency, the SDS-PAGE was Western blotted using an antibody raised against the DWNN domain of RBBP6. Lanes 5 and 6 of Fig. 4.2(b) show that species with molecular weights greater than that of Hsp70 do indeed contain the DWNN domain. These species are not due to DWNN-DWNN cross-linking, since they do not appear when only the DWNN is cross linked (Fig. 4.2. b), nor do they contain Hsp70, since lane 2 shows that there is no cross-reactivity between the anti-DWNN antibody and Hsp70. Hence we conclude that the high molecular weight bands in lanes 5 and 6 corresponding to DWNN-Hsp70 cross-linking.

4.4 MS analysis of cross-linked proteins

A piece of the SDS-PAGE gel containing the high molecular weight species (indicated with a red rectangle in lane 6 of Fig. 4.2 (a)) was excised and subjected to liquid chromatography coupled to an Orbitrap Velos (Thermo Scientific, Waltham, Massachusetts, USA) in the laboratory of Prof. Henning Urlaub, Max Planck Institute for Biophysical Chemistry, Göttingen, Germany. Ionization was achieved through ESI. Peptides were analyzed using the cross-linking application forming part of the MASCOT suite. Using the sequences of the DWNN domain as Hsp70 protein as input, as well as the cross-linker involved, the algorithm searched the MS data for fragments of both proteins, as well as for intramolecular cross-linked fragments. Although the search was able to identify Hsp70 (Fig. 4.3), no evidence of DWNN was found.

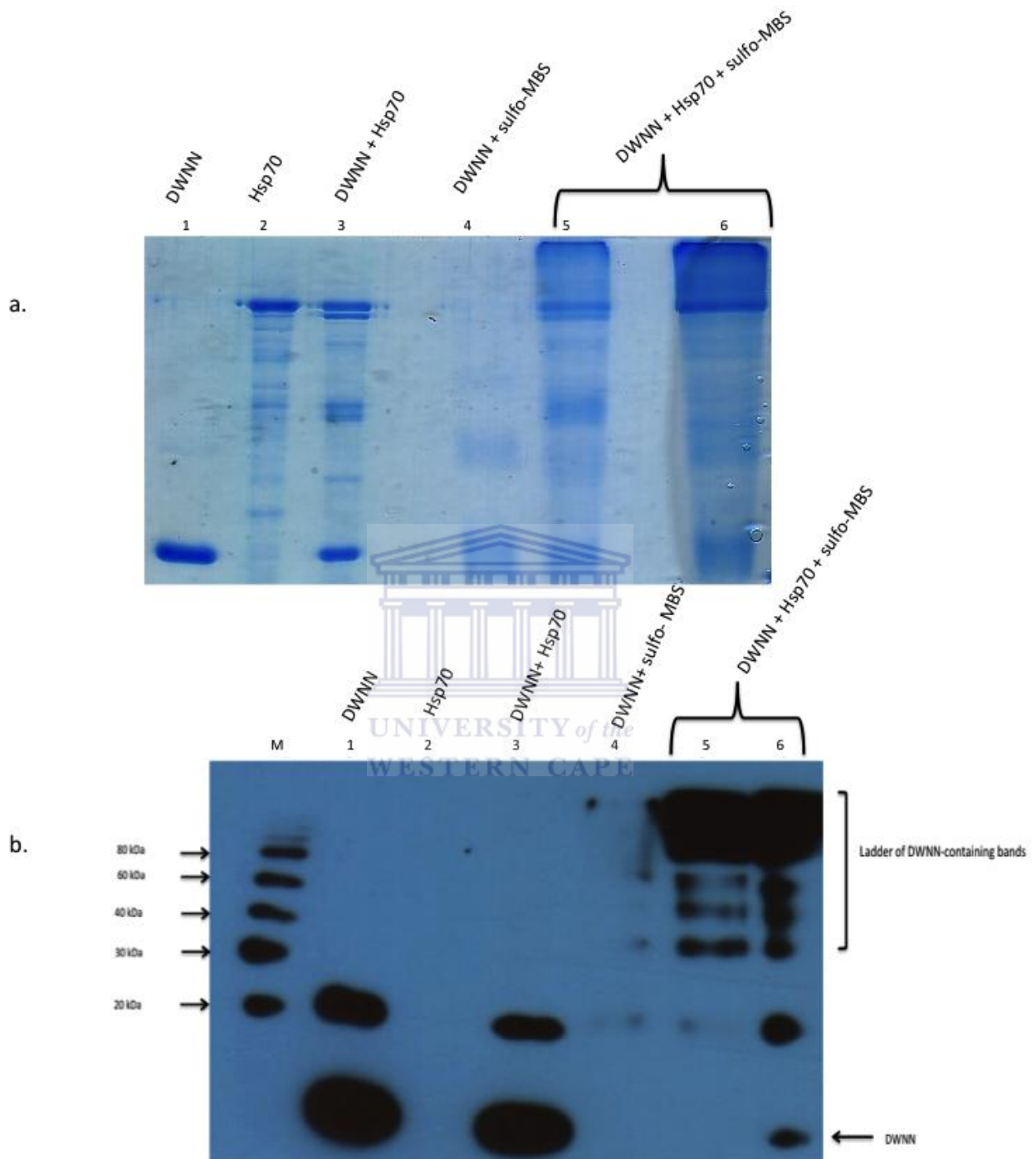
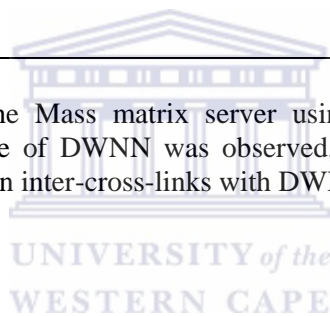


Figure 4.2 Analysis of cross-linked species. a) SDS-PAGE following cross-linking of DWNN and Hsp70. b) Western blot of cross-linking assay using monoclonal anti-DWNN antibody. The addition of the hetero-bifunctional cross-linker sulfo-MBS creates high molecular weight bands that exceed the molecular weight of Hsp70 (70 kDa). These do not correspond to Hsp70-Hsp70 complexes because the antibody does not recognize Hsp70 at all (lane 2) nor to DWNN-DWNN complexes as they do not appear to any significant content in lane 4, where DWNN alone is cross-linked.

Protein Mass: 33110.077 (monoisotopic) 33130.185(average) Protein Score: **89**

Protein pp: **2149.6** Hsp 70 Sequence:AKAAAIGIDL GTTYSCVGVF QHGKVEIIAN
DQGNRTTPSY VAFDTERLI GDAAKNQVAL NPQNTVFDAK RLIGRKFGDP
VVQSDMKHWP FQVINDGDKP KVQVSYKGET KAFYPEEISS MVLTKMKEIA
EAYLGYPVTN AVITVPAYFN DSQRQATKDA GVIAGLNCLR IINEPTAAAI
AYGLDRTGKG ERNVLIFDLG GGTFDVSILT IDDGIFEVKA TAGDTHLGGE
DFDNRLVNHF VEEFKRKHKK DISQNKRAVR RLRTACERAK RTLSSSTQAS
LEIDSLFEGI DFYTSITRAR

Figure 4.3 Data generated from the Mass matrix server using the cross-linking application identified Hsp70 whilst no evidence of DWNN was observed, thus revealing intra-cross-links between the Hsp70 protein rather than inter-cross-links with DWNN.



While it was disappointing that mass spectrometry was unable to confirm the presence of the DWNN domain in the gel slice, the evidence of the Western blot in Fig. 4.2b is difficult to dispute. It is more likely that our search of the MS data was non-optimal and that it failed to identify the DWNN that was present. Further optimization of the search was not attempted due to time constraints.

4.5 Size exclusion chromatography of DWNN and Hsp70

In a further attempt to cross-link the DWNN domain and Hsp70, size exclusion chromatography was first used to isolate the interacting complex, prior to cross-linking. Equal concentrations of the DWNN domain and Hsp70 were mixed together and incubated at 4 °C before loading them on a Superdex 75 16/600 (GE healthcare, Pittsburgh, USA) size exclusion column. A small peak, eluting before the main Hsp70 peak, was present only when the DWNN domain was present (Fig. 4.4.a and b.) It therefore represents a putative non-covalent complex between Hsp70 and the DWNN domain. SDS-PAGE analysis (Fig. 4.4.c) revealed a band consistent with that of the DWNN domain. The band was excised from the gel and subjected to tryptic digest and MS as before. MS confirmed that DWNN was present in the band (Fig. 4.5). Using the MASCOT server database to search for peptides identified yielded result for a possible significant hit, as RBBP6 is identified as one of the candidates identified (Fig. 4.5.a). Owing to the novelty of the technique hits relating to keratin and trypsin are expected. However, when the DWNN domain sequence is used as the input for the peptide search, 5 peptides covering 68 % of the DWNN sequence were identified. The presence of the DWNN domain, which has a mass of only 9 kDa, in a fraction corresponding to a molecular weight of greater than 70 kDa is clear evidence that it forms a non-covalent interaction with Hsp70.

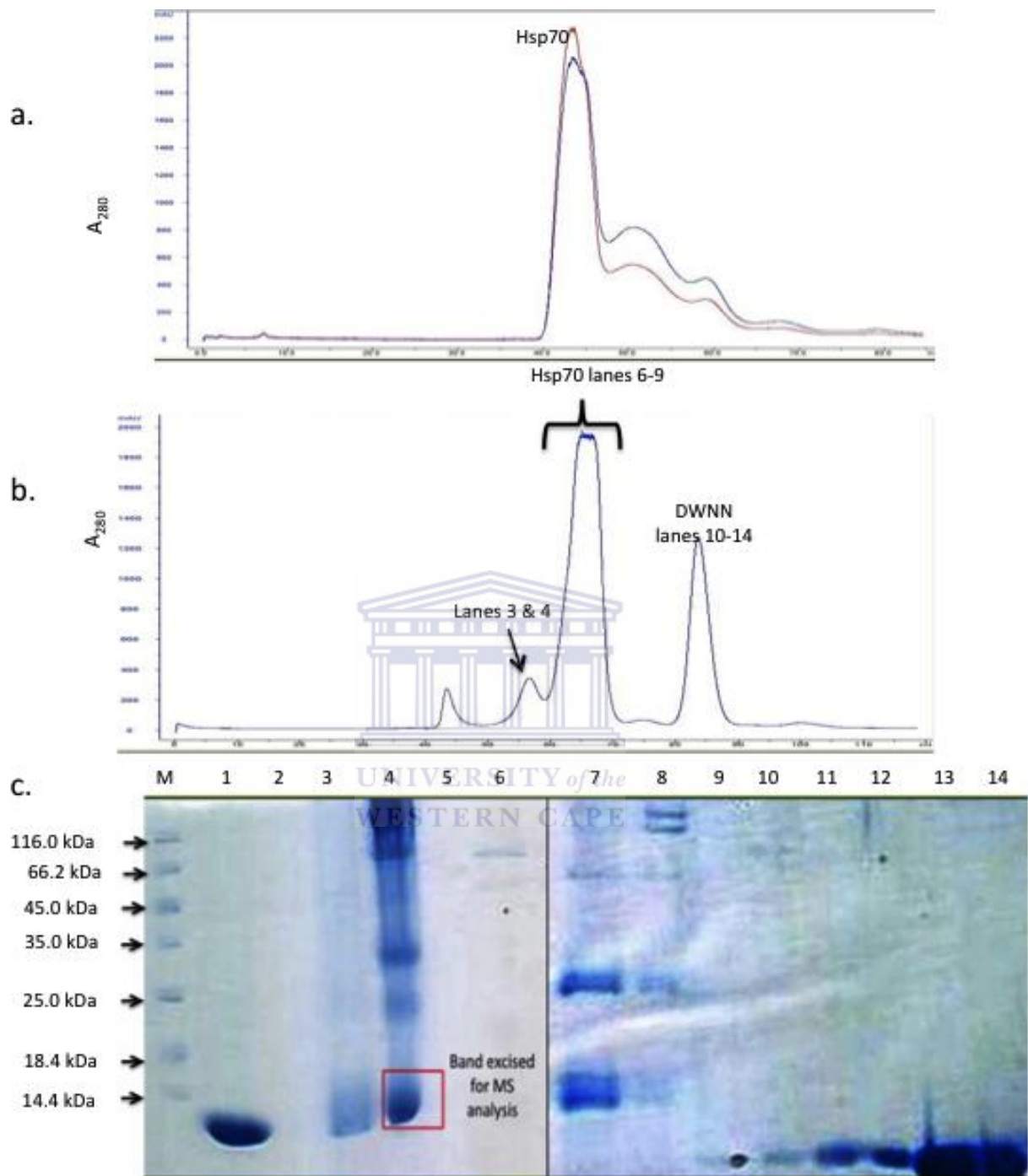


Figure 4.4 Isolation of an interacting complex between the DWNN domain and Hsp70. (a) Size exclusion chromatogram of Hsp70 alone. (b) Size exclusion chromatogram of DWNN and Hsp70. The labels refer to the lanes in (c). (c) SDS-PAGE of fractions corresponding to the fractions indicated in (b). The small peak eluting prior to Hsp70 contains a band consistent with the DWNN domain (lanes 3 and 4), which is seen on its own in lane 1. The bulk of the DWNN domain elutes much later, consistent with its molecular weight of only 9 kDa.

a.

Accession	Description	Score	Coverage	# Proteins	# Unique Peptides	# Peptides	# AAs	MW [kDa]	calc. pI
P04264	Keratin, type II cytoskeletal 1 OS=Homo sapiens GN=KRT1 PE=1 SV=6 - [K2C1_HUMAN]	130.1.32	62.11	5	18	40	644	66.0	8.12
P35527	Keratin, type I cytoskeletal 9 OS=Homo sapiens GN=KRT9 PE=1 SV=3 - [K1C9_HUMAN]	966.98	62.60	1	26	31	623	62.0	5.24
P35908	Keratin, type II cytoskeletal 2 epidermal OS=Homo sapiens GN=KRT2 PE=1 SV=2 - [K22E_HUMAN]	794.56	52.90	1	15	28	639	65.4	8.00
P13645	Keratin, type I cytoskeletal 10 OS=Homo sapiens GN=KRT10 PE=1 SV=6 - [K1C10_HUMAN]	726.91	47.26	3	10	27	584	58.8	5.21
Q6EIZ0	Keratin, type I cytoskeletal 10 OS=Canis familiaris GN=KRT10 PE=2 SV=1 - [K1C10_CANFA]	393.40	27.46	3	1	18	568	57.7	5.15
P08779	Keratin, type I cytoskeletal 16 OS=Homo sapiens GN=KRT16 PE=1 SV=4 - [K1C16_HUMAN]	262.27	51.59	2	9	21	473	51.2	5.05
P00761	Trypsin OS=Sus scrofa PE=1 SV=1 - [TRYP_PIG]	251.39	35.93	1	6	6	231	24.4	7.18
Q6E1Y9	Keratin, type II cytoskeletal 1 OS=Canis familiaris GN=KRT1 PE=2 SV=1 - [K2C1_CANFA]	245.75	19.87	1	1	17	619	63.8	7.84
A7YWK3	Keratin, type II cytoskeletal 73 OS=Bos taurus GN=KRT73 PE=2 SV=1 - [K2C73_BOVIN]	226.51	11.48	2	1	7	540	58.8	7.23
Q6P6Q2	Keratin, type II cytoskeletal 5 OS=Rattus norvegicus GN=Krt5 PE=1 SV=1 - [K2C5_RAT]	197.62	22.05	2	2	17	576	61.8	7.80
P02538	Keratin, type II cytoskeletal 6A OS=Homo sapiens GN=KRT6A PE=1 SV=3 - [K2C6A_HUMAN]	182.71	32.62	2	5	21	564	60.0	8.00
P02533	Keratin, type I cytoskeletal 14 OS=Homo sapiens GN=KRT14 PE=1 SV=4 - [K1C14_HUMAN]	174.03	41.74	3	1	18	472	51.5	5.16
Q7Z6E9	Retinoblastoma-binding protein 6 OS=Homo sapiens GN=RBBP6 PE=1 SV=1 - [RBBP6_HUMAN]	156.66	3.07	1	5	5	1792	201.4	9.64

b.

Accession	Description	Score	Coverage	# Proteins	# Unique Peptides	# PSMs	# AAs	MW [kDa]	calc. pI
A0000	test OS=David Pugh	281.38	67.90	1	5	19	81	9.1	8.29

MSCVHYKFS S **KLNYDTVTFD GLHISLCDLK** KQIMGREK**LK AADCDLQITN AQTKEEYTD**
NALIPKNSSV IVRRIPIGGV K

Figure 4.5 Identification of DWNN from excised band. Using the database as the input the MASCOT server identified mainly keratin and trypsin (a), which are a result of sample preparation prior to MS. However, peptides identified match that of the RBBP6 gene. When subjecting the server to the DWNN domain sequence as input (b) the server identified peptides covering 68 % of the DWNN domain sequence (highlighted in green).

Further attempts to localize this interaction are currently under way, with the peptide-binding domain of Hsp70 being the preferred candidate involved in the interaction with the DWNN domain.

4.6 Interaction between RBBP6 and Murine-double minute 2 (MDM2)

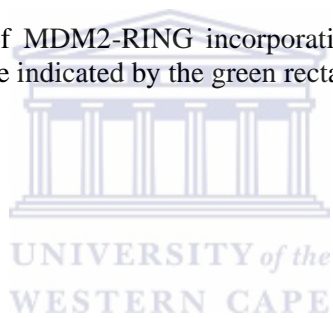
RBBP6 has been reported to interact directly with MDM2 *in vitro* (Li *et al.* 2007), and to facilitate the ubiquitination of p53 by MDM2 in a manner that requires the presence of the RING finger domain of RBBP6. Our unpublished data confirms that RBBP6 cooperates with MDM2 in the ubiquitination of p53 in *in vitro* ubiquitination assays, in a manner depending on its RING finger domain, and that it interacts directly with MDM2 *in vitro* (A. Faro and D.J.R. Pugh, unpublished data). Together this data suggests that RBBP6 and MDM2 may interact through their respective RING finger domains. MDM2 is known to heterodimerize with MDMX (through their RING finger domains (Baer & Ludwig, 2002), and a number of other E3 ubiquitin ligases, including BRCA1 and BARD1 are known to do the same (Christensen & Klevit, 2009).

4.6.1 Affinity pull-down assay

The RING finger from human RBBP6 was expressed and purified as described previously (Section 3). A sequence corresponding to residues 438-478 of human MDM2 (NM_002392) was amplified from the pCMV-Myc3-HMD2 construct obtained from Addgene (20935) using the primers shown in Fig. 4.6. Sequencing confirmed the construct to be 100 % correct. The construct was expressed in *E. coli* and was found to be soluble and stable while the GST tag was still attached, although it showed evidence of insolubility once GST was removed using pre-scission protease.

Primer	Sequence
Forward	5'- GAG GCG GGA TCC GAA GAA ACC CAA GAC AAA GAA G -3'
Reverse	5'- GAG GCG CTC GAG TTA TTA GGG GAA ATA AGT TAG CAC AAT-3'

Fig 4.6 Primers for amplification of MDM2-RING incorporating BamHI and XhoI restriction sites (red rectangles). Stop codons are indicated by the green rectangle.



GST-pulldown assays were conducted with GST-MDM2-RING as bait and RBBP6-RING as prey, detecting with a polyclonal antibody against the RBBP6-RING. However, due to cross-reactivity between the antibody and GST-MDM2-RING, most probably due to the fact that the antibody had been raised using RBBP6 RING purified from a GST-fusion construct (GST-RBBP6-RING), these assays were not pursued.

As an alternative strategy, the MDM2 RING was re-amplified and cloned into the NdeI and XhoI sites of the pET28a vector so that it could be expressed with a C-terminal 6His tag (Fig. 4.7.a) The reverse primer incorporated a stop codon immediately prior to the XhoI site, obviating the C-terminal 6His tag (Fig. 4.7.b).

Only one positive clone was obtained following the cloning of the MDM2-RING into the pET28a vector. Sequencing of the clone revealed a base change from adenine to guanine (Fig.4.8.b), which fortunately left the amino acid sequence unchanged since codons CAA and CAG both code for the amino acid glutamine. The MDM2-RING-His6 was found to express solubly and stably in *E. coli*. The expressed protein was kindly expressed by Dr. A. Faro.

GST-affinity pull-down assays were conducted to establish whether an interaction exists between the RING finger domains of RBBP6 and MDM2, with GST-RBBP6-RING as bait and MDM2-RING as prey (Fig. 4.9). Western blotting was carried out using a monoclonal antibody recognizing an epitope within residues 383-491 of MDM2 (AB11, Merck Millipore, Darmstadt). Fig. 4.9 confirms that the antibody detects MDM2 (lanes 3 and 4) but not GST-RBBP6-RING (lanes 1 and 2). GST-RBBP6-RING was able to precipitate MDM2-RING (lane 6), but a dummy GST-fusion protein was not (lane 5).

Primer	Sequence
Forward	5'- GAG GCG GGA TCC GAA GAA ACC CAA GAC AAA GAA G -3'
Reverse	5'- GAG GCG CTC GAG TTA TTA GGG GAA ATA AGT TAG CAC AAT -3'

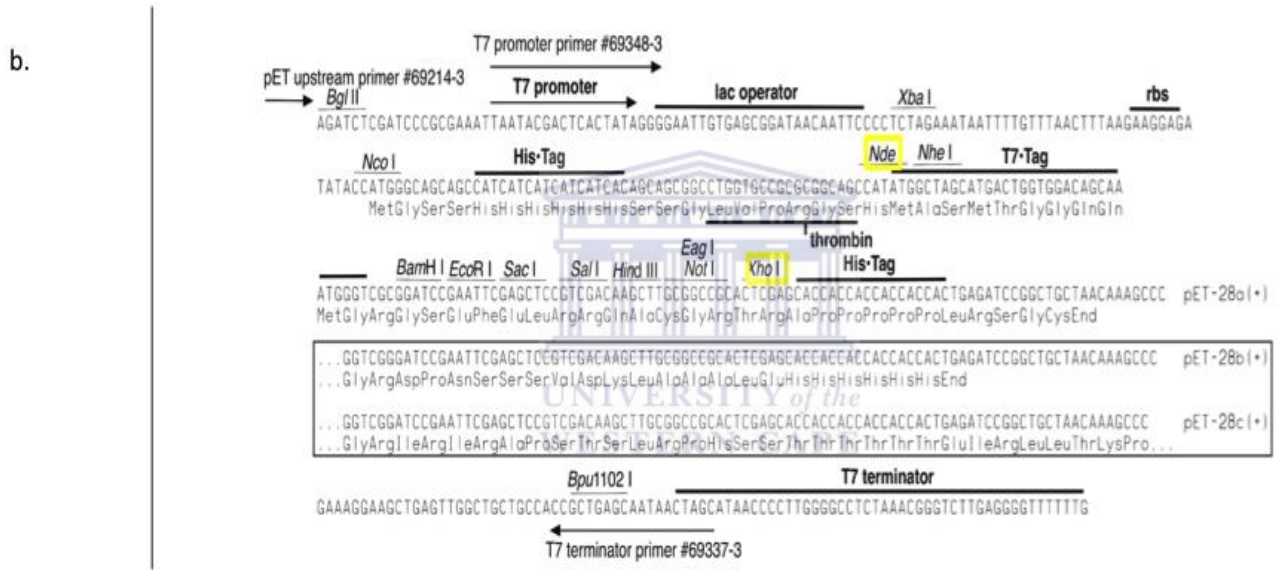


Figure 4.7 (a) Primers for amplification of MDM2-RING, incorporating an N-terminal NdeI and a C-terminal XhoI site (red boxes) as well as two stop codons immediately following the end of the gene. (b) Cloning into the NdeI and XhoI sites was chosen so as to incorporate an N-terminal 6His tag. Incorporation of a C-terminal 6His tag was obviated by the stop codons incorporated into the reverse primer. Figure adapted from <http://www.staff.ncl.ac.uk/p.dean/pET.pdf>, accessed 04/07/2013.

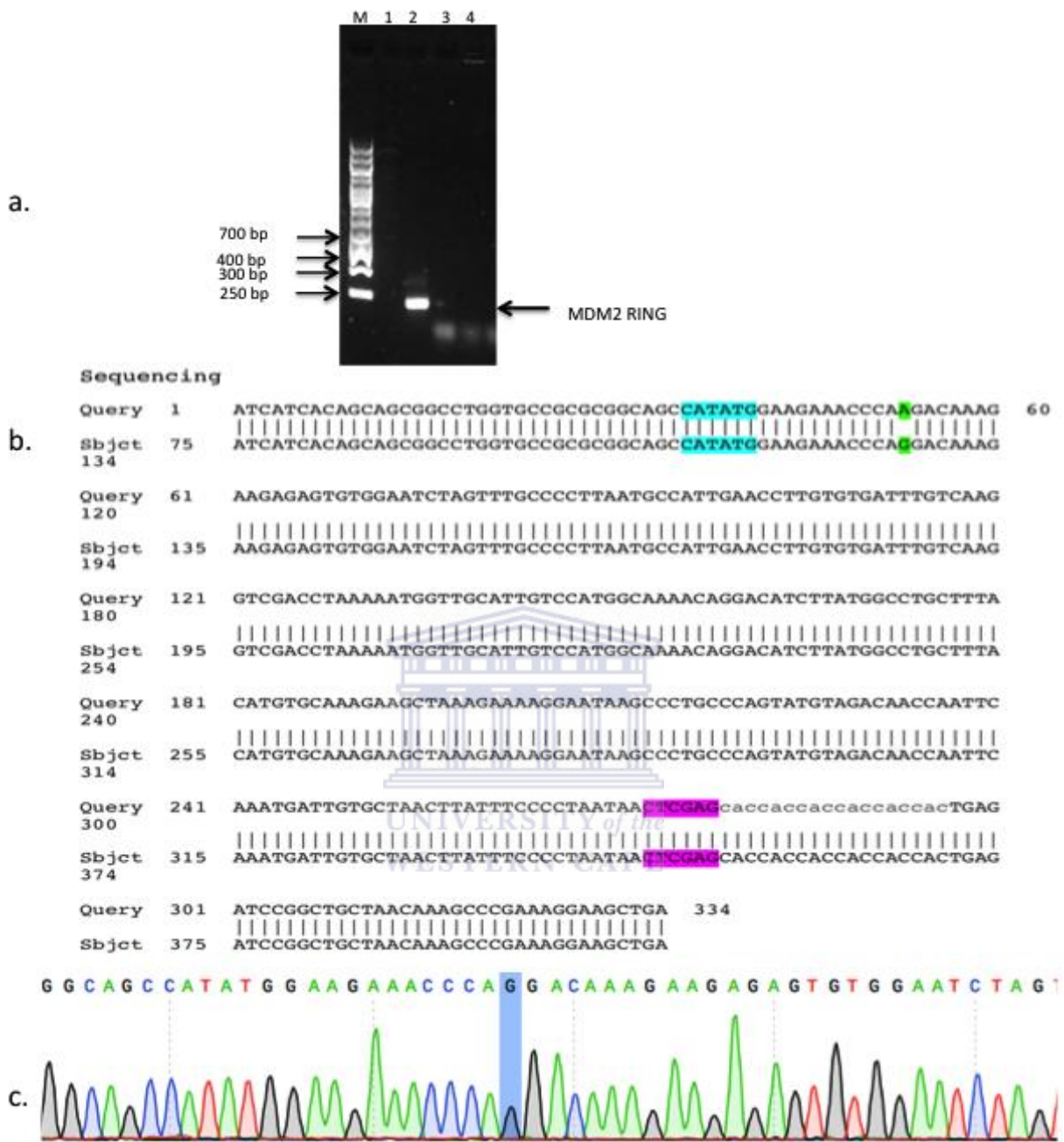


Figure 4.8 a) Colony PCR screen of putative clones identified one positive colony (lane 2), which was subjected to sequencing. b) Comparison of the experimental sequence (Query) showed that the construct contained a mismatch (indicated in green). Inspection of the sequencing trace (c) confirmed that the mismatch was indeed present and was not due an error in base calling. Fortunately the mismatch was found to have no effect on the amino acid sequence.

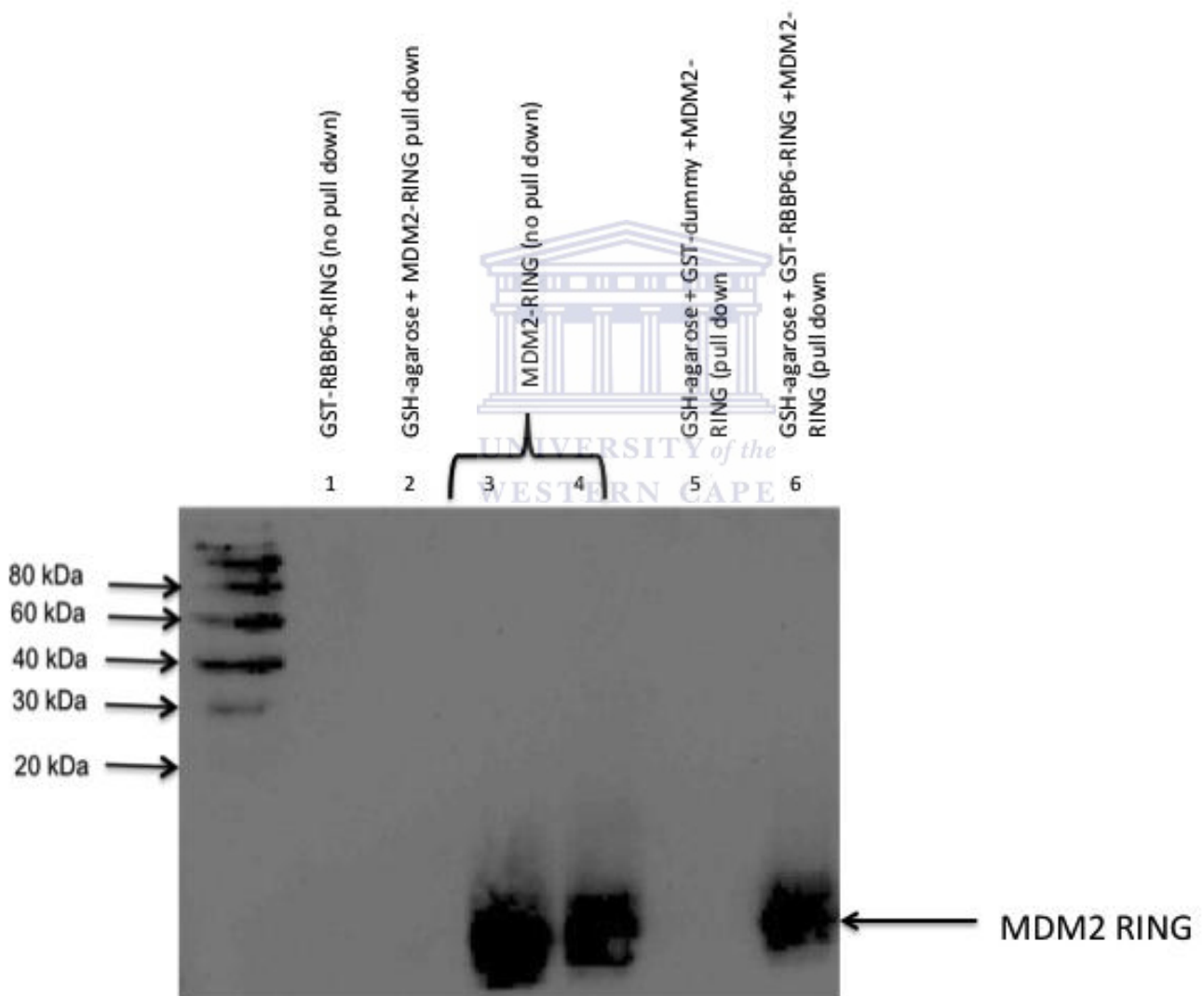


Figure 4.9 GST-affinity pull-down assay using GST-RBBP6-RING as bait and MDM2-RING-6His as prey. MDM2-RING was detected using monoclonal antibody 4B11 against full length MDM2. GST-RBBP6-RING was able to pull down MDM2-RING-6His (lane 6), but a dummy GST-fusion was not (lane 5).

This important result was confirmed by replacing pull down of GST-RBBP6-RING by immunoprecipitation of RBBP6-RING using the polyclonal antibody discussed previously. Co-precipitation of MDM2-RING-6His was detected using a monoclonal antibody (Merck Millipore, Darmstadt, Germany). The cross-reactivity of the anti-RBBP6-RING polyclonal antibody mentioned earlier is not problematic in this context because the pre (MDM2-RING) no longer incorporated a GST tag (Fig. 4.10.a). As before, MDM2-RING-6His was precipitated by anti-RBBP6-RING in the presence of RBBP6-RING (lane 6) but not in the absence of RBBP6-RING (lane 5). Alternatively, GST-RBBP6-RING was able to co-precipitate MDM2-RING-6His in the presence of anti-RBBP6-RING (lane 6), but not in the presence of anti-HA (lane 4), an antibody that does not recognize RBBP6-RING.

The interaction between the RING finger domains of RBBP6 and MDM2 was further confirmed by immunoprecipitating MDM2-RING-6His using the anti-MDM2 antibody discussed above and probing for co-precipitation of RBBP6-RING using the polyclonal antibody against the RBBP6-RING (Fig. 4.10.b). Again the cross-reactivity of this antibody is not significant in this context because either detection of GST or of RBBP6-RING would be evidence of co-precipitation of RBBP6-RING by MDM2-RING-6His. Despite the poor quality of the Western blot, which is due to the crude nature of the anti-RBBP6-RING anti-serum, it is clear that anti-MDM2 is able to precipitate RBBP6-RING in the presence of MDM2-RING-6His (lane 5) but not in the absence of MDM2-RING-6His (lane 4). Alternatively, MDM2-RING-6His is able to precipitate RBBP6-RING in the presence of anti-MDM2 (lane 5), but not in the presence of anti-HA, which does not recognize MDM2-RING-6His.

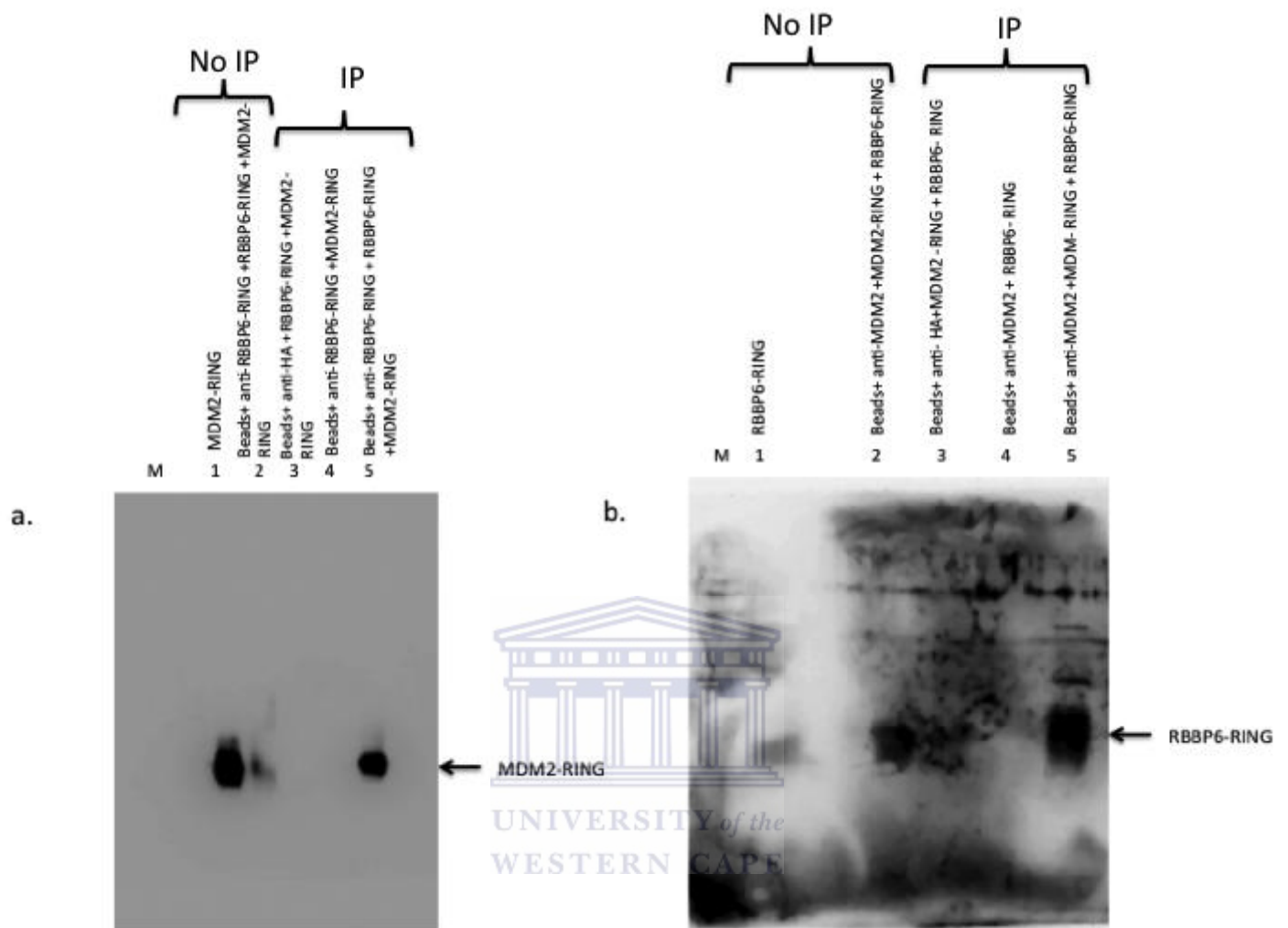


Figure 4.10. Co-immunoprecipitation of MDM2-RING-6His and RBBP6-RING. a) Using anti-RBBP6-RING coupled to an Affi-gel matrix, RBBP6-RING (bait) was used to precipitate MDM2-RING-6His (prey) using monoclonal antibody 4B11 against full length MDM2. b) Using MDM2-RING-6His as bait the RBBP6-RING was precipitated, as detected using a polyclonal antibody against the RBBP6-RING.

Chapter 5: Discussion and Conclusion

The aim of the project was to implement two novel mass spectrometry-based methods for analyzing protein function: i) non-denaturing MS to investigate zinc binding on proteins in their native state and ii) cross-linking mass spectrometry to investigate protein-protein interactions.

Whereas the RING finger domain from human RBBP6 has been shown using NMR to bind two zinc ions, in line with all other RING fingers, analysis of the amino acid sequences of orthologues from *S. cerevisiae* and *A. niger* suggested that these may bind fewer than two zinc ions. In addition to demonstrating the power of the technique for analyzing proteins in their native state – unfolded proteins being unable to bind any zinc ions – the identification of RING finger domains binding fewer than two zinc ions would be of great interest in itself. In particular, it may provide support for the hypothesis proposed by Kappo and co-workers (Kappo *et al.* 2012) that the RBBP6 RING finger-like domains represent a structural intermediate between RING fingers and U-boxes.

The non-denaturing mass spectrometry data supports the hypothesis in that it shows that the *Sc*RBBP6-RING binds only one zinc ion and, based on NMR spectra, is a folded, presumably functional protein, thereby possibly being further stabilized by salt bridges and hydrogen bonds. If so, it is the first reporting of a RING finger-like domain that binds only one zinc ion, yet is stable and functional. The only other RING finger-like protein reported to bind a single zinc ion is the SP-RING domain found in members of the PIAS family, in which the first binding site has been lost, but the second is preserved in the form CHCC (Yunus & Lima, (2009)). Interestingly PIAS family proteins play the role of

E3 ligases for SUMO ubiquitin-like modifiers, raising the question of whether RBBP6 may have a role in SUMOylation.

There have been previous reports on RING fingers that coordinate zinc ions through an aspartic residue. Régnier and coworkers (1995) identified the RING finger domain of CART1 to have an aspartic acid in the second zinc binding pocket, thereby coordinating zinc in a C3HC3D motif. The sequence of the RING finger from *Aspergillus niger* suggested that one of the zinc-coordinating cysteines has been replaced with an aspartic acid, giving a CDCC coordination pattern in site 1 and a C4 pattern in site 2. The question was therefore whether site 1 would bind a zinc ion with a CDCC motif, or whether the protein bound only one zinc ion in site 2. Non-denaturing mass spectrometry clearly showed that the *A. niger* RING bound 2 zinc ions. It is therefore similar to the RING from Rbx1 and CART1, in which one of the zinc ions is coordinated by a CCCD configuration. However, with these two RINGs the aspartic acid is located in the second binding site for zinc. The *AnRING* has the aspartic acid in site 1, and can therefore be classified in a class of its own.

Structural studies of the *ScRING* and *AnRING* domains using NMR would further substantiate the mass spectrometry data, potentially leading to re-classification of these RING finger-like domains as evolutionary intermediates between RING fingers and U-boxes.

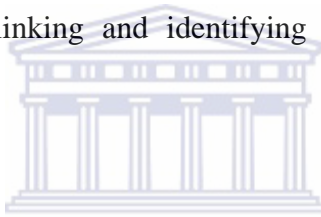
Experiments pertaining to protein-protein interactions were conducted in the hope of localizing the regions of interaction at the amino acid level. Affinity pull-down assays aided in confirming the interaction between proteins, as well as partial localization, in the

case of RBBP6. We were able to identify the N-terminal DWNN domain of RBBP6 as the interacting partner of Hsp70, and hypothesized its interaction with the peptide-binding domain of Hsp70, as the yeast two-hybrid results published by the group (Chibi et al. 2008) identified the peptide-binding domain of Hsp70 as the interacting partner of RBBP6.

Initial attempts to cross-link the DWNN domain of RBBP6 and Hsp70 had failed, as the addition of a cross-linker yielded intra-cross-links between individual proteins, rather than inter-cross-links between proteins. The lack of expertise could also be attributed to the failure to generate good cross-linking data as the technique is novel to Africa, so optimization can be tedious. Owing to the novelty of the technique, software and algorithms too require much needed work as those currently available are beyond reach. However, the western blot data suggest that we have convincingly created inter-molecular cross-links between the DWNN domain and Hsp70. Due to time constraints the cross-linking experiment could not be repeated as the analyzed excised band was subjected to MS whilst on a workshop relating to protein-protein interactions using MS. Therefore optimization and enrichment of cross-links could not be attempted.

Using size exclusion chromatography we attempted to generate a complex between the DWNN domain and Hsp70, but were unsuccessful, as the complex obtained was not stable enough to be cross-linked. However, further work pertaining to this interaction is currently being pursued as the SEC and MS data conclusively provide the platform for the interaction to be further pursued.

A drawback from using SEC for the complex generation is that the DWNN domain from RBBP6 has no tyrosine or tryptophan amino acids, so absorbance values at A_{280} recorded during SEC do not pick up the total amount of protein present. When generating a complex using SEC, the elution profiles of the individual proteins under scrutiny are aligned and compared to that of the complex elution profile. The size difference between the DWNN and Hsp70 is not significant enough to cause a peak shift in the elution profile thereby confirming the complex formation. Future work pertaining to this interaction would be to confirm that the peptide-binding domain from Hsp70 indeed is responsible for the interaction with the DWNN domain from RBBP6, produce enough quantities of the peptide-binding domain of Hsp70 as well as the DWNN domain, and force a complex between the two, before cross-linking and identifying amino acids involved in the interaction.



The interaction between RBBP6 and Hsp70 is interesting in itself and needs much more attention as it implicates RBBP6 further in the stress response as well as chaperone-mediated ubiquitination. Hsp90 has previously been identified as a potential interactor of RBBP6 (Witte and Scott, 1997). Owing to the function of Hsp90, which include protein folding and degradation, it is possible to hypothesize that RBBP6 is implicated in chaperone-mediated /ubiquitination, as well as pre-mRNA processing.

The RING finger domain of RBBP6 has been shown to act with MDM2 during the process of ubiquitination (Faro, A and Pugh, DJR, unpublished data), thereby leading us to the hypothesis that a potential interaction might occur between the RING finger domains of these proteins. We can conclusively state that an interaction between RBBP6 and MDM2 has been established through interaction of their respective RING finger

domains. MDM2, a homodimer, has previously been reported to heterodimerize with MDMX during ubiquitination. It has been reported that RBBP-RING too forms homodimers, as we have seen with non-denaturing ESI and NMR. This, in conjunction with the notion that these relatively small domains are too small to carry out a function independently, led to us hypothesizing that heterodimerization would enhance the functionality of this complex.

We attempted to form the heterodimer between RBBP6 and MDM2 using their isolated RING fingers. Initial results indicate that the heterodimer can be made using SEC, but ongoing experimentation should confirm it, thereby allowing us to perform the necessary experiments to try to localize their regions of interaction. Once the complex is stable cross-linking assays can be conducted and the interacting residues can be identified using MS. Validation of these interactions will be achieved through Isothermal Titration Calorimetry (ITC) to determine all binding parameters, or chemical shift perturbation experiments using NMR. Constructs with the interacting residues mutated can then be generated and the abolished interaction observed using NMR or ITC.

In addition, affinity purification MS (APMS) can be used in conjunction with the above mentioned for confirmation of the amino acids involved in the interaction.

The data presented provides a building block into the workings of RBBP6, which has many functions, as a full-length protein, as well as individual domains of the protein.

References

- Aebersold, R. & Goodlett, D. R. (2001) Mass Spectrometry in Proteomics. *Chemical Reviews* 101, 269-295.
- Aebersold, R., & Mann, M. (2003) Mass spectrometry-based proteomics. *Nature* 422, 198-208.
- Andersen, P., Kragelund, B.B., Olsen, A.N., Larsen, F.H., Chua, N.H., Poulsen, F.M., & Skriver, K. (2004) Structure and Biochemical Function of a Prototypical Arabidopsis U-box Domain. *Journal of Biological Chemistry* 279, 40053–40061.
- Aravind, L. & Koonin, E. V. (2000) The U-box is a modified RING finger - a common domain in ubiquitination. *Current Biology* 10, R132-4.
- Back, J.W., de Jong, L., Muijsers, A.V., de Koster, C.G. (2003) Chemical cross linking and mass spectrometry for protein structural modeling. *Journal of Molecular Biology* 331, 303-313.
- Baer, R., & Ludwig, T. (2002) The BRCA1/BARD1 heterodimer, a tumor suppressor complex with ubiquitin ligase activity. *Current opinion in Genetics and Development* 12 (1), 86-91.
- Baldwin, M. A. (2004) Protein Identification by Mass Spectrometry. *Molecular and Cellular Proteomics* 3, 1-9.

- Bantscheff, M., Eberhard, D., Abraham, Y., Bastuck, S., Boesche, M., Hobson, S., Mathieson, T., Perrin, J., Raida, M., Rau, C., Reader, V., Sweetman, G., Bauer, A., Bouwmeester T., Hopf, C., Kruse, H., Neubauer, G., Ramsden, N., Rick, J., Kuster, B., & Drewes, G. (2007) Quantitative chemical proteomics reveals mechanisms of action of clinical ABL kinase inhibitors. *Nature Biotechnology* 25, 1035–1044.
- Barlow, P. N., Luisi, B., Milner, A., Elliott, M. & Everett, R. (1994) Structure of the C3HC4 Domain by 1H-nuclear Magnetic Resonance Spectroscopy: A New Structural Class of Zinc-finger. *Journal of Molecular Biology* 237, 201-211.
- Bax, A., & Grzesiek, S. (1993) Methodological Advances in Protein NMR. *Accounts of Chemical Research* 26, 8.
- Benesch, J.L.P., Aquilina, A., Ruotolo, B.T., Sobott, F., Robinson, C.V. (2006) Tandem Mass Spectrometry Reveals the Quaternary Organization of Macromolecular Assemblies. *Chemistry and Biology* 13, 597-605.
- Benesch, J.L.P., & Robinson, C.V. (2006) Mass spectrometry of macromolecular assemblies: preservation and dissociation. *Current opinions in Structural Biology* 16, 245-251.
- Berg, J. M., & Shi, Y. (1996) The Galvanization of Biology: A Growing Appreciation for the roles of Zinc. *Science* 271, 5.
- Capili, A. D., Edghill, E. L., Wu, K. & Borden, K. L. (2004) Structure of the C-terminal RING finger from a RING-IBR-RING/TRIAD motif reveals a novel zinc-binding domain distinct from a RING. *Journal of Molecular Biology* 340, 1117-29.

- Chasapis, C. T., Christos, T., Spyroulias, J., & Georgios, A. (2009) RING Finger E3 Ubiquitin Ligases: Structure and Drug Discovery. *Current Pharmaceutical Design* 15(31), 3716-3731.
- Chen, Z. A., Jawhari, A., Fischer, L., Buchen, C., Tahir, S., Kamenski T., Rasmussen, M., Lariviere, L., Bukowski-Wills J.C., Nilges, M., Cramer P., & Rappsilber, J. (2010) Architecture of the RNA polymerase II-TFIIF complex revealed by cross-linking and mass spectrometry. *The EMBO Journal* 29, 717-726.
- Chibi, M., Meyer, M., Skepu, A., Rees, D.J.R. Moolman-Smook, J. C. & Pugh, D.J.R (2008) RBBP6 interacts with multifunctional protein YB-1 through its RING finger domain, leading to ubiquitination and proteosomal degradation of YB-1. *Journal of Molecular Biology* 384, 908-16.
- Christensen, D.E., & Klevit, R.E. (2009) Dynamic interactions of proteins in complex networks: identifying the complete set of interacting E2s for functional investigation of E3-dependent protein ubiquitination. *FEBS Journal* 276 (19), 5381-5389.
- Deriziotis, P., & Tabrizi, S.J. (2008) Prions and the proteasome. *Biochimica et Biophysica Acta* 1782, 713-722.
- Deshaies, R. J. & Jaozeiro, C. A. P. (2009) RING Domain E3 Ubiquitin Ligases. *Annual Reviews in Biochemistry* 78, 399-434.
- Dominguez, C., Folkers, G.E., Boelens, R. (2004) Biological Introduction: RING domain proteins. *Handbook of Metalloproteins* 3, 338-351.
- Domon, B. & Aebersold, R. (2006) Mass Spectrometry and Protein Analysis. *Science* 312, 212-219.

- Dudev, T. L. C. (2003) Principles Governing Mg, Ca, and Zn Binding and Selectivity in Proteins. *Chemistry Reviews* 103, 773–787.
- Figeys, D., McBroom, L. D., & Moran, M. F. (2001) Mass Spectrometry for the study of protein-protein interactions. *Methods* 24, 230-239.
- Friebolin, H. (2010) *Basic one- and two-dimensional NMR spectroscopy*, Weinheim, WILEY-VCH, Germany, ISBN 978-3-527-32782-9.
- Gao, Q., Xue, S., Doneanu, C. E., Shaffer, S.A., Goodlett, D.R. ,& Nelson, S.D. (2006) Pro-crosslink. Software tool for cross-linking and Mass Spectrometry. *Analytical Chemistry* 78, 2145-2149.
- Gao, S. & Scott, R. E. (2003) Stable overexpression of specific segments of the P2P-R protein in human MCF-7 cells promotes camptothecin-induced apoptosis. *Journal of Cell Physiology* 197, 445-52.
- Gaskell, S. J. (1997) Electrospray: Principles and Practice. *Journal of Mass Spectrometry* 32, 677-688.
- Gehrig, P.M., You, C., Dallinger, R., Gruber, C., Brouwer, M., Kägi, J.H., Hunziker, P.E. (2000) Electrospray ionization mass spectrometry of zinc, cadmium, and copper metallothioneins: Evidence for metal-binding cooperativity. *Protein Science* 9, 395-402.
- Glish, G. L. & Vachet, R. W. (2003) The basics of Mass Spectrometry in the twenty-first century. *Nature Reviews: Drug Discovery* 2, 140-150.
- Griffiths, W. J., Jonsson, S.U., Rai, D. K., & Wang, Y. (2001) Electrospray and tandem mass spectrometry in biochemistry. *Biochemistry Journal* 355, 545-561.

- Gstaiger, M. & Aebersold, R. (2009) Applying mass spectrometry-based proteomics to genetics, genomics and network biology. *Nature Reviews: Genetics* 10 (9), 617-627.
- Hanzawa, H., De Ruwe, M. J., Albert, T. K., Van der Vliet, P. C., Timmers, H. T. & Boelens, R. (2001) The structure of the C4C4 ring finger of human NOT4 reveals features distinct from those of C3HC4 RING fingers. *Journal of Biological Chemistry* 276, 10185-10190.
- Hashizume, R., Fukuda, M., Maeda, I., Nishikawa, H., Oyake, D., Yabuki, Y. Ogata, H., & Ohta, T. (2001) The RING heterodimer BRCA1-BARD1 is a ubiquitin ligase inactivated by a breast cancer-derived mutation. *Journal of Biological Chemistry* 276, 14537-14540.
- Hick, L., Schubert, H. L., & Hill, C.P. (2005) Ubiquitin-binding domains. *Nature Reviews: Molecular Cell Biology* 6, 610-621.
- Houben, K., Waseilewski, E., Dominguez, C., Kellenberger, E., Atkinson, R.A., Timmers, H.T., Kieffer, B., & Boelens, R. (2005) Dynamics and Metal Exchange Properties of C4C4 RING Domains from CNOT4 and the p44 Subunit of TFIIH. *Journal of Molecular Biology* 349, 621–637.
- Kamura, T., Koepp, D. M., Conrad, M. N., Skowyra, D., Moreland, R.J., Iliopoulos, O., Lane, W.S., Kaelin, W.G., Elledge, S.J., Conaway, R.C., Harper, J.W., & Conaway, J.W. (1999) Rbx1, a component of the VHL tumor suppressor complex and SCF ubiquitin ligase. *Science* 284, 657-661.
- Kappo, M.A., AB, E., Hassem, F., Atkinson, R.A., Faro, A., Muleya, V., Mulaudzi, T., Poole, J.O., McKenzie, J.M., Chibi, M., Moolman-Smook, J.C., Rees, D.J.G., & Pugh, D.J.R. (2012) Solution structure of the RING finger-

like domain of Retinoblastoma Binding Protein-6 (RBBP6) suggests it functions as a U-Box. *Journal of Biological Chemistry* 287 (10), 7146-7158.

Katoh, S., Hong, C., Tsunoda, Y., Murata, K., Takai, R., Minami, E., Yamazaki, T., & Katoh, E. (2003) High precision NMR structure and function of the RING-H2 finger domain of EL5, a rice protein whose expression is increased upon exposure to pathogen-derived oligosaccharides. *Journal of Biological Chemistry* 278, 15341-8.

Kellenberger, E., Dominguez, C., Fribourg, S., Wasielewski, E., Moras, D., Poterszman, A., Boelens, R., & Kieffer, B. (2005) Solution Structure of the C-terminal Domain of TFIIF P44 Subunit Reveals a Novel Type of C4C4 Ring Domain Involved in Protein-Protein Interactions. *Journal of Biological Chemistry* 280, 20785-20792.

Kerscher, O., Felberbaum, R., & Hochstrasser, M. (2006) Modification of Proteins by Ubiquitin and Ubiquitin-Like Proteins. *Annual Review of Cell and Developmental Biology* 22, 159-180.

Kirkin, D. (2007) Role of ubiquitin- and Ubl-binding proteins in cell signaling. *Current Opinion in Cell Biology* 19, 199–205.

Kostic, M., Matt, T., Martinez-Yamout, M.A., Dyson, H.J., & Wright, P.E. (2006) Solution Structure of the Hdm2 C2H2C4 RING, a Domain Critical for Ubiquitination of p53. *Journal of Molecular Biology* 363, 433–450.

Kühn-Hölsken, E., Lenz, C., Dickmanns, A., Hsiao, H., Richter, F.M., Kastner, B., Ficner, R., & Henning, U. (2010) Mapping the binding site of

snurportin 1 on native U1 snRNP by cross-linking and mass spectrometry. *Nucleic Acids Research* 38, 5581-5593.

Laganowsky, A., Reading, E., Hopper, J.T.S., Robinson, C.V. (2013) Mass spectrometry of intact membrane complexes. *Nature Protocols* 8 (4), 639-651.

Leitner, A., Walzthoeni, T., Kahraman, A., Herzog, F., Rinner, O., Beck, M., & Aebersold, R. (2010) Probing native protein structures by chemical cross-linking, mass spectrometry, and bioinformatics. *Molecular and Cellular Proteomics* 9, 1643-1649.

Li, L., Deng, B., Xing, G., Teng, Y., Tian, C., Cheng, X., Yin, X., Yang, J., Gao, X., Zhu, Y., Sun, Q., Zhang, L., Yang, X., & He, F. (2007) PACT is a negative regulator of p53 and essential for cell growth and embryonic development. *Proceedings of the National Academy of Science USA* 104, 7951-6.

Linares, L. K., Hengstermann, A., Ciechanover, A., Müller, S., & Scheffner, M. (2003) HdmX stimulates Hdm2-mediated ubiquitination and degradation of p53. *Proceedings of the National Academy of Science USA* 100, 12009-12014.

Maiolica, A., Cittaro, D., Borsotti, D., Sennels, L., Ciferri, C., Tarricone, C., Musacchio, A., & Rappsilber, J. (2007) Structural analysis of multi-protein complexes by cross-linking, mass spectrometry, and database searching. *Molecular Cell Proteomics* 6, 2200-2211

Ohi, M. D., Vander Kooi, C.W., Rosenberg, J.A., Chazin, W.J., & Gould, K.L. (2003) Structural insights into the U-box, a domain associated with multi-ubiquitination. *Nature Structural Biology* 10, 250-255.

- Pugh, D. J.R., AB, E., Faro, A., Luty, P. T., Hoffmann, E., & Rees, D. J.G. (2006) DWNN, a novel ubiquitin-like domain, implicates RBBP6 in mRNA processing and ubiquitin-like pathways. *BMC Structural Biology* 6, 1.
- Ramalho, T. C., Martins, T.L.C., Borges, L.E, de Pinho, M.H., de Avillez, R.R., & da Cunha, E.F. (2009) Influence of Zn-Cd substitution: Spectroscopic and theoretical investigation of 8-hydroxyquinoline complexes. *Spectrochimica Acta, Part A*, 4.
- Rappsilber, J. (2011) The beginning of beautiful friendship: Cross-linking/mass spectrometry and modeling of proteins and multi-protein complexes. *Journal of Structural Biology* 173(3), 530-540.
- Régnier, C.H., Tomasetto, C., Moog-Lutz, C., Chenard, M.P., Wendling, C., Basset, P., Rio, M.C. (1995) Presence of a conserved domain in CART1, a novel member of the tumor necrosis factor receptor-associated protein family, which is expressed in breast carcinoma. *The Journal of Biological Chemistry* 270, 25715-25721.
- Sakai, Y., Saijo, M., Coelho, K., Kishino, T., Niikawa, N. & Taya, Y. (1995) cDNA sequence and chromosomal localization of a novel human protein, RBQ-1 (RBBP6), that binds to the retinoblastoma gene product. *Genomics* 30, 98-101.
- Schilling, B., Row, R.H., Gibson, B.W., Guo, X., & Young, M.M. (2003) MS2Assign, automated assignment and nomenclature of tandem mass spectra of chemically crosslinked peptides. *Journal of the American Society for Mass Spectrometry* 14, 834–850.

- Schulze, W. X. & Usadel, B. (2010) Quantitation in Mass-Spectrometry-Based Proteomics. *Annual Reviews in Plant Biology* 61, 491-516.
- Schwartz, J.C., Senko, M.W., Syka JE. (2002) A two-dimensional quadrupole ion trap mass spectrometer. *Journal of the American Society for Mass Spectrometry* 13, 659–669.
- Seebacher, J., Mallick, P., Zhang, N., Eddes, J.S., Aebersold, R., & Gelb, M.H. (2006) Protein Cross-linking analysis using Mass Spectrometry, Isotope-coded cross-linkers, and integrated computational data processing. *Journal of Proteome Research* 1-13.
- Sharon, M., Taverner, T., Ambroggio, X.I., Deshaies, R.J. & Robinson, C.V. (2006) Structural organization of the 19S proteasome lid: insights from MS of intact complexes. *PLoS Biology* 4, e267.
- Simons, A., Melamed-Bessudo, C., Wolkowicz, R., Sperling, J., Sperling, R., Eisenbach, L. & Rotter, V. (1997) PACT: cloning and characterization of a cellular p53 binding protein that interacts with Rb. *Oncogene* 14, 145-155.
- Singh, P., Panchaud, A., & Goodlett, D. R. (2010) Chemical cross-linking and mass spectrometry as a low-resolution protein structure determination technique. *Analytical Chemistry* 82 (7), 2636-2642.
- Sinz, A. (2006) Chemical cross-linking and Mass spectrometry to map Three-dimensional protein structures and protein-protein interactions. *Mass Spectrometry Reviews* 25, 663-682.
- Siuzdak, G. (1994) The emergence of mass spectrometry in biochemical research. *Proceedings of the National Academy of Science* 91, 11290-11297.

- Steen, H. & Mann, M. (2004) The ABC's (and XYZ's) of Peptide Sequencing. *Nature Reviews: Molecular Cell Biology* 5, 699-711.
- Stengel, F., Aebersold, R., & Robinson, C.V. (2012) Joining forces: Integrating Proteomics and Cross-Linking with the Mass Spectrometry of Intact Complexes. *Molecular and Cellular Proteomics* 11, 1-13.
- Tang, X., Munske, G. R., Siems, W. F., & Bruce, J. E. (2005) Mass Spectrometry Identifiable cross-linking strategy for studying protein-protein interactions. *Analytical Chemistry* 77, 311-318.
- Veenstra, T. D. (1999) Electrospray ionization mass spectrometry in the study of biomolecular non-covalent interactions. *Biophysical Chemistry* 79, 63-79.
- Vo, L. T., Minet, M., Schmitter, J. M., Lacroute, F. & Wyers, F. (2001) Mpe1, a zinc knuckle protein, is an essential component of yeast cleavage and polyadenylation factor required for the cleavage and polyadenylation of mRNA. *Molecular Cell Biology* 21, 8346-56.
- Woelk, T., Sigismund, S., Penengo, L., & Polo, S. (2007) The ubiquitination code: a signalling problem. *Cell Division* 2, 12.
- Wüthrich, K. (1995) NMR – this other method for protein and nucleic acid structure determination. *Acta Crystallographica Section D* 51, 249-270.
- Yates, J. R. (1998) Mass Spectrometry and the Age of the Proteome. *Journal of Mass Spectrometry* 33, 1-19.
- Yates, J. R., Ruse, C. I., & Nakorchevsky, A. (2009) Proteomics by Mass Spectrometry: Approaches, Advances, and Applications. *Annual Review of Biomedical Engineering* 11, 49-79.

- Yunus, A. A. & Lima, C. D. (2009) Structure of the Siz/PIAS SUMO E3 Ligase Siz1 and Determinants Required for SUMO Modification of PCNA. *Molecular Cell* **35**, 669-682.
- Wang, X. & Jiang, X. (2012) MDM2 and MdmX partner to regulate p53. *FEBS Letters* **586** (10), 1390-1396.
- Witte, M. M. & Scott, R. E. (1997) The proliferation potential protein-related (P2P-R) gene with domains encoding heterogeneous nuclear ribonucleoprotein association and Rb1 binding shows repressed expression during terminal differentiation. *Proc Natl Acad Sci U S A* **94**, 1212-7.
- Zhang, H., Cui, W., Wen, J., Blankenship, R.E., & Gross, M.L. (2011) Native Electrospray and Electron-Capture Dissociation FTICR Mass Spectrometry for Top-down Studies of Protein Assemblies. *Analytical Chemistry* **83** (14), 5598-5606.

